

**UCGE Reports**

**Number 20134**

Department of Geomatics Engineering

**Determining Heading and Pitch  
Using a Single Difference  
GPS/GLONASS Approach**

by

**JiunHan Keong**

**November 1999**



Calgary, Alberta, Canada

THE UNIVERSITY OF CALGARY

**Determining Heading and Pitch Using a Single Difference  
GPS/GLONASS Approach**

by

Jiun Han Keong

A THESIS

SUBMITTED TO THE FACULTY OF GRADUATE STUDIES  
IN PARTIAL FULFILMENT OF THE REQUIREMENTS FOR THE  
DEGREE OF MASTER OF SCIENCE

DEPARTMENT OF GEOMATICS ENGINEERING

CALGARY, ALBERTA

DECEMBER, 1999

© Jiun Han Keong 1999

## ABSTRACT

This thesis presents an approach to combine GPS and GLONASS measurements, using a single differencing technique with a common frequency and time standard, to determine the heading and pitch parameters using a pair of non-dedicated GPS/GLONASS receivers. The theory behind the use of GPS for attitude determination is well known. Augmentation of GPS with GLONASS is not straightforward however. This is because the latter system, besides having other differences with the former system, employs the frequency division multiple access (FDMA) technique to distinguish the signals from different satellites. The fact that each GLONASS signal has its own slightly different frequency makes the double differencing (DD) of the carrier phase measurements no longer possible without modification. GPS uses the code division multiple access (CDMA) technique, which has a common frequency for all satellites, and hence does not experience the same problem. To get around this problem, the use of between-receiver single differencing (SD) of the carrier phase measurements is proposed. In this case however, receiver clock and other errors do not cancel out. An external frequency and time standard is used to serve as a common oscillator for the two receivers. Remaining time and other biases are estimated using a low-pass averaging filter. The SD carrier phase integer ambiguities can then be resolved and the heading and pitch can be determined with a relatively good level of accuracy. A software algorithm was written to estimate the heading and pitch parameters from GPS and GLONASS measurements using the above approach. Static and kinematic tests conducted with a pair of GPS/GLONASS receivers are used to validate the approach. Under reduced visibility, the combined GPS/GLONASS approach is shown to yield superior availability.

## ACKNOWLEDGEMENTS

First and foremost, I thank my parents, my grandparents, and the rest of my family members with heart for being a constant source of support, both spiritually and materialistically, throughout my whole life. Without them, I would not have made it that far, across the oceans, to Canada and would not have made myself to higher education. All they have been giving me in the past 25 years are certainly invaluable and irreplaceable.

Deep gratitude and appreciation are extended to my supervisor, Dr. Gérard Lachapelle, for his excellent supervision and financial support during my study here in the University of Calgary. I am certain that the many discussions he has had with me, in both the professional and the personal aspects, will be very helpful in my future careers.

Special thanks go to the members in my MSc examining committee, Dr. Gao, Dr. El-Sheimy, and Dr. Ulieru for taking the time and effort, not only sitting in the oral examination, but also reading my thesis and providing feedback. Guidance from Dr. Cannon is very appreciated. Courses I took from Dr. Schwarz, Dr. Brunner, Dr. Maybeck, Dr. Nowrouzian, Dr. Salychev and Mr. Geier are beneficial and I would like to thank all of them.

Many teachers who thought me in Sam Tet Primary School and Shen Jai Secondary School in Malaysia as well as the professors in the University of New Brunswick during my undergraduate study have always been remembered and thanked. In particular, I would like to thank Mr. Choy, Mr. Toh, Mdm. Chow, Mr. Goh, Dr. Kleusberg, Dr. Nichols, and Dr. Secord.

JiHong and Ning, my two good friends from China and “partners” in the office, are specially thanked for many things. These include great helps in academic matters, exchange of thoughts, advises in daily life, opportunities given to me, dinners, outings, card games, sports, and a lot of others.

My special Indian colleague, Jayanta, is particularly thanked for proofreading the first draft of this thesis and being an excellent source of knowledge in the areas of GPS and Electronic Engineering. Peers within our research group, Sun, Rakesh, Jim, Sam, Mark, and many others, are also thanked for providing answers when in doubts. Other friends in the “trailer” have been nice for creating an interesting environment for both working (daytime/weekday) and “living” (nighttime/weekend).

Friends in Canada are kind, friendly, and helpful and have enlightened my life a lot. I must say without knowing all these friends and being together with them, my life in Canada, especially the last two years in Calgary, would have not been that meaningful, colourful, and exciting.

Last but not least, my *mm* is especially thanked for being understanding, considerate and always being there when needed.

## TABLE OF CONTENTS

APPROVAL.....	ii
ABSTRACT.....	iii
ACKNOWLEDGEMENTS.....	iv
TABLE OF CONTENTS.....	vi
LIST OF FIGURES.....	x
LIST OF TABLES.....	xii
LIST OF ABBREVIATIONS.....	xiii
LIST OF SYMBOLS.....	xvi
LIST OF OPERATORS.....	xviii
<b>CHAPTER ONE</b>	
<b>INTRODUCTION.....</b>	<b>1</b>
1.1 Background.....	1
1.2 Objective and Proposed Approach.....	3
1.3 Outline.....	5
<b>CHAPTER TWO</b>	
<b>REVIEW OF GPS AND ITS ERROR SOURCES.....</b>	<b>7</b>
2.1 Overview of GPS.....	7
2.1.1 GPS Signals.....	8
2.1.2 Code Pseudorange Observation Equation.....	10
2.1.3 Solutions and Accuracy from Code Pseudorange.....	11
2.2 Carrier Phase Observable.....	13
2.2.1 Carrier Phase Observation and Differencing Equations.....	14
2.2.2 Receiver Measurement Noise.....	17
2.2.3 Multipath.....	19
2.2.4 Other Errors.....	22

## **CHAPTER THREE**

<b>GLONASS: CHARACTERISTICS AND DIFFERENCES WITH GPS .....</b>	<b>26</b>
3.1 Overview of GLONASS .....	26
3.1.1 Satellites, Control, and Users Components .....	27
3.1.2 Performances: Visibility, Accuracy, and Coverage .....	30
3.1.3 Carrier Frequencies .....	32
3.2 Difference between GPS and GLONASS .....	34
3.2.1 Time Reference Systems .....	35
3.2.2 Coordinate Reference Systems .....	37
3.2.3 Signal Multiplexing Techniques .....	42
3.2.3.1 Single Difference with a Common Clock .....	43
3.2.3.2 Modified Double Difference Technique .....	44
3.2.4 Other Differences between GLONASS and GPS .....	45
3.3 Future of GLONASS .....	47

## **CHAPTER FOUR**

<b>ATTITUDE PARAMETERS AND COORDINATE FRAMES .....</b>	<b>48</b>
4.1 Coordinate Systems and Rotation Matrices .....	48
4.1.1 Conventional Terrestrial System .....	49
4.1.2 Local Level System .....	50
4.1.3 Wander Frame .....	53
4.1.4 Vehicle Platform Coordinate System .....	54
4.1.5 Antenna Body Coordinate System .....	55
4.2 Deriving the Heading and Pitch Parameters .....	59
4.2.1 Twin-Antenna System .....	60
4.2.2 Multi-Antenna System .....	62
4.3 Accuracy of the Attitude Parameters .....	65
4.3.1 Deriving DOP for Attitude Parameters .....	66
4.3.2 Error Sizes and Other Impacts .....	69

## **CHAPTER FIVE**

<b>ATTITUDE DETERMINATION USING GPS/GLONASS .....</b>	<b>71</b>
5.1 SD Carrier Phase .....	71
5.2 SD Carrier Phase Ambiguity Resolution in an Attitude System.....	76
5.2.1 Defining the Ambiguity Search Space/Volume .....	78
5.2.2 Selecting the Ambiguities Candidates.....	82
5.2.3 Ambiguities Distinguishing Testing.....	84
5.2.3.1 Variance Factor Test .....	84
5.2.3.2 Known Baseline Constraint Test.....	86
5.2.3.3 Ratio Test .....	87
5.3 SD Clock Offset and Line Bias Residuals .....	89
5.3.1 Estimating the SD Biased Residuals .....	91
5.3.2 Shadow Test .....	93
5.3.3 Clock Test: Rubidium vs. OCXO .....	95
5.3.4 Multipath in SD GPS/GLONASS .....	98

## **CHAPTER SIX**

<b>SYSTEM ARCHITECTURE, TEST RESULTS AND ANALYSIS .....</b>	<b>103</b>
6.1 System Architecture .....	103
6.1.1 Hardware .....	103
6.1.2 Software .....	106
6.2 Static Test I.....	111
6.2.1 10° Elevation Mask .....	111
6.2.2 35° Elevation Mask .....	113
6.3 Kinematic Test I.....	115
6.3.1 10° Elevation Mask .....	116
6.3.2 30° Elevation Mask .....	118
6.4 Kinematic Test II.....	120
6.4.1 Open Sky Area .....	121
6.4.2 Residential Area .....	123

**CHAPTER SEVEN**

**CONCLUSIONS AND RECOMMENDATIONS ..... 129**

7.1 Conclusions ..... 129

7.2 Recommendations ..... 131

**LIST OF REFERENCES ..... 134**

## LIST OF FIGURES

Figure 2.1: Single Differencing and Double Differencing of GPS Measurements.....	16
Figure 2.2: Receiver Multipath from Satellite .....	20
Figure 3.1: (a) GPS and (b) GLONASS Satellite Constellation .....	29
Figure 3.2: Location of GLONASS Satellites in October 1999.....	29
Figure 3.3: GPS and GLONASS Satellite Visibility on October 1999.....	31
Figure 3.4: Transformation between WGS84 and PZ90 [Misra et al., 1996] .....	40
Figure 4.1: Relationship between the CT Frame and LL Frame.....	51
Figure 4.2: Defining Heading and Pitch in a Vehicle Platform Coordinate System.....	54
Figure 4.3: Antenna Body Frame of a Twin-antenna System.....	56
Figure 4.4: Antenna Body Frame of a GPS/GLONASS Multi-antenna System .....	62
Figure 5.1: Ambiguity Baseline Constraint Cube Search Concept.....	79
Figure 5.2: Ambiguity Pitch Constraint Spherical Surface Search Volume Concept.....	81
Figure 5.3: Key Procedures in a typical Integer Ambiguity Resolution Process.....	89
Figure 5.4: Residuals for Selected GPS SVs.....	90
Figure 5.5: Residual Bias Estimates for Four SVs.....	92
Figure 5.6: SD Residuals after Bias Estimate Feedback.....	93
Figure 5.7: Heading and Pitch Estimates with 2-Sigma Bounds .....	94
Figure 5.8: Residuals, before and after Bias Removal.....	95
Figure 5.9: Heading and Pitch using Rubidium and OCXO as Common FTS.....	98
Figure 5.10: Site of Static Roof Test for Multipath .....	99
Figure 5.11: Heading and Pitch Estimates from Day 1 and Day 9 .....	100
Figure 6.1: Hardware Installation for GPS/GLONASS Attitude System.....	105
Figure 6.2: Flowchart of the Ambiguity Resolution Process in HEADG <sup>2</sup> ™.....	107

Figure 6.3: Flowchart of the Residuals Feedback System .....	110
Figure 6.4: Number of SVs, ADOP, and EDOP for 10° Elevation Mask – Static Test..	112
Figure 6.5: GPS and GG Heading and Pitch Estimates for 10° Elevation Mask – Static Test.....	112
Figure 6.6: Number of SVs, ADOP, and EDOP for 35 ° Elevation Mask – Static Test .....	114
Figure 6.7: GPS and GG Heading and Pitch Estimates for 35° Elevation Mask – Static Test.....	114
Figure 6.8: Reference Estimates of Heading and Pitch from Standard GPS DD Technique – Kinematic Test I.....	116
Figure 6.9: Number of SVs, ADOP, and EDOP for 10° Elevation Mask – Kinematic Test I.....	117
Figure 6.10: Differences in SD Heading and Pitch Estimates with respect to (w.r.t.) GPS DD for 10° Elevation Mask – Kinematic Test I.....	117
Figure 6.11: Number of SVs, ADOP, and EDOP for 30° Elevation Mask – Kinematic Test I.....	119
Figure 6.12: Differences in SD Heading and Pitch Estimates w.r.t. GPS DD for 30° Elevation Mask – Kinematic Test I.....	119
Figure 6.13: Reference Estimates of Heading and Pitch using a Standard GPS DD Technique – Kinematic Test II.....	121
Figure 6.14: Number of SVs, ADOP, and EDOP for Open Sky – Kinematic Test II ....	122
Figure 6.15: Differences in SD Heading and Pitch Estimates w.r.t. GPS DD for Open Sky – Kinematic Test II.....	122
Figure 6.16: Number of SVs, ADOP, and EDOP for Residential Area – Kinematic Test II .....	124
Figure 6.17: Differences in SD Heading and Pitch Estimates w.r.t GPS DD for Residential Area – Kinematic Test II.....	124
Figure 6.18: Attitude Accuracy as a function of Inter-Antenna Distance .....	1247

## LIST OF TABLES

Table 3.1: GLONASS / GPS Comparison in Space Segment.....	28
Table 3.2: Defining Parameters of the PZ90.....	37
Table 3.3: Differences between GLONASS and GPS .....	46
Table 5.1: Statistics for Heading and Pitch Estimates for Day 1 and Day 9 – Static Multipath Test .....	101
Table 6.1: Accuracy of Ashtech GG24 <sup>TM</sup> as a Function of Mode at 95%.....	104
Table 6.2: Statistics of GPS and GLONASS Augmentation for 10° and 30° Elevation Mask – Kinematic Test I.....	120
Table 6.3: Statistics of GPS and GLONASS Augmentation for Open Areas and Residential Areas – Kinematic Test II .....	125
Table 6.4: Accuracy of Heading and Pitch with Different Inter-antenna Distances.....	126

## LIST OF ABBREVIATIONS

AB	Antenna Body
ADOP	azimuth dilution of precision
AFM	ambiguity function method
AS	anti-spoofing
C/A-code	coarse acquisition code
CDMA	code division multiple access
CS	central synchronizer
CT	conventional terrestrial
CTS	command tracking stations
DD	double difference / double differencing / double differenced
DGPS	Differential Global Positioning System
DoD	Department of Defence
DOP	dilution of precision
ECEF	Earth-Centred Earth-Fixed
EDOP	elevation dilution of precision
EU	European Union
FARA	fast ambiguity resolution approach
FASF	fast ambiguity search filter
FDMA	frequency division multiple access
FTS	frequency and time standard
GEO	Geostationary-Earth-orbiting
GLONASS	Global Navigation Satellite System (from Russian <i>Global'naya Navigatsionnaya Sputnikovaya Sistema</i> )
GLONASST	Global Navigation Satellite System Time
GNSS	Global Navigation Satellite Systems
GPS	Global Positioning System

GPST	Global Positioning System Time
HP	high precision
ICD	Interface Control Document
INS	Inertial Navigation System
IERS	International Earth Rotation Services
ITRF94	International Terrestrial Reference Frame 1994
ITU	International Telecommunications Union
KNITs	Coordination Scientific Information Centre (from Russian <i>Koordinatsionny Nauchno-Informatsionny Tsentr</i> )
LEO	low-Earth-orbiting
LL	Local Level
LSAST	least-squares ambiguity search technique
MEO	medium-Earth-orbiting
NAVSTAR	Navigation Satellite using Timing and Ranging
OCXO	oven-controlled crystal oscillator
P-code	precise code
PDOP	position DOP
PPS	precise positioning service
PRN	pseudorandom noise
PZ90	Parameters of the Earth System 1990 (from Russian <i>Parametry Zemli 1990</i> )
RA	right ascension
RDOP	relative DOP
REDOP	relative DOP for easting
RMS	root-mean-squares
RNDOP	relative DOP for northing
RVDOP	relative DOP for height
SA	selective availability
SCC	system control centre
SD	single difference / single differencing / single differenced

SNR	signal-to-noise ratio
SP	standard precision
SPS	standard positioning service
STD	system-time-difference
SU	Soviet Union
SV	satellite vehicle
TAI	International Atomic Time
TDMA	time division multiple access
URE	user equivalent range error
UHF	ultra-high-frequency
US	United States
USD	United States Dollars
UTC	Universal Coordinated Time
UTC_SU	Universal Coordinated Time, Soviet Union standard
UTC_BIPM	Universal Coordinated Time, international standard (from French <i>Bureau International des Poids et Mesures</i> )
UTC_USNO	Universal Coordinated Time, United States Naval Observatory standard
VKS	[Russian] Military Space Forces (from Russian <i>Voенно-Kосмический Силы</i> )
WGS84	World Geodetic System 1984

## LIST OF SYMBOLS

$\alpha$	wander angle used in the wander frame
$\varepsilon$	error in measurements which includes receiver noise, multipath, etc
$\phi$	geodetic latitude
$\lambda$	geodetic longitude
$\psi$	heading parameter of a moving platform
$\theta$	pitch parameter of a moving platform
$\varphi$	roll parameter of a moving platform
$\delta t$	time difference between two epoch epochs
$\rho$	true geometric range between the antennas of satellite and receiver
$\sigma^2$	variance
$\tau_c$	tolerance criterion in the phase rate method
$\tau_d$	tolerance criterion in the baseline constraint method
$v$	measurement residuals
$\chi^2$	chi-squares percentile,
$\Phi$	measured carrier phase,
$\Phi_{L1}$	carrier phase measurement on L1
$\Phi_{L2}$	carrier phase measurement on L2
$\Phi_{L1,L2}$	ionospheric-free carrier phase measurement
$a$	semi-major axis
$b$	semi-minor axis
$cdt$	satellite clock offset from GPST
$cdT$	receiver clock offset from GPST
$comb$	combined term for the receiver clock offset and line bias
$C$	covariance matrix
$dp$	orbital error along the line of sight from satellite to receiver

df	degree of freedom
dIon	ionospheric delay
dTrop	tropospheric delay
est	estimate of the residual bias over time
E	easting (or longitude)
$f_{L1}$	frequency for L1 carrier
$f_{L2}$	frequency for L2 carrier
h	geodetic height
lb	line bias delay caused by the physical length of the cable
k	channel number used in GLONASS frequency division
L	baseline length (or inter-antenna distance) in an attitude system
$n_e$	total number of epoch used
$n_s$	total number of satellites
N	carrier phase integer ambiguity
N	northing (or latitude)
$N_{float}$	vector of the floating ambiguity states
$N_{int}$	vector of the potential integer ambiguity states
$N_p$	prime vertical radius of the curvature at point p
p	measured pseudorange
$p_{L1}$	pseudorange measurement on L1
$p_{L2}$	pseudorange measurement on L2
$p_{L1,L2}$	ionospheric-free pseudorange measurement
Res	estimate of the residual bias in an epoch
$R_1$	rotation matrix for rotation about the x-axis
$R_2$	rotation matrix for rotation about the y-axis.
$R_3$	rotation matrix for rotation about the z-axis
Up	vertical component (or height)

## LIST OF OPERATORS

<b>a</b>	vectors are in bold and lower-case
<b>A</b>	matrices are in bold and upper-case
$\Delta a$	is the between-receiver differencing of quantity $a$
$\nabla a$	is the between-satellite differencing of quantity $a$
$\delta a$	is the between-epoch differencing of quantity $a$
$\nabla\Delta a$	is the between-satellite between-receiver double differencing of quantity $a$
$\mathbf{A}^{-1}$	is the inverse of $\mathbf{A}$
$\mathbf{A}^T$	is the transpose of $\mathbf{A}$
$\hat{a}$	is the estimated value for $a$
$\dot{a}$	is the rate of change of $a$
$ a $	is the absolute value of quantity $a$
$\text{int}[a]$	is the nearest integer operation on quantity $a$ ,

## **CHAPTER ONE**

### **INTRODUCTION**

In this thesis, an approach to estimate the heading and pitch attitude parameters using Global Positioning System (GPS) and Global Navigation Satellite System (GLONASS) measurements is studied and presented.

This chapter first provides readers with a background knowledge of GPS attitude determination. It then introduces the objective of this study which is the determination of heading and pitch using GPS/GLONASS. A brief introduction of the remaining chapters is also given.

#### **1.1 Background**

The application of attitude determination is essential for a wide range of navigation, guidance, and control tasks. Most aircraft, marine vessels, space vehicles, and some automotive vehicles are equipped onboard with one type of attitude system or another. The types of attitude systems available commercially in the market range from the simplest traditional magnetic compass to the most advance, expensive and accurate inertial-based devices such as the Inertial Navigation System (INS).

It is also well known that GPS, when employed in differential GPS (DGPS) mode, can be used to estimate the three attitude parameters: heading (yaw), pitch, and roll (e.g.

[Schleppé, 1996], [Cohen, 1992] and [Lu, 1995]). Heading and pitch can be adequately determined using two GPS antennas. This is similar in theory to the determination of azimuth and elevation in a local coordinate system using relative positioning.

In addition to the GPS code pseudorange observable, higher precision GPS carrier phase is yet another required observable for attitude determination. Carrier phase differential technique relies upon measurements of the accumulated phase of the GPS carrier. The number of cycles of the carrier at the start of accumulation, known as the carrier phase ambiguity, is not known and hence absolute GPS carrier phase measurement without solving the ambiguity is meaningless. The most accurate DGPS technique requires the carrier phase ambiguity to be resolved as an integer number. Float number ambiguity may also be used, however, the attainable accuracy may be degraded by approximately an order of magnitude.

Millimetre level relative positioning accuracy is required in attitude determination for sub-degree attitude accuracy with antenna baseline lengths at the metre level. (The term “antenna baseline lengths”, strictly speaking, should be called the “inter-antenna distances” as the term “baseline” constitutes special meaning in geomatics of being static and fixed. However, due to the popularity of the term “antenna baseline lengths” for attitude applications in common literature, it will be used interchangeably with the term “inter-antenna distances” throughout this thesis). Since a float solution would not provide a good accuracy, therefore, fixing the carrier phase integer ambiguity is essential in attitude determination. To resolve the carrier phase integer ambiguity, the technique of double differencing is commonly used in practice.

This double difference technique differenced the carrier phase observation equations twice, between the antennas and between the satellites, to eliminate errors due to satellite and receiver clock offsets. The double difference technique also significantly reduces the spatially correlated errors due to the orbits and the atmosphere in case of a short baseline. One of the requirements for performing the double differencing technique is to have at

least four satellites commonly tracked by the two antennas. The availability of additional satellites is nonetheless highly desirable. It provides redundancy of measurements, accelerates the integer ambiguity resolution process, and increases the success rate. However, the availability of additional satellites may pose significant difficulties in areas of reduced visibility, such as automotive navigation in urban canyons or under foliage, marine navigation in fjords, etc.

There have been several solutions proposed to this problem. One that has been widely used in practice is to integrate GPS measurements with INS measurements to determine the attitude parameters (e.g. [Sun, 1994]). The advantages are that INS is capable of yielding better accuracy, especially for pitch and roll, and it is able to provide a data rate that is as high as ten times that of GPS. Most importantly, INS has no obstruction problem and/or loss of lock problem and hence it is able to provide continuous measurements without outage. Thus, INS is an excellent source to complement GPS by bridging outages when the latter is temporarily not available. The main disadvantage of GPS/INS integration is that INS is very expensive at this time. Also, INS without GPS update may drift as much as several arc-minutes/minute and this shorten the period of using INS as a sole-mean navigation system when GPS measurements are not available.

## **1.2 Objective and Proposed Approach**

One of the increasingly popular alternatives to the GPS/INS integration approach is the augmentation of GPS with GLONASS, its Russian counterpart. GLONASS is very similar to GPS in many aspects. It offers many great advantages to the augmentation. First, there can be as many as twice the number of satellites with the augmentation of GLONASS and hence improve the situations where signal masking and reduced visibility is a problem. Second, the geometry of the satellites is likely to be strengthened with the augmentation of GPS with GLONASS. Third, GLONASS as an independent system is free from GPS system biases and blunders. Therefore, the improvements in availability,

geometry, integrity, and reliability are some direct advantages of combining the GPS and GLONASS measurements.

Upon combining the measurements from GPS and GLONASS, some of the major differences between GPS and GLONASS have to be accounted for. GLONASS differs from GPS in the time reference system, coordinate reference system, and the signal multiplexing technique. The differences in the signal multiplexing technique constitute the most challenging aspect of this research. GLONASS employs the technique of frequency division multiple access (FDMA), rather than code division multiple access (CDMA) as is the case for GPS, to distinguish the signals from different satellites. The fact that each GLONASS satellite signal has a slightly different frequency makes double differencing of the carrier phase measurements no longer possible. Similar to many other engineering problems, many different approaches and solutions exist for meeting the challenges to some degrees or another.

To combine the GPS and GLONASS carrier phase measurements, a between-receiver single differencing approach is studied herein. The single differencing approach has some advantages over the standard double differencing approach. There is a lower noise in the carrier phase and there is an extra satellite observation available for the ambiguity resolution process in attitude determination. In this case however, the receiver clock offset and the line bias errors do not cancel out. Therefore, an external time and frequency standard is used as a common oscillator for the two receivers to reduce errors due to the receiver clocks. There is however a remaining bias between the two receivers and a special treatment has to be used [Keong & Lachapelle, 1998]. A low-pass averaging filter is first employed to estimate the bias in the residuals. The single differenced ambiguities can then be resolved with the bias removed. The heading and pitch parameters can finally be determined with satisfactory accuracy under benign visibility conditions. Under signal masking or reduced visibility conditions, the combined GPS/GLONASS attitude system yields superior availability and here lie the main contribution of this study.

*In summary, the approach taken in this research study is to combine measurements from a pair of non-dedicated, off-the-shelf, GPS/GLONASS receivers with a common time and frequency standard for the determination of heading and pitch attitude parameters using a single difference carrier phase technique.*

### **1.3 Outline**

This thesis consists of seven chapters. A brief introduction of the remaining chapters is subsequently given as follows.

Chapter Two reviews GPS and its error sources. It begins with an overview of the GPS technology. The carrier phase observable and its errors, particularly those affecting the accuracy of attitude determination, are described in details. The techniques of single differencing and double differencing for carrier phase measurements are also discussed.

Chapter Three focuses on the GLONASS system. First, it presents an overview of GLONASS with some of its unique characteristics. It then addresses the major differences between GLONASS and GPS: in time and coordinate referencing and in signal multiplexing. The FDMA related problems in GLONASS are presented in details and two corresponding solutions are discussed. The future of GLONASS is also briefly discussed.

Coordinate frames and rotation matrices related to attitude determination are reviewed in Chapter Four. The conventional terrestrial, the local level and the antenna body frames are defined and rotation matrices between these frames are presented. Attitude parameters referenced to these coordinate frames are defined. A direct method to derive the attitude parameters from measurements in twin- and multi-antenna systems is given.

It is then followed by a discussion of the error analysis of the estimated attitude parameters.

Chapter Five discusses the technique of single differencing of the GPS/GLOASS carrier phase in greater details. It first presents the technique of single differencing in theory. It is then followed by a discussion of the ambiguity resolution mechanism for SD carrier phase in an attitude system. The problems faced with single differencing, namely the existence of a bias residual, is discussed and a solution is given. Lastly, the results of several tests, including a shadow test and a clock test, are presented to validate the SD carrier phase approach. The GPS/GLONASS multipath effect on attitude parameter is also investigated.

The system architecture of a GPS/GLONASS attitude system is first presented in Chapter Six, with emphasis on the hardware installation and software implementation. It then compares the performance of the approach described in Chapter Five against that using a standard GPS double differencing approach. The results and analysis from one static and two kinematic tests are presented.

Chapter Seven summarizes this thesis with conclusions based upon the present findings. Last but not least, recommendations for future work are suggested.

## CHAPTER TWO

### REVIEW OF GPS AND ITS ERROR SOURCES

A review of GPS and its sources of errors is the main focus of this chapter. It begins with an overview of the GPS technology. The carrier phase observable and its errors, particularly those affecting the accuracy of attitude determination, are described in details. The techniques of single differencing and double differencing for carrier phase measurements are also discussed.

#### 2.1 Overview of GPS

Formally known as the Navigation Satellite using Timing and Ranging GPS (Navstar GPS), GPS is the first radio-based navigation systems to provide timing and positioning services at all times, under all weather conditions, on a worldwide and free-of-charge basis, to an unlimited number of users [Wells et al., 1986]. GPS is developed and currently administrated by the United States (US) Department of Defence (DoD). Since its beginning in 1980, it has attracted the attentions of users from around the world with a wide range of applications. The GPS system has three inter-related segments: the space, the control system, and the users.

The space segment consists of a constellation of 21 plus 3 active spare satellites since the announcement of full operational status in 1995. Occasionally, the number of active and healthy satellites reaches 27 as new satellites are launched before the life span of old satellites expire. The GPS satellites are unevenly distributed in six evenly spaced orbital

planes. The nominal height of the satellites is 20,183 km. All GPS satellites have orbital periods of 12 sidereal hours, i.e. exactly half the rotation period of the Earth, and therefore the ground tracks of the satellites repeat themselves after two revolutions.

The functions of the control segment are, among others, to monitor the health of the satellites, to model the satellite orbit, to upload the navigation data and to synchronize the satellite and system clocks. There are four control stations located on islands in three oceans near the equator. A master control station is located in Colorado Springs.

The military and civilian users make up the third and, by far, the largest segment. The total number of users, in term of the number of receivers, is estimated to exceed four millions by 2000. The worldwide civilian users outnumber the military users by an increasing ratio of 20 to 1. In term of market value, the civilian-military ratio is doubled with an estimate of \$5 billion US Dollars (USD) [Jacobson, 1999]. A user typically uses a GPS antenna to track satellite signals and a GPS receiver, equipped with a microprocessor chipset, to extract navigation messages, compute positions from ranging information, and/or display solutions output.

### **2.1.1 GPS Signals**

From the users' point of view, GPS is a passive one-way timing and ranging system, i.e., the signal are transmitted by the satellite and the users can only do the "listening". All GPS satellites have several Cesium and Rubidium atomic clocks on board. These clocks are set to a fundamental frequency,  $f_0$ , of 10.23 MHz. All signals transmitted from the GPS satellites are derived from this fundamental frequency. These signals are centred on two ultra-high-frequency (UHF) radio frequencies: the L1 1575.42 MHz (i.e.  $154 \cdot f_0$ ), and the L2 1227.60 MHz (i.e.  $120 \cdot f_0$ ).

The two UHF signals are generated in the satellites as pure sinusoidal waves, known as the carrier. The carrier is then modulated in order to carry information for timing and

ranging. Modulation is a process to alter the identical sinusoidal waves in a certain derivable random-like manner. The binary-phase-shift-keying (BPSK) method, with instantaneous phase changes of  $0^\circ$  and  $180^\circ$ , is the digital modulation technique used in all GPS signals.

The signal modulated on the GPS carrier is a pseudorandom noise (PRN) code. The L1 signal is modulated by two PRN codes, the precise P-code and coarse-acquisition C/A-code. The L2 carrier, on the other hand, only carries the P-code signal.

The C/A-code has 1023 binary bits (or chips) and it is repeated every millisecond. Therefore, it has a wavelength (or chip-length) of 293.3 metres. Due to the frequent repeatability of 1 ms of the C/A-code, a GPS receiver can quickly lock onto the signal and begin matching the received code with a replica generated by the receiver. The chip length of the P-code, on the other hand, is only 29.3 metres long, one tenth of that of C/A-code. A shorter P-code wavelength naturally gives rise to a higher precision measurement. The period of the P-code signal is extremely long compared to that of C/A-code: 266 days (or 37 weeks) versus 1 millisecond.

The P-code is currently transmitted on both the L1 and L2 carriers whereas the C/A-code is transmitted only on the L1. A modulo-2 addition technique combines the two binary data streams from the P- and C/A-code into the L1 carrier. All codes are initialized once per week at Saturday/Sunday midnight, thus effectively creating the GPS week as a major unit of time.

As described above, all the satellites transmit PRN signals on two identical L1 and L2 frequencies. In order for receivers to uniquely identify the origins of signals, the signal of each GPS satellite is differed by code. This is a technique known as the code division multiple access (CDMA). GLONASS, on the other hand, uses the technique of frequency division multiple access (FDMA), which will be discussed in Chapter Three.

### 2.1.2 Code Pseudorange Observation Equation

Ranging determination is made possible through a time delay measurement. It compares a receiver-replicated code against the satellite-transmitted code received by an antenna using an auto-correlation method. The difference between the two is a time offset, the interval of time it takes for a signal to propagate from the satellite antenna to the receiver antenna. This time offset, multiplied by the speed of light, is then the GPS *pseudorange* measurement from the satellite to the receiver. It is referred to as a pseudorange because the receiver clock offset and other errors corrupt the true geometric range.

The pseudorange observation equation is given as follows [Wells et al., 1986]:

$$p = \rho + d\rho + cdt - cdT + lb + dIon + dTrop + \varepsilon \quad (2.1)$$

where,

- $p$  is the measured pseudorange,
- $\rho$  is the true (but unknown) range,
- $d\rho$  is the orbital error along the line of sight from satellite to receiver,
- $cdt$  is the satellite clock offset from GPS Time (GPST),
- $cdT$  is the receiver clock offset from GPST,
- $lb$  is the line bias delay caused by the physical length of the cable,
- $dTrop$  is the tropospheric delay,
- $dIon$  is the ionospheric delay, and
- $\varepsilon$  is the error term which includes measurement noise, multipath, etc.

To define the position for a given receiver, a three-dimensional position vector and a bias in the receiver clock offset must be estimated, requiring pseudoranges to a minimum of four satellites at any given instant. However, with clock aiding, it is possible to navigate with less than four satellites. Augmenting GPS with clock and height constraints require

only as few as two satellites measurements to provide a two-dimensional solution (e.g. [Zhang, 1997]).

### 2.1.3 Solutions and Accuracy from Code Pseudorange

The user equivalent range error (UERE) is a measure of quality of the GPS measurements. Dilution of Precision (DOP), on the other hand, is a measure of the quality of satellite geometry. The accuracy of GPS solutions can then be estimated *a priori* as the product of UERE and DOP. Under normal circumstances, GPS is capable of providing positioning accuracy to some tens of metres and timing accuracy at sub-microsecond level.

Seeing the above mentioned accuracy as a threat to the national security, the US DoD implements a procedure, known as selective availability (SA), to purposely degrade the accuracy provided to civilian users. SA can be implemented through two methods: satellite clock dithering and orbital accuracy degradation. However, only the former, a technique to cause the satellite clock corrections to drift according to a polynomial with fast changing coefficients, has actually been implemented. The only guaranteed limitation to clock dithering SA is that the rate of change of the polynomial will not exceed 2 m/s and the acceleration will not exceed 19 mm/s<sup>2</sup>. With SA implemented, the positioning accuracy of a civilian user is then limited to about 100 m horizontally and 150 m vertically at two-dimensional root-mean-square (RMS), or at a 95% confidence level. This is what GPS, at its cheapest and easiest, is capable of providing. This standard positioning service (SPS) is a committed service provided by US DoD to civilian users worldwide.

There is yet another level of service known as the precise positioning service (PPS), which provides positioning accuracy to better than 30 metres horizontally and vertically at two-dimensional RMS. PPS is available only to some authorized (military) users who can remove the effect of SA through a decryption capability. Encryption is a procedure

in SA and in anti-spoofing (AS) to deny the access of the high precision P-code signal by unauthorized users. AS is done by the US DoD to prevent a deception jammer from broadcasting a beacon that mimics the actual GPS signals. When the P-code is encrypted, it becomes the Y-code. Therefore, a semi-codeless GPS receiver, using a squaring or cross-correlation technique, is required for civilian users to make measurements on the P(Y)-code in differential mode.

The SPS level of accuracy obviously do not serve the requirements of many users. However, it is possible to improve the accuracy of GPS by as many as five orders of magnitude. With Differential GPS (DGPS) where the users have the luxury of employing one or more GPS receivers at some presumably known and fixed locations, the relative positioning accuracy could be improved to the sub-centimetre level. Attitude determination of sub-degree accuracy usually requires the relative vector of the antenna-pair(s) to be determined at a sub-centimetre level.

High accuracy positioning and navigation, therefore, require a better and finer GPS observable in certain applications including attitude determination. GPS *carrier phase* is a more precise observable than its code pseudorange counterpart and therefore it becomes the primary observable in high accuracy applications. In attitude determination however, there is still a role for the code solution to play. Code solution provides the coordinates of the platform with single point accuracy. It also determines the size of the search space in the integer ambiguity resolution process. More importantly, it defines the origin of a local level coordinate system from which the platform attitude is referred to.

The phase of the received carrier is related to the phase of the carrier at the satellite through signal propagation time between the satellite and the receiver. The carrier generated by the satellite nominally has a constant frequency, but the received carrier by the receiver is changing in frequency due to a shift induced by the satellite-receiver relative motion. The beat frequency usually refers to the difference between these two frequencies. This yet another GPS observable, the *Doppler*, is very useful in the velocity

determination of a moving platform, as the range rate is proportional to the Doppler shift of the received carrier frequency. The range rate is the change in the satellite-receiver range over an interval of time divided by the interval.

Given that attitude determination uses the GPS carrier phase as its primary observable, the characteristics of the carrier phase observable will be discussed in greater detail in the following section.

## **2.2 Carrier Phase Observable**

The carrier, as its name suggests, is generated to carry the code and other navigation data. However, it has been discovered since the early GPS development stage that phase measurements on the carrier is much more accurate than pseudorange measurements. One of the reasons contributing to this is that the carrier phase has a significantly lower noise level than the code pseudorange. This is due to the fact that the wavelength of the carrier is several orders of magnitude smaller. The L1 carrier has a typical wavelength of 0.19 metre, given the fact the speed of light is 299 792 458 m/s. A 0.19-metre wavelength is considerably smaller than the 293-metre wavelength for the C/A-code. Therefore, a measurement accuracy of the carrier phase at the millimetre level can be obtainable.

The carrier phase is measured by beating the received Doppler-shifted satellite carrier with a locally generated replica in a GPS receiver. The information in the carrier transmitted by a satellite can be extracted either by complete knowledge of the C/A-code (civilian and military users) and P-code (military users only). As mentioned previously, civilian users who do not have knowledge of the P-code use semi-codeless signal processing technique, such as squaring or cross-correlation, to make measurements on L2.

### 2.2.1 Carrier Phase Observation and Differencing Equations

The equation describing the relationship between the measured phase of the carrier and the spatial distance, in units of length, is as follows [Wells et al., 1986]:

$$\Phi = \rho + dp + \lambda N + cdt - cdT + lb - dIon + dTrop + \epsilon \quad (2.2)$$

where,

- $\Phi$  is the measured carrier phase,
- $\rho$  is the true (but unknown) range,
- $dp$  is the orbital error along the line of sight from satellite to receiver,
- $\lambda$  is the wavelength of the carrier phase,
- $N$  is the carrier phase integer ambiguity,
- $cdt$  is the satellite clock offset from GPST,
- $cdT$  is the receiver clock offset from GPST,
- $lb$  is the line bias delay caused by the physical length of the cable,
- $dTrop$  is the tropospheric delay,
- $dIon$  is the ionospheric delay, and
- $\epsilon$  is the error term which consists of measurement noise and multipath.

The carrier phase measurements can be collected at equally spaced nominal GPST epoch. An observation of the carrier phase observable would be the sum of the total number of full carrier cycles and a fractional cycle between the antennas of a satellite and that of a receiver at any instant. The spatial distance between the two antennas is then an integer number of cycles plus the fractional cycle of the carrier multiplied by the wavelength of the carrier. However, a GPS receiver has no way to distinguish one cycle of the carrier from another and there are effectively millions of cycles between the two antennas considering the distance of the satellites from Earth. The unknown number of cycles is commonly known as the carrier phase integer ambiguity,  $N$ . It must be determined along with other unknowns in order for the measurements to make sense. Chapter Five will

describe the theory of integer ambiguity resolution in the application of attitude determination in greater details.

The negative sign of the  $dI_{on}$  term in Equation (Eq.) (2.2) is due to the dispersive nature of the ionosphere. Thus, it causes the speed of propagation of the carrier to increase, rather than to slow down as in the case of pseudorange. As will be discussed later, the effect of measurement noise and multipath is different on the measured phase than they are on a measured pseudorange.

One effective way to reduce these errors is to difference the measurements between receivers and satellites. Differencing measurements collected simultaneously by two receivers on the same satellite eliminates the satellite clock offset and greatly reduces orbital and atmospheric errors. This process is known as the between-receiver single differencing (SD) method. Similarly, differencing measurements simultaneously collected by one receiver on two satellites eliminate the receiver clock offset. This process is known as between-satellite SD. If the between-receiver SD measurements for two different satellites are further differenced, the process is known as the between-satellite between-receiver double differencing (DD). There is yet another differencing technique, known as the between-epoch differencing, which takes the difference of the same satellite-receiver measurements between two different epochs. The between-epoch differencing cancel neither the receiver nor satellite clocks. However, it does eliminate the integer ambiguity term,  $N$ , provided that no cycle slip occurs between the two epochs.

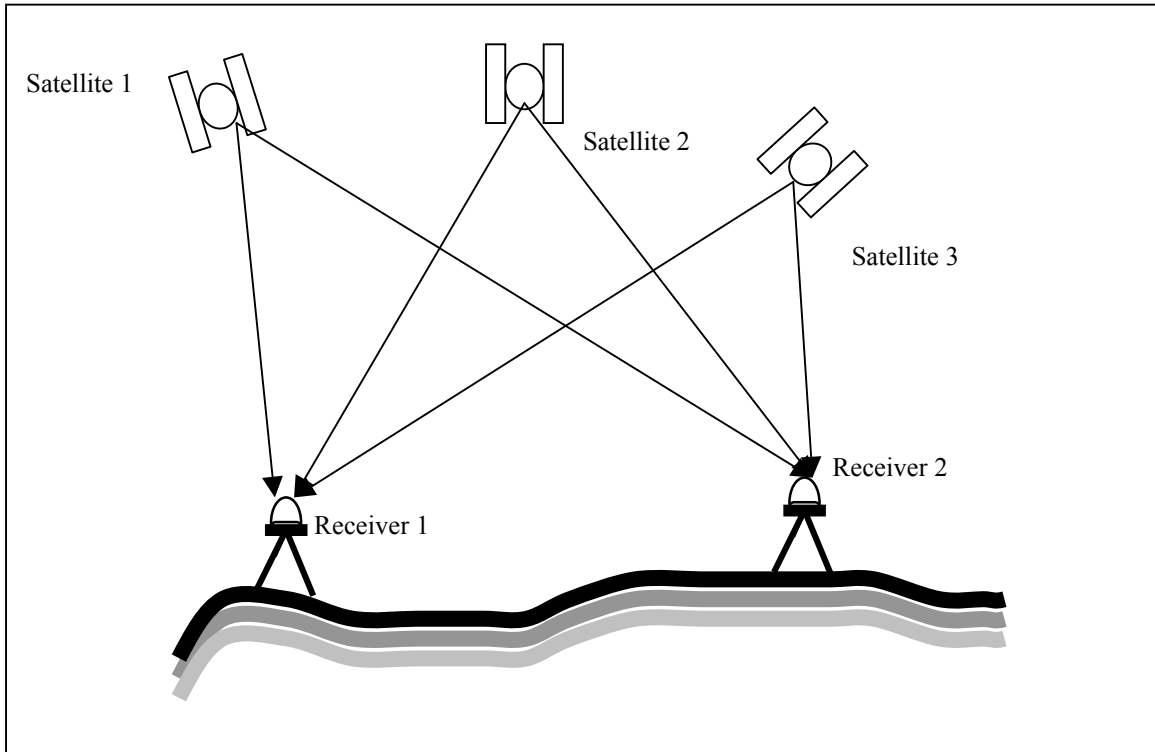


**Figure 2.1: Single Differencing and Double Differencing of GPS Measurements**

The between-receiver SD and the between-satellite between-receiver DD observation equations for carrier phase are usually expressed as follows:

$$\Delta\Phi = \Delta\rho + \Delta d\rho + \lambda\Delta N - c\Delta dT + \Delta lb - \Delta dIon + \Delta dTrop + \Delta\epsilon \quad (2.3)$$

$$\nabla\Delta\Phi = \nabla\Delta\rho + \nabla\Delta d\rho + \lambda\nabla\Delta N + \nabla\Delta lb - \nabla\Delta dIon + \nabla\Delta dTrop + \nabla\Delta\epsilon \quad (2.4)$$

where  $\Delta$  is the operator for between-receiver differencing and  $\nabla$  denotes the operation for between-satellite differencing.  $\delta$  usually refers to the operation that denotes the between-epoch differencing.

The offset errors due to the satellite clock can be eliminated using the technique of between-receiver differencing, and the one due to receiver clock can be eliminated using the technique of between-satellite differencing. The orbital, tropospheric and ionospheric

errors can also be largely reduced after the differencing(s) of the measurements. Short antennas separation in a twin-antenna attitude system offers great advantages for error reduction. The spatially correlated ionospheric and troposphere errors as well as the orbital errors, as indicated in Eq. (2.3) and Eq. (2.4) are virtually eliminated by differencing and their effects on the relative positioning are negligible.

The multipath and measurement noise are the remaining errors that cannot be eliminated or reduced. These errors actually increase with differencing(s). These remaining errors hence determine the ultimate accuracy achievable by an attitude determination system and are discussed in details below.

### **2.2.2 Receiver Measurement Noise**

Receiver measurement noise is generated by the receiver in the process of taking code or phase measurements. It is considered to be white noise for the sampling interval normally present in GPS receivers. There is also no correlated noise between separate measurements taken at the same point in time, because independent tracking loops are used for each separate measurement, and the noise is primarily generated by tracking loop jitter.

A general rule-of-thumb for receiver noise in both carrier phase and code pseudorange is that it is normally well below 0.5% of the observable wavelength. For GPS, noise on C/A-code should therefore be less than 1.5 m and noise on P-code should be less than 0.15 m. For GLONASS, the amount of the code noise can be double the amount. This is due to the fact that the wavelengths of both the GLONASS C/A-code and P-code, as described in Chapter Three, are exactly two times longer than that of GPS. For L1 carrier, the wavelength of both GPS and GLONASS is about 20 cm and thus the carrier phase noise should be less than one millimetre. It is shown in Cannon et al. [1993] that the RMS single difference carrier phase noise for low cost receivers manufactured in the early 90's ranges from 0.9 to 2.0 mm.

The receiver noise can be measured using a “zero-baseline” test. In this test, the satellite signal from a single antenna is split and sent to two different receivers. A DD operation, as described by Eq. (2.4), cancels all the error terms except the measurement noise. For the carrier phase, the integer ambiguities term,  $\nabla\Delta N$ , does not cancel out, but it can easily be determined or simply eliminated by rounding to the nearest integer number. Take note that after DD, the measurement noise also increases by a factor of  $\sqrt{2}$  twice, the true value for the measurement noise is the value obtained from double difference divided by a factor of two.

A zero-baseline test was carried out in order to investigate the noise level of GPS and GLONASS L1 carrier from an Ashtech GG24<sup>TM</sup>, the receiver used for this research. Data was collected for a period of 90 minutes and it was found that for L1 C/A-code, the magnitudes of the noise were 1.1 m and 2.4 m for GPS and GLONASS respectively. The carrier phase noise was found to be 1.1 mm for both GPS and GLONASS. Therefore, it can be concluded that the accuracy of L1 carrier of GLONASS is comparable to that of GPS. Raquet [1998] has also found similar statistics with the Ashtech Z-12: the code measurement noise is of the order of metres while the phase measurement noise is of the order of millimetres. This is in accordance to the fact that, compared to GPS, the wavelength of GLONASS code is twice as long and the wavelength of GLONASS phase is about the same.

Note that when anti-spoofing (AS) is on, receiver noise on the GPS P(Y)-code and L2 carrier phase obtain using a semi-codeless method may be significantly increased. It is also found that the measurement noise is increased as the signal-to-noise ratio (SNR) decreases [Spilker, 1996]. Because the SNR tends to decrease with decreasing elevation, measurement noise can be expected to increase with decreasing in elevation.

### 2.2.3 Multipath

Multipath errors occur when the signal arriving from the satellite at the antenna has travelled more than one path. This results in the received signal being split in a direct line of sight signal and one or more others of different pathlengths. The difference in pathlengths causes the signals to interfere among themselves at the antenna thereby corrupting the ranging information brought by the direct line of sight signal. There are two different kinds of multipath, namely, the satellite multipath and the receiver multipath. The satellite multipath is the different propagation paths resulting from the reflection at the transmitting GPS satellite in space, whereas the receiver multipath is the one resulting from the reflection in the surrounding of the receiver antenna. The one that is commonly known to the user is the receiver multipath as the effect of satellite multipath is effectively eliminated in DGPS, including in attitude determination which utilizes short baselines. This is due to the fact that the effect of satellite multipath is virtually identical for the receivers within the same area [Georgiadou & Kleusberg, 1988]. The multipath signal and direct line-of-sight signal are shown in Figure 2.2.

The effect of multipath is indeed site dependent. Different sites generally exhibit different effects of multipath. To be exact, the occurrence of multipath depends on the reflectivity of the antenna environment, i.e., the satellite-reflector-antenna geometry. Therefore, if the position and orientation of the antenna remain constant, the effect of multipath reoccurs exactly after one sidereal day. A sidereal day is about 4 minutes less than a solar day. The period of a GPS satellite is exactly one half of a sidereal day and this is the reason why, after one sidereal day, the satellite-reflector-antenna geometry repeats itself. Thanks to this characteristic, users are able to investigate the effect of the multipath at a particular site over a long enough period of time. The results and analyses of a repeatability test are presented in Chapter Five to assess the effect of GPS/GLONASS multipath on attitude parameters.

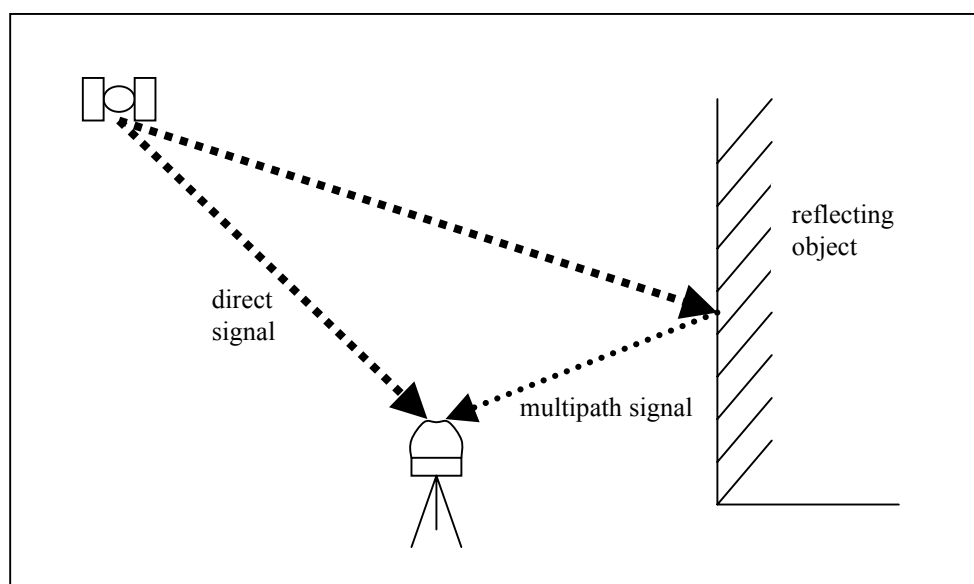


**Figure 2.2: Receiver Multipath from Satellite**

Multipath is notorious as it affects the pseudorange and the carrier phase in both absolute and differential modes of GPS operations. Even the most advanced military users have no alternative but to deal with it.

Strictly speaking, the code multipath especially in a static environment may not be a zero mean process [van Nee, 1994]. However, the effect of multipath in kinematic applications, when averaged over a long enough time for the relative phase of the direct and reflected signals to have changed by at least one cycle, will be considerably reduced [Langley, 1996]. Along the same argument, Cannon & Lachapelle [1992] assumed that code kinematic multipath behaves in a random manner with a zero mean over a sufficiently long enough periods and hence could be averaged out. For the carrier phase multipath, Georgiadou & Kleusberg [1988] showed that a theoretical maximum of a quarter of the cycle of the wavelength, which is about five cm at the L1 frequency, is obtained.

Phase centre variation of the antenna, unlike multipath, is independent of the site environment. The variation of the phase centre is due to the non-spherical pattern of the

phase of the antenna. Therefore, Tranquilla [1986] argued that the term “phase centre” is actually misleading. A more appropriate term for describing the measuring centre of an antenna would be the “centre of the best-fit-sphere” as the term “phase centre” has a rigorous meaning of referring to the centre of the curvature of the non-spherical phase pattern. A result of the non-spherical pattern of the antenna is that the centre point of the measured phase of the same signal varies in space as the signal comes in at different azimuth angles as well as elevation angles. For the accuracy obtained by differential code measurements, the error induced by the variation of the phase centre is certainly negligible. This is especially true in current technology where the magnitude of the error for the average quality antennas is at the millimetre level. For attitude determination requiring a high level of accuracy however, error due to phase centre variation of the antenna could be significant. One solution is to use the same model antennas in the attitude system and to place them in the same azimuth. By performing a between-receiver differencing operation, the error due to phase centre variation can then be effectively removed.

Imaging, the twin of multipath, is an interference effect of the signal due to the existence of nearby “unfriendly” obstacles. It is one of the errors, in addition to the phase centre variation, originating at the GPS antenna. The occurrence of imaging results from the changes in the antenna phase pattern induced by objects in the immediate vicinity of the antenna [Tranquilla, 1986]. These objects produce an “image” of the antenna and this causes the change of the amplitude and phase characteristics of the antenna as it is no longer an isolated antenna. The pattern of the antenna would be deformed to the one formed from the combination of the antenna and its image. Therefore, it also can be seen as an environmentally induced phase centre variation [Georgiadou & Kleusberg, 1988].

Similar to the effect of multipath, the effect of antenna imaging will repeat itself after exactly one sidereal day if the position and orientation of the antenna remain unchanged. It is suspected that the characteristics of the error due to imaging are comparable to that due to phase centre variation [Georgiadou & Kleusberg, 1988]. The effects of the phase

centre variation and the antenna imaging cannot easily be averaged out over long period of time.

Scattering is another phenomenon related to multipath. It is caused by the interference of the incoming signal. It has been reported that a GPS signal scattered from the surface of a pillar on which a GPS antenna is mounted interferes with the direct signal. According to [Langley, 1996], the error in signal scattering depends on the elevation angle of the satellite, and varies slowly with elevation angle and time. It does not necessarily cancel out by having different antenna set-ups and/or baseline lengths, and hence may introduce systematic error at the centimetre level.

As will be shown in Chapter Five, the effect of multipath, perhaps together with the errors described above, typically reaches 1-2 cm. This level of relative positioning accuracy translates to an accuracy of  $0.1^\circ$  in attitude determination with a one-metre antenna baseline length used. Carrier phase multipath therefore remains the most dominant error source for attitude determination. A more detailed discussion of carrier phase multipath can be found in [Braasch, 1996] and [van Nee, 1994].

#### **2.2.4 Other Errors**

Besides measurement noise and multipath error, the residual errors of troposphere and ionosphere after differencing may still affect the process of ambiguity resolution to a certain degrees.

The troposphere is the portion of the atmosphere from the ground extending up to 60 km above the surface of the Earth. A tropospheric error refers to a refraction delay of the satellite signal when the signal travels through the troposphere entering the Earth from space. Normally, around 10-20% of the delay is due to the wet portion of the troposphere, which is contained within the first 10 km. This is also the most difficult portion to model as it is effected by weather patterns, temperatures, pressure, humidity,

and satellite elevation. At low satellite elevations, the tropospheric error can reach up to 30 m.

As mentioned earlier, differencing measurements between receivers over short baselines practically removes the tropospheric error. Even for short baselines however, if the height difference between the two antennas is significantly different, the tropospheric errors can have a significant impact in the integer ambiguity resolution process. For baselines of a few metres, the residual after modelling is however negligible.

There are several models available to estimate the tropospheric errors. The best known models are the Hopfield model [Hopfield, 1969], the modified Hopfield model [Goad and Goodman, 1974], and the Saastamoinen model [Saastamoinen, 1973]. Goad and Goodman [1974] has shown that the modified Hopfield model gives the best results for low elevation satellites and all other models should give similar results for satellites above 20 degrees.

The effect of the troposphere on carrier phase positioning and residuals is demonstrated in Tiemeyer et al. [1994] and Zhang [1999]. It was also shown that an unmodelled troposphere could contribute up to several centimetres to the carrier phase residuals when using DGPS and for a distance larger than a few km between the receivers. When no tropospheric modelling was implemented, incorrect ambiguity of a new satellite entering the solution would be found even though all of the other ambiguities were correct before a new satellite arose. An approach to estimate the tropospheric delay of a new rising satellite using data from a wide area GPS network has been successfully developed by Zhang [1999].

The ionosphere is the portion of the atmosphere in which free ionized electrons exist. It is above the troposphere and can extend up to 1000 km above the surface of the Earth. Unlike the troposphere, the effects of the ionosphere on radio waves with frequencies greater than 100 MHz include group delay, carrier phase advance, polarization rotation,

angular refraction, and amplitude and phase scintillation [Skone, 1998]. The most significant factors affecting the ionosphere include the time of day, time of year, solar cycle of 19.6 years, and the geomagnetic latitude. The solar cycle was at minimum in 1995 while the solar maxim is expected to occur in 2001, which may have a significant impact on some high precision GPS applications.

The group delay, which is equal in magnitude to the phase advance, is directly proportional to the total electron content and inversely proportional to the frequency squared. The total electron content varies with the local time, weather, solar cycle, geomagnetic latitude, and sunspot activity [Skone, 1998].

The ionospheric error can be handled in one of three ways. Firstly, if differenced observations are used, the error is significantly reduced, depending on the baseline length. Secondly, an ionospheric correction is broadcast with the almanac data that can be used by single frequency users. Finally, given that GPS signals are dispersive in ionosphere, the ionospheric free observations can be computed if dual frequency receivers are available [Leick, 1995].

The equation for an ionospheric-free pseudorange in a dual-frequency receiver is as follows [Leick, 1995]:

$$p_{L1,L2} = \frac{f_{L1}^2}{f_{L1}^2 - f_{L2}^2} p_{L1} - \frac{f_{L2}^2}{f_{L1}^2 - f_{L2}^2} p_{L2} \quad (2.5)$$

where,

- $p_{L1,L2}$  is the ionospheric-free pseudorange measurement,
- $f_{L1}$  is the frequency for L1 carrier (1575.42 MHz),
- $f_{L2}$  is the frequency for L2 carrier (1227.60 MHz),
- $p_{L1}$  is the pseudorange measurement on L1, and
- $p_{L2}$  is the pseudorange measurement on L2.

The ionospheric-free phase can also be computed as follows [Leick, 1995]:

$$\Phi_{L1,L2} = \frac{f_{L1}^2}{f_{L1}^2 - f_{L2}^2} \Phi_{L1} - \frac{f_{L2}^2}{f_{L1}^2 - f_{L2}^2} \Phi_{L2} \quad (2.6)$$

where,

- $\Phi_{L1,L2}$  is the ionospheric-free carrier phase measurement,
- $\Phi_{L1}$  is the carrier phase measurement on L1, and
- $\Phi_{L2}$  is the carrier phase measurement on L2.

In the case that a dual frequency receiver is not available, the differencing technique is generally used to reduce the ionospheric error. If the separation between the two receivers is, for e.g., larger than 30 km, the differencing technique may not be adequate to reduce the ionospheric error [Neumann et al., 1996]. In that case, ionospheric-free observables are often used in combination with a differencing technique. Aside from the increased noise of the ionospheric-free phase, one major drawback is that the ambiguities no longer retain their integer properties. Thus, the ambiguities can only be estimated as floating numbers. In the case of attitude determination where the inter-antenna distances are typically metres apart, the differencing technique is adequate in practically eliminating the ionospheric error.

## CHAPTER THREE

### GLONASS: CHARACTERISTICS AND DIFFERENCES WITH GPS

This chapter describes the GLONASS system. First, it presents an overview of GLONASS with some of its unique characteristics. It then addresses the major differences between GLONASS and GPS: in time and coordinate referencing and in signal multiplexing. The FDMA related problems in GLONASS are presented in details and two corresponding solutions are discussed. The future of GLONASS is also briefly discussed at the end.

#### 3.1 Overview of GLONASS

Similar to GPS in many aspects, GLONASS or the Global Navigation Satellite System (translation from *Global'naya Navigatsionnaya Sputnikovaya Sistema*) offers users continuous worldwide three-dimensional positioning and navigation services at no cost. Developed and administrated by the Russian Military Space Forces (VKS, which is the acronym of Russian *Voенно-Kosmicheski Sily*) at its Department of Defence, GLONASS was not available to the civilian users until the very late 80's. Since then, GLONASS serves as a great tool to the new and existing GPS users. Civilian users can obtain official information about the general descriptions of GLONASS from the VKR operated Coordination Scientific Information Centre (KNITs, which is the acronym of Russian *Koordinatsionny Nauchno-Informatsionny Tsentr*) in Russia. There is an English GLONASS page in the official website of KNITs at <http://www.rssi.ru/>.

The Russian authority, for the first time, released the Interface Control Document in 1995 (ICD-95) [KNITs, 1995]. This document describes the system, its components, and the signal structures and the navigation message of GLONASS to the users. The document states that this version of the ICD-95 “was produced with the purpose of contributing to the development of global navigation satellite system(s) Standards and Recommended Practices”. In early 1998, an English Version 4.0 of ICD-98 was published to replace the ICD-95 [KNITs, 1998]. The 44-page ICD-98 provides further up-to-date details on GLONASS and a clearer direction of the system. A 5-page list of changes/corrections/comments to ICD-98 was revealed in April 1999. The list eliminates some inconsistencies in designations of parameters given in the two ICDs. It provides clarifications on some parameters, misprints, and vague statements that appeared in ICD-98.

### **3.1.1 Satellites, Control, and Users Components**

The system of GLONASS includes three components:

- constellation of satellites (space segment equivalent of GPS);
- ground-based control facilities (control segment equivalent of GPS); and
- users equipment (users segment equivalent of GPS).

A full constellation of GLONASS consists of 21 active plus 3 spare satellites. These satellites are evenly spaced in three orbital planes, separated from each other by 120 degrees. The satellites within a plane are also evenly separated by an argument of latitude of 45 degrees. Satellites in adjoining planes, on the other hand, are shifted in argument of latitude by 15 degrees. The satellites are placed into planes with target inclination of 64.8 degrees, considerably higher than that of GPS. GLONASS orbits are also highly circular with eccentricities smaller than that of GPS and closer to zero. The satellites have a radius of 25,510 km, which gives an altitude of 19,130 km [KNITs, 1998].

The GLONASS orbit planes are numbered one to three and contain orbital slots 1-8, 9-16, and 17-24, respectively. The satellites are sent up to three at a time by the Proton DM (SL-12) booster from the Baikonur Cosmodrome near Leninsk in Kazakhstan. Compared to GPS, GLONASS has a shorter orbital period (11 hours 15 minutes 44 seconds) due to its lower altitude. The ground tracks of the satellites therefore repeat themselves after a long 17-revolution (eight sidereal days) period. Besides capable of broadcasting radio-navigation signals, each GLONASS satellite also carries a laser ranging retro-reflector for satellite time synchronization, precise orbit determination and other geodetic research applications [Langley, 1997].

Table 3.1 summarizes some of the important features of the space segment, for GLONASS and GPS. Shown in Figure 3.1 is the satellite constellation of GPS and GLONASS. Figure 3.2 shows the location of GLONASS satellites as of October 1999. As can be seen in Figure 3.2, there are only less than half of the full satellite constellation (11 healthy satellites) at time of writing.

**Table 3.1: GLONASS / GPS Comparison in Space Segment**

	GLONASS	GPS
No. of satellites	24	24
Launch vehicle	Proton K/DM-2	Delta 2-7925
No. of satellites / launch	3 (occasionally 2)	1
Launch site	Baikonur Cosmodrome, Kazakstan	Cape Canaveral, US
No. of orbital planes	3	6
Orbital inclination	64.8°	55°
Orbit altitude	19,130 km	20,180 km
Period of revolution	11h 15m 40s	11h 58m 00s

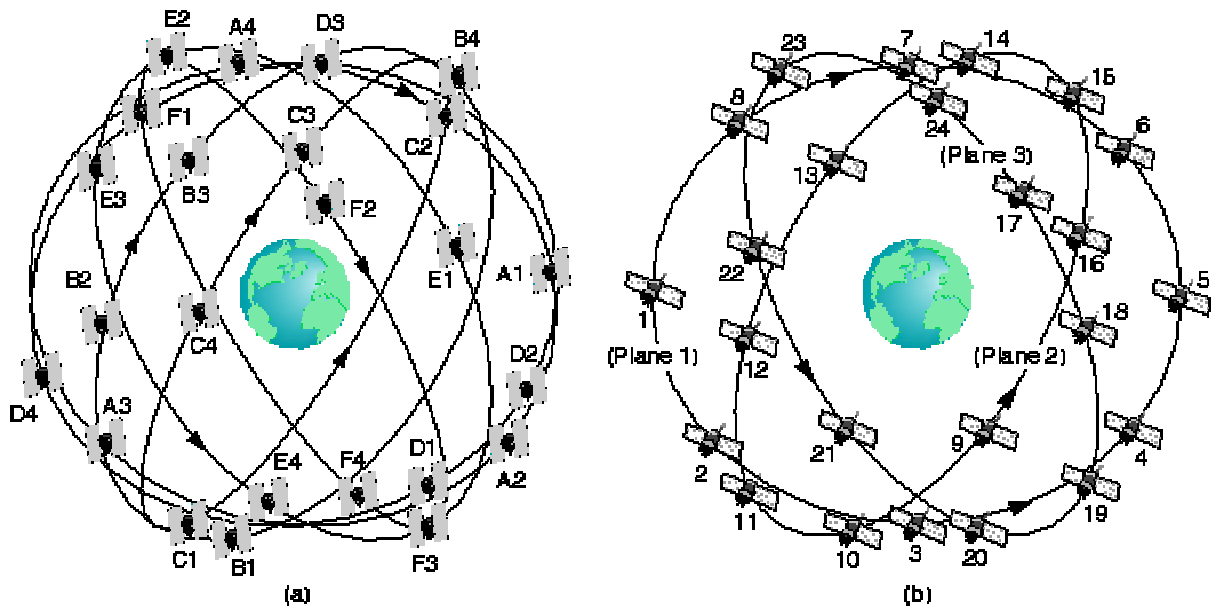


Figure 3.1: (a) GPS and (b) GLONASS Satellite Constellation

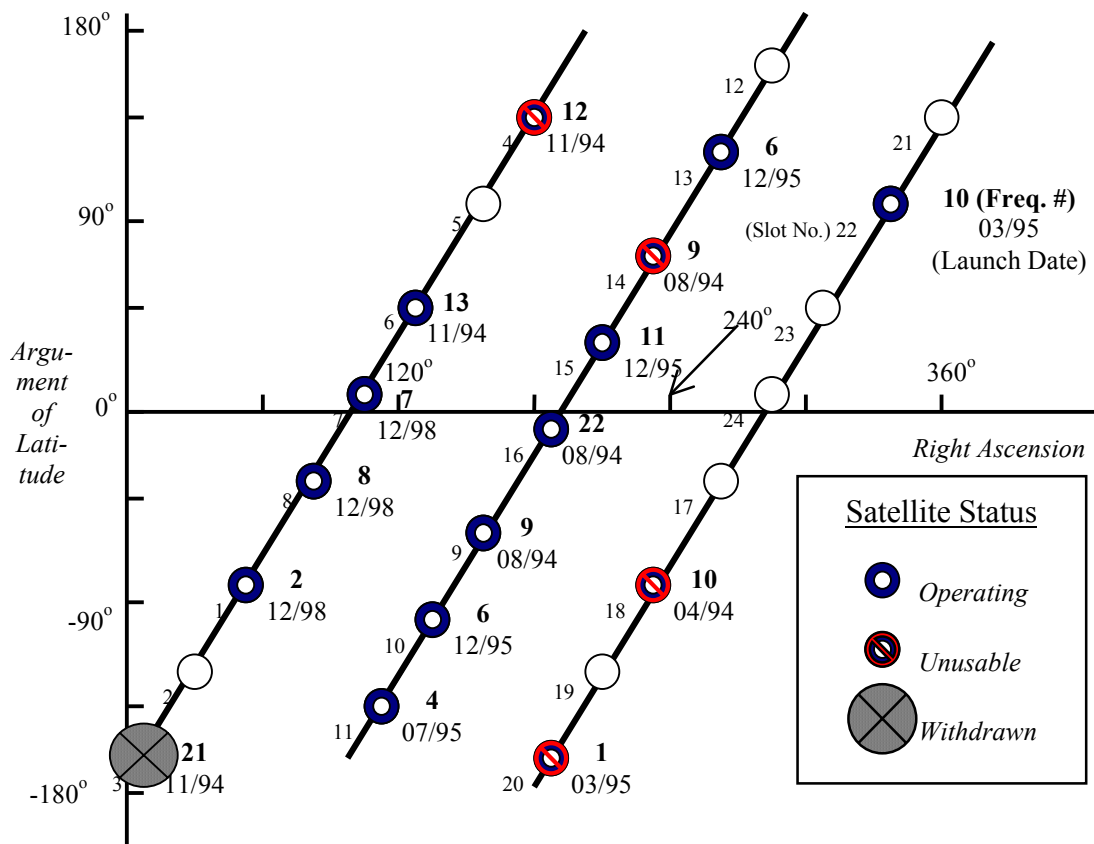


Figure 3.2: Location of GLONASS Satellites in October 1999

Referred to as the ground-based control facilities, the control segment of GLONASS consists of the system control centre (SCC) in Moscow and a network of several command tracking stations (CTS) in the former Soviet Union (SU) territories. SCC and CTS have functions similar to the GPS master control station in Colorado Springs and the other four monitor stations in the US territories. The control segment monitors, among others, the status of all the GLONASS satellites. It determines the ephemerides and satellite clock offsets with respect to GLONASS time and the Russian National Etalon time scale. It also provides uploads of the navigation data to the GLONASS satellites. Different from GPS which uploads its navigation data to the satellites once per day, uploads for GLONASS occur twice per day. Therefore technically speaking, the GLONASS ephemerides should be more precise than that of GPS.

Military and civil users constitute the user segment. The military has been playing a significant role in the use of the system even up until the 90's when the number of civilian users started growing. The first commercial GLONASS civilian receivers did not appear until the early 90's. Unlike GPS receivers that have been commonly available in a wide range of selections, the selection of GLONASS receivers have been quite limited. This is particularly true for low cost and average quality receivers, which is the reason for its growth. The lack of readily available GLONASS receivers at costs comparable with GPS unit posed a stumbling block to the widespread use of the system [Langley, 1997].

### **3.1.2 Performances: Visibility, Accuracy, and Coverage**

The GLONASS system began in 1982 with its first satellite launched in August 30 that year. A full constellation of 24 satellites was reached on Jan 18, 1996. The Russian authority, for one reason or another, has failed to maintain the full constellation after a year [Holmes et al., 1998]. A possible lack of funding for launches together with an aging satellite population put the system operating with 10 to 16 healthy satellite since September 1997. Another explanation for lack of urgency to launch new satellites

thereby maintaining a full constellation is that most of the current satellites are operating well (with more than 80% of Russia covered) even though many of them have exceeded their design lifetime of three years. Figure 3.3 shows that the number of GLONASS satellites is always two to four lesser than the number of GPS satellites in the Boston area at 42.5° N latitude and 71.3° W longitude.

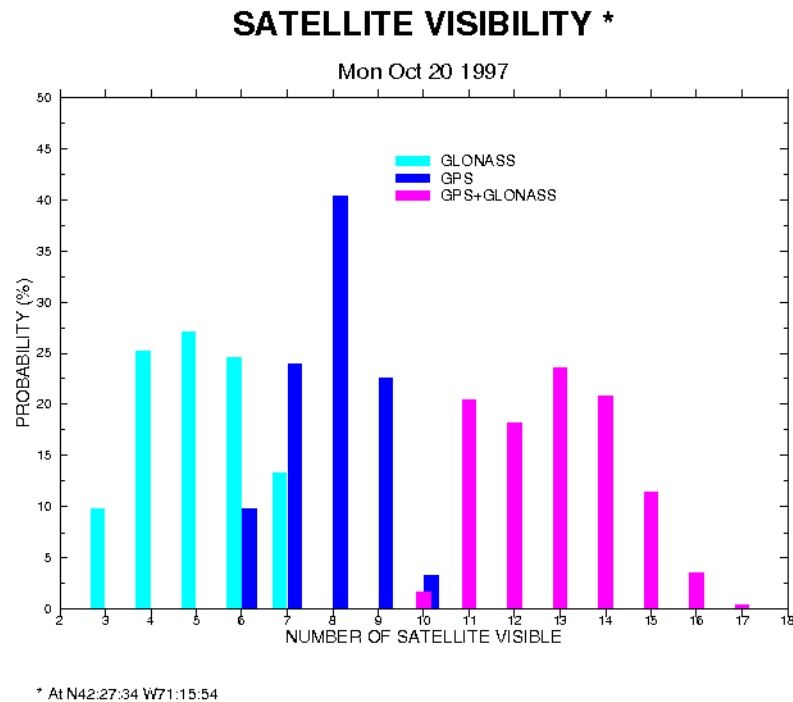


**Figure 3.3: GPS and GLONASS Satellite Visibility on October 1999**

Despite some of the less-than-encouraging news from the recent GLONASS constellation, there is however a number of inherent advantages GLONASS has over GPS. The most beneficial one is that GLONASS has no SA or any other technique implemented to purposely degrade its ranging accuracy. No SA mode in GLONASS played an important role in many stand-alone GLONASS applications. In terms of accuracy, the UERE of GLONASS has been reported at 10 metres level [Daly & Misra,

1994]. Compared to the 25 metres UERE from GPS with SA on (7 metres UERE with SA off), GLONASS is advantageous. It is hence able to meet the requirements of many users in Russia and worldwide. In terms of coverage, users in higher latitude areas, such as Canada, obtain better GLONASS derived dilution of precision (DOP) than that of GPS. This is due to the high inclination angle of GLONASS: 64.8 degrees compared to 55 degrees for GPS.

### **3.1.3 Carrier Frequencies**

Currently, the system transmits the signals within two bands: L1 sub-band (from 1602.5-1616 MHz, with frequencies spaced by 0.5626 MHz) and L2 sub-band (from 1246.4-1256.5 MHz, with frequencies spaced by 0.4375 MHz). This arrangement provides 25 channels at each sub-band such that each satellite in the full 24-satellite constellation could be assigned a unique frequency (with the remaining channel reserved for testing). Such a technique characterizing simultaneous multiple access/transmission is known as frequency division multiple access (FDMA). This FDMA signal multiplexing technique distinguishes GLONASS from GPS, which uses a code division multiple access (CDMA) technique.

Some of the GLONASS L1 sub-band transmissions, however, were found to cause interference to radio astronomers, who study very weak natural radio emissions in the vicinity of the GLONASS frequencies. Radio astronomers use the frequency bands of 1610.6-1613.8 and 1660-1670 MHz to observe the spectral emissions from hydroxyl radical clouds in interstellar space. The International Telecommunications Union (ITU) in the early 90's has given the radio astronomers primary user status for this spectrum space [Langley, 1997]. The ITU also has allocated the 1610-1626.5 MHz band to operators of low-Earth-orbiting mobile communication satellites. As a result, the GLONASS authorities, working with the ITU, have decided to reduce the number of frequencies used by the satellites and shift the bands to slightly lower frequencies [KNITs, 1998].

Eventually, the system will use only 12 primary frequency channels (plus two additional channels for testing purposes). The bands will be shifted to 1598.0625 – 1604.25 MHz for L1 and 1242.9375 – 1247.75 MHz for L2. In order to accommodate 24 satellites in 12 channels, antipodal technology must be used for two satellites to share the same channel. By having satellites in the same orbit plane separated by 180 degrees in argument of latitude. This approach is quite feasible because a user at any location on or near Earth will never simultaneously receive the signals from such a pair of satellites at any time.

The reallocation to new frequency assignments started in September 1993 with the initial pairing of satellite channels. As can be seen in Figure 3.2, several pairs of satellites share currently channels. The current and future GLONASS frequency channels can be formulated as follows [KNITs, 1998]:

$$\begin{aligned} f_{L1} &= 1602 \text{ MHz} + k \cdot 0.5625 \text{ MHz} \\ f_{L2} &= 1246 \text{ MHz} + k \cdot 0.4375 \text{ MHz} \end{aligned} \quad (3.1)$$

where,  $k$  is the channel number.

The plan stated in ICD-98 is that up until 1998,  $k$  in Eq. (3.1) ranges from 0 to 24 (0 for testing). From the period of 1998 – 2005,  $k$  ranges from -7 to 12. After 2005,  $k$  ranges from -7 to 6 (with 5 and 6 for testing) to avoid using frequency beyond 1610 MHz. However, there is yet a reallocation of frequency to occur and  $k$  still ranges from 0 to 24 at the present time of writing (October 1999). No official information has been released by the Russian authority in relation to the current status on reallocation of the GLONASS carrier frequencies.

The wavelength of the carrier is useful to understand in many applications. For GPS, it is shown in Chapter Two that the L1 carrier has a wavelength of 19 cm. For GLONASS however, the wavelengths of the L1 carrier are different for each GLONASS satellite due

to the different frequencies used. An understanding of the magnitude of the wavelength differences within the L1 carrier sub-band is crucial for ambiguity resolution. Looking at the largest separation within the L1 sub-band, an 18.71-cm wavelength for 1602.5 MHz frequency (minimum) and an 18.55-cm wavelength for 1616 MHz frequency (maximum) occurs. The wavelength difference between the two extremes is 0.15 cm in length, which is less than 0.01 L1 cycle.

GLONASS satellites transmit two types of signals, namely, standard precision (SP) and high precision (HP). GLONASS transmits the P-code HP signal on both L1 and L2, with the C/A-code SP only on the L1. The C/A-code of GLONASS is 511 chip long with a rate of 511,000 chip per second, giving a repetition interval of 1 millisecond with a wavelength of 586.7 metres. The P-code is 33,554,432 chip long with a rate of 5,110,000 chips per second, giving a wavelength of 58.7 metres. The code sequence is truncated to give a repetition interval of one second. The wavelengths of the two pseudorandom noise codes of the GLONASS signal are about twice that of GPS, giving noisier measurements, which reflects in the results shown in Chapter Two. Unlike GPS satellites, all GLONASS satellites transmit the identical code pattern. The timing and frequency references of the signals are derived from one of three onboard cesium atomic clocks operating at 5.0 MHz. The signals are right-hand circularly polarized, like GPS signals, and have a comparable signal strength.

### **3.2 Difference between GPS and GLONASS**

GPS and GLONASS are two autonomous systems, each with its own time scale and coordinate frame from which a three-dimensional time-varying position can be reference to. Upon combining GPS and GLONASS, some of the differences between GPS and GLONASS may have to be accounted for. These major differences can be found in the time reference system, the coordinate reference system, and the signal multiplexing technique.

### 3.2.1 Time Reference Systems

GLONASS uses the Universal Coordinated Time, Soviet Union (UTC\_SU) standard as its reference time frame [KNITs, 1998]. The Russian National Time and Frequency Services maintains the UTC\_SU standard. UTC\_SU is synchronized to the international standard of UTC, UTC\_BIPM (*Bureau International des Poids et Mesures*) within one microsecond after an adjustment of nine microseconds was made in 1996 [KNITs, 1998].

GLONASS Time (GLONASST) is the time standard for the system. It has an exact offset of three hours from UTC\_SU due to the geographic location of Moscow. The offset between the GLONASST and the UTC\_SU is known to 50 nanoseconds. GPST, on the other hand, is referenced to the UTC standard maintained by United States Naval Observatory (USNO), UTC\_USNO. The uncertainty between the UTC\_SU and UTC\_USNO is about 50 nanoseconds. GPST is accurate to UTC\_USNO to the nanosecond level.

GLONASS satellites are equipped with Cesium clocks onboard to provide time and frequency standards. The Cesium clocks have daily frequency stabilities of  $5 \cdot 10^{-13}$ . With the clock corrections uploaded to satellites twice a day, this Cesium standard provides an accuracy of satellite time synchronization relative to GLONASST to about 15 nanoseconds at one sigma level. GLONASST is generated by the central synchronizer (CS) time. Daily stabilities of the CS Hydrogen clocks are one order of magnitude better than the Cesium, at about  $5 \cdot 10^{-14}$ . The absolute difference of GLONASST relative to UTC\_SU is always less than one millisecond. The accuracy of the difference is always known to sub-microsecond level [Gouzhva et al., 1992].

The fundamental time scale for all the time keeping standard on Earth, including all the UTC, is the International Atomic Time (TAI). TAI is a continuous time scale and hence it has two inherent problems in practical use: its scale is slightly different from that of the

Earth's rotation and the Earth's rotation with respect to the sun is slowing down by a small amount. Thus UTC, which runs at the same rate as TAI, would eventually become inconveniently out of synchronization with the solar day. This problem has been overcome by introducing 1-second jumps, known as leap seconds, to UTC each time when necessary at the end of either June or December.

GLONASST follows when UTC is incremented by a leap second. Therefore, there is no integer-second difference between GLONASST and UTC. However there is a constant offset of three hours between GLONASST and UTC\_SU due to the geographic location of the GLONASS SCC. GPST, on the other hand, is not incremented by leap seconds. There are hence an integer-second differences, which will be increasing as time goes, between GPST and UTC (also GLONASST). The following equations depict the relationships among GPST, UTC, GLONASST, and TAI:

$$\text{GLONASST} = \text{UTC} + 03 \text{ h } 00 \text{ m } 00 \text{ s} \quad (3.2)$$

$$\text{GPST} - \text{UTC} (\cong \text{GLONASST} - 3 \text{ h}) = +13 \text{ s (at time of writing)} \quad (3.3)$$

$$\text{TAI} - \text{UTC} = +32 \text{ s (at time of writing)} \quad (3.4)$$

$$\text{TAI} - \text{GPST} = +19 \text{ s (at any instant)} \quad (3.5)$$

Users interested in the integrated use of GPS/GLONASS must be able to determine the instantaneous time scale difference between the two. The problem can be thought of as estimating a position from two sets of pseudoranges, each with an unknown clock bias, and hence giving five unknowns in all. Obviously, one of the two systems could carry information about the difference in time scales in the navigation messages. Before this information is available in real time, users could solve for this additional unknown by “sacrificing” a measurement. The integrated use of GPS and GLONASS offers amply redundant measurements, and the additional unknown does not usually create a problem.

### 3.2.2 Coordinate Reference Systems

The coordinate reference system for GLONASS, since 1993, is the so-called Parameters of the Earth 1990 System (PZ90, which is the acronym of Russian *Parametry Zemli 1990*). Similar to World Geodetic System 1984 (WGS84), the reference system for GPS, PZ90 is an Earth-Centred Earth-Fixed (ECEF) terrestrial frame. An ECEF is a non-inertial system, i.e. it is fixed to the Earth and rotates with it, and its origin is at the centre of the mass of the Earth. It is the closest practical approximation of the geocentric natural system and is probably the most important system in geodesy [Vaníček & Krakiwsky, 1986]. The PZ90 however, adopts a set of different parameters from that of WGS84. The realization of the system is also different from WGS84. PZ90 is accomplished through a network of geodetic points in the former SU territories. Table 3.2 lists the values of some of the defining parameters of PZ90 [KNITs, 1998].

**Table 3.2: Defining Parameters of the PZ90**

Parameter	Value
Earth rotation rate	$7.292115 \cdot 10^{-5}$ radians/second
Gravitational constant	$3.9860044 \cdot 10^{14}$ metre <sup>3</sup> /second <sup>2</sup>
Gravitational constant of atmosphere	$3.5 \cdot 10^8$ metre <sup>3</sup> /second <sup>2</sup>
Speed of light	299 792 458 metres / second
Second zonal harmonic of the geo-potential	$-1.08262 \cdot 10^{-3}$
Ellipsoid semi-major axis	6 378 136 metres
Ellipsoid flattening	1 / 298.257
Equatorial acceleration of gravity	978 032.8 mgal
Correction to acceleration of gravity due to atmosphere	-0.9 mgal

An offset in origin and a difference in scale and orientation exist between PZ90 and WGS84. These are due to the fact that PZ90 adopts some different defining parameters and that it is realized on a set of different points than WGS84. Combining measurements from GPS and GLONASS therefore requires the users to estimate a transformation between the two frames. Several research groups have estimated the transformation parameters between WGS84 and PZ90. However, the findings from these groups vary from one to another due to, beside others, the limited number of measurements available. Investigations into the transformation parameters between the two systems can generally be done by two approaches. Using the baseline approach, one may use GLONASS receivers to compute the PZ90 baseline vectors on a number of known WGS84 sites or vice versa. Alternatively, one may use the orbital approach to inter-compare the satellite orbital coordinates of GPS or GLONASS in the two reference frames.

The transformation parameter set adopted in this research is the one reported by Rossbach et al. [1996]. A rotation of 0.33 arcsecond about the z-axis is required to transform the coordinates in PZ90 to WGS84. Dual frequency GPS/GLONASS receivers capable of tracking the GLONASS high precision P-code signals are located in six geodetic sites in Europe, including one in Russia, to collect measurements for the determination process. The researchers determined the transformation parameter between PZ90 and the International Terrestrial Reference Frame 1994 (ITRF94) using the baseline approach. The assumption made is that ITRF94 is identical to WGS84, which is not exactly the case as can be seen later. The transformation equation reported by Rossbach et al. [1996] is as follows:

$$\begin{bmatrix} x \\ y \\ z \end{bmatrix}_{WGS84} = \begin{bmatrix} 1 & -1.6 \cdot 10^{-6} & 0 \\ 1.6 \cdot 10^{-6} & 1 & 0 \\ 0 & 0 & 1 \end{bmatrix} \begin{bmatrix} u \\ v \\ w \end{bmatrix}_{PZ90} \quad (3.6)$$

The rotation of  $1.6 \cdot 10^{-6}$  radian, or 0.33 arcsecond, gives a displacement of about 10 metres along the equator. Rossbach et al. [1996] also estimated seven- and four-

parameter transformations using the baseline approach, but conclude that the additional estimated transformation parameters are not statistically significant.

Another transformation relating PZ90 and WGS84 that has been widely used in practice is the one reported by Misra et al. [1996]. The scarcity of a widely distributed GLONASS receiver reference network leads the researchers to use the orbital approach. Rather than relating the coordinates of receivers on the Earth's surface in the two systems as in [Rossbach et al., 1996], they relate the orbital positions of two GLONASS satellites expressed in the two systems.

The positions of the satellites in the PZ90 frame are obtained from the broadcast ephemerides and those in the WGS84 frame are obtained from a global network of tracking stations. Estimates of one-, two-, four- and seven-parameter transformations reveal that only a rotation of 0.4 arcsecond about the z-axis and possibly a 2.5 metres upward shift along the y-axis is statistically significant. The major source of errors in the transformation determination process is likely to be the broadcast GLONASS ephemerides. The transformation equation reported by Misra et al. [1996], in unit of metres and radians, is as follows:

$$\begin{bmatrix} x \\ y \\ z \end{bmatrix}_{WGS84} = \begin{bmatrix} 0 \\ 2.5 \\ 0 \end{bmatrix} + \begin{bmatrix} 1 & -1.9 \cdot 10^{-6} & 0 \\ 1.9 \cdot 10^{-6} & 1 & 0 \\ 0 & 0 & 1 \end{bmatrix} \begin{bmatrix} u \\ v \\ w \end{bmatrix}_{PZ90} \quad (3.7)$$

Figure 3.4 shows the same transformations between PZ90 and WGS84. To transform a set of PZ90 coordinates to WGS84, a rotation of 0.4 arcsecond about the z-axis and a 2.5 metres upward shift along the y-axis is needed.

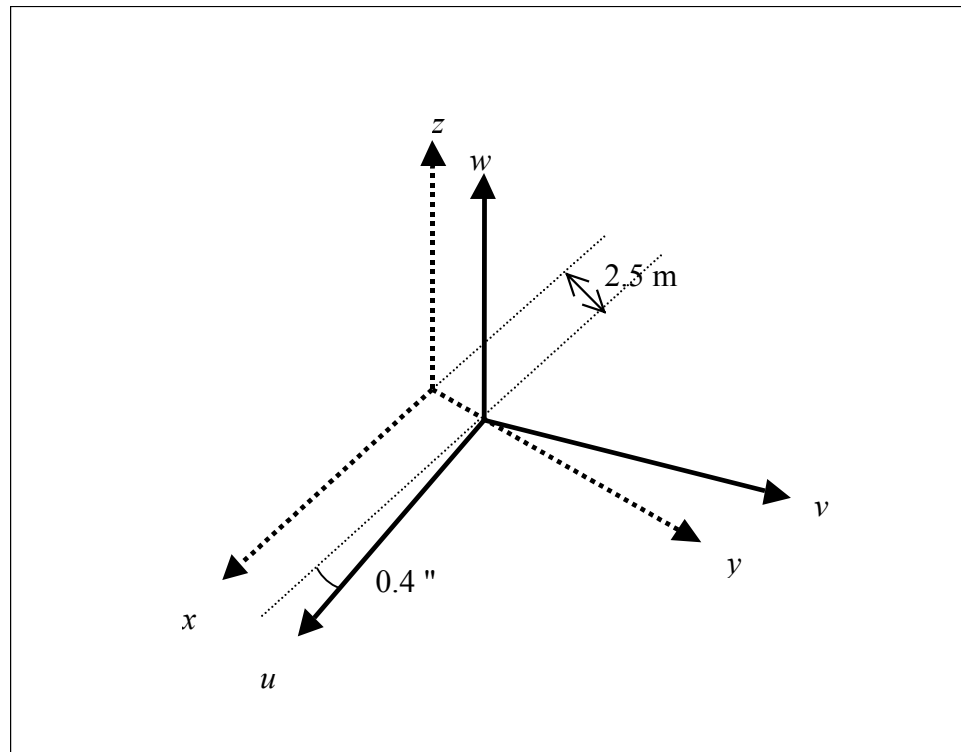


**Figure 3.4: Transformation between WGS84 and PZ90 [Misra et al., 1996]**

Another two sets of transformation parameters between WGS84 and PZ90 more recently were reported by Mitrikas et al. [1998] based on 20 months of laser data using the orbital approach. Similar to Rossbach et al. [1996], preliminary transformations between the ITRF94 and PZ90 have to be first determined. However, the relatively small ITRF94 to WGS84 transformation, as shown in the 1995 Annual Report of International Earth Rotation Services (IERS) [IERS, 1996], has been applied to obtain the PZ90 to WGS84 transformation from PZ90 to ITRF94. The equation required to transform coordinates from WGS84 to ITRF94, in unit of metres and radians, is as follows:

$$\begin{bmatrix} x \\ y \\ z \end{bmatrix}_{ITRF94} = \begin{bmatrix} -0.02 \\ 0.01 \\ -0.01 \end{bmatrix} + \begin{bmatrix} 1 & -0.017 \cdot 10^{-6} & 0.015 \cdot 10^{-6} \\ 0.017 \cdot 10^{-6} & 1 & 0.003 \cdot 10^{-6} \\ -0.015 \cdot 10^{-6} & -0.003 \cdot 10^{-6} & 1 \end{bmatrix} \begin{bmatrix} u \\ v \\ w \end{bmatrix}_{WGS84} \quad (3.8)$$

The transformation parameters between the reference frames of the two systems have been determined for the 20 month time period. Thus, there is a time-dependent effect of the transformation parameters. The transformation parameters are found to be highly correlated with differences between the Earth orientation parameters (EOP) used in regular GLONASS orbit determination and final IERS values. The estimated accuracy of the transformation is expected to be at the 20 to 30 cm level after removing the EOP difference.

The two sets of transformations presented in Mitrikas et al. [1998] to transform coordinates from PZ90 to WGS84 are as follows:

$$\begin{bmatrix} x \\ y \\ z \end{bmatrix}_{WGS84} = \begin{bmatrix} -0.47 \\ -0.51 \\ -1.56 \end{bmatrix} + (1 + 22 \cdot 10^{-9}) \begin{bmatrix} 1 & -1.728 \cdot 10^{-6} & -0.017 \cdot 10^{-6} \\ 1.728 \cdot 10^{-6} & 1 & 0.076 \cdot 10^{-6} \\ 0.017 \cdot 10^{-6} & -0.076 \cdot 10^{-6} & 1 \end{bmatrix} \begin{bmatrix} u \\ v \\ w \end{bmatrix}_{PZ90} \quad (3.9)$$

$$\begin{bmatrix} x \\ y \\ z \end{bmatrix}_{WGS84} = \begin{bmatrix} -0.47 \\ -0.51 \\ -2.00 \end{bmatrix} + (1 + 22 \cdot 10^{-9}) \begin{bmatrix} 1 & -1.728 \cdot 10^{-6} & 0.005 \cdot 10^{-6} \\ 1.728 \cdot 10^{-6} & 1 & -0.012 \cdot 10^{-6} \\ -0.005 \cdot 10^{-6} & 0.012 \cdot 10^{-6} & 1 \end{bmatrix} \begin{bmatrix} u \\ v \\ w \end{bmatrix}_{PZ90} \quad (3.10)$$

Both transformations are fully populated, i.e. all seven parameters (the X-, Y-, Z-axes translations and rotations and the scale factor) in the 3-D similarity transformation are found to be significant. Eq. (3.9) is based on the average transformation from the direct comparison between improved orbits in PZ90 and the same orbits in ITRF94, while Eq. (3.10) is the transformation yield from the reference frame of GLONASS tracking facilities or from true PZ90, which is free of errors from the polar motion. There is no exact verdict as which one is the best to be used in a combined GPS/GLONASS application. Strictly speaking, Eq. (3.9) is more appropriate but it also averages errors in

GLONASS from the polar motion determination reflected in regular ephemeris [Mitrikas et al., 1998].

To facilitate the combined use of GLONASS and GPS, Russian authorities plan to include the differences between the time and position references of the two systems in the navigation message [Langley, 1997]. Again, the information has not been available in the navigation message at the time of writing. Therefore, the differences between the two still have to be taken into considerations by the users. As described, the difference in the timing systems can be estimated at the cost of an additional satellite. A transformation in coordinate reference systems has to be carried out, usually when computing the satellite orbital positions, to transform the GLONASS PZ90 coordinates to GPS WGS84 coordinates.

### **3.2.3 Signal Multiplexing Techniques**

To distinguish the signals received from different satellites, three primary signal multiplexing techniques are available. There are the frequency division multiple access (FDMA), code division multiple access (CDMA), and time division multiple access (TDMA).

CDMA is a method in which satellites share time and frequency allocations, and the signals are channellized by assigning each satellite a distinct code. The signals are separated at the receiver by using a correlator that accepts only the signal from the desired channel using an auto-correlation function. FDMA is a multiple access method in which satellites are assigned specific frequency bands. The satellite has sole right of using the frequency band thereby transmitting signal without interference. TDMA is an assigned frequency band shared among the satellites. However, each satellite is allowed to transmit in predetermined time slots. Hence, channellization of signals in the same frequency band with the same code can be achieved through separation in time.

The major problem in implementing the integration of GLONASS and GPS arises from the fact that GLONASS uses the FDMA technique to distinguish signals from different satellites. As shown in Eq. (3.1), the frequency offset between satellites in the L1 band is 562.5 kHz and that in L2 is 437.5 kHz. The FDMA characteristic presents several difficulties in using the popular standard DD technique for integer ambiguity resolution.

Firstly, the integer nature of the ambiguity term after between-satellite differencing cannot be preserved and hence cannot be fixed. Secondly, each of the signals experiences a different ionospheric delay. Moreover, these delays can be temperature (receiver) dependent. Thirdly, the fact that each measurement is made at a different time in the two receivers means that an extra error is present when the clock errors are scaled by the different frequencies. Again, this is not a problem for GPS since there is only one frequency. Finally, a much wider bandwidth is used in the channel design to receive the range of GLONASS frequencies. This potentially leads to noisier observations and may have a negative impact on ambiguity resolution.

To get around this problem, there are generally two solutions available. One may use a SD technique with certain constraints and/or aiding to resolve the GLONASS carrier phase ambiguity. Alternatively, one may modify the standard DD technique to accommodate the different GLONASS satellite frequencies. These two approaches will be discussed briefly in the following two sub-sections.

### **3.2.3.1 Single Difference with a Common Clock**

Given the fact that the difficulties in DD GLONASS carrier phase arise from the fact that the between-satellite differencing causes problems, an immediate solution to the problem is simply not to perform between-satellite differencing when dealing with GLONASS carrier phase. This yields the SD solution to solve for the GLONASS carrier phase ambiguity. However, a between-receiver SD solution alone, as observed in Eq. (2.3), does not eliminate the receiver clock offset and some other errors. An external frequency and time standard is therefore used as a common oscillator for the two receivers in an

attitude system. Remaining time and other biases are estimated using a low-pass (averaging) filter. This is the approach proposed and validated in this research and will be presented in greater details in Chapter Five.

### **3.2.3.2 Modified Double Difference Technique**

There have been several modified DD solutions discussed in the common literature. These solutions use different techniques to resolve the ambiguities from GLONASS carrier phase measurements.

The first solution proposed is to estimate the receiver clock term from the pseudoranges and substitute it back in the DD carrier phase measurements accordingly. To achieve this, the pseudoranges must be measured with high precision. Current technology allows the receiver clock term to be estimated from pseudoranges to an accuracy of tens of nanoseconds. However, an error in the receiver clock term of 1 nanosecond causes a carrier phase error in double difference of about 1 cycle. In order to fix the L1 carrier phase ambiguity, a measurement accuracy better than a few millimetres (less than 0.1 cycle) is highly desirable. Therefore, estimating the receiver clock term from pseudoranges is not readily available with the current technology [Leick, 1998].

The second solution to DD is to scale all the frequencies in L1 GLONASS frequency band to a mean frequency. With this, the receiver clock term can also be eliminated after DD. The mean frequency can be located at the middle of the L1 GLONASS frequency band at 1.60875 GHz. The drawback with this solution is that the new DD ambiguity term is no longer an integer linear combination of the SD ambiguities. Most of the popular techniques in fixing DD ambiguities to integers therefore cannot readily be used in this approach. Not having the ambiguity fixed results in having accuracy at the one decimetre level [Landau & Vollath, 1996]. Clearly, accuracy at this level is insufficient for the determination of attitude parameters.

The third solution is to scale all the frequencies in the L1 GLONASS frequency band to a common frequency by finding an auxiliary wavelength. This is to preserve the integer characteristic of the ambiguity term after DD. However, as shown in Rossbach & Hein [1996], the auxiliary wavelength is extremely small for GLONASS L1 carrier. The 65 micrometres auxiliary wavelength makes solving and fixing the integer from carrier phase measurements practically impossible since the latter have a noise level in the millimetre level.

The solution to GLONASS DD can be found if one has access to dual frequency carrier phase measurements [Leick et al., 1995]. This approach is similar to the resolution of wide-lane ambiguities from a dual-frequency receiver. The largest limitation to this approach is the need for a dual-frequency receiver and the need for accurate pseudoranges to compute the initial ambiguity estimate with sufficient confidence. Therefore, users without access to the L2 frequency cannot take advantage of this solution.

### **3.2.4 Other Differences between GLONASS and GPS**

Aside from the differences described above, there are some other differences which users have to take into consideration. The knowledge of these differences are important especially when dealing data from the GLONASS satellites.

Substantially different from GPS, the GLONASS ephemerides provide the satellite positions in state vectors rather than in Keplerian orbital elements as in the case of GPS. The other differences between GLONASS and GPS are in terms of format in almanac, frequency range, signal coding, navigation message, and etc. Table 3.3 contains a list of comparisons between GLONASS and GPS.

**Table 3.3: Differences between GLONASS and GPS**

Items		GLONASS	GPS	
Ephemeris representation		Position, velocity and acceleration in Earth-centered, Earth-fixed coordinates	Kepler parameters	
Almanac	Length	152 bits	120 bits	
	Duration	12m 30s	2m 30s	
	Content	Day of validity	Day of validity	week of validity
		Channel number	Channel number	S/C identifier
		Eccentricity	Eccentricity	eccentricity
		Inclination	Inclination	inclination
		Equator time	Equator time	almanac time
		validity of almanac	validity of almanac	health
		equatorial longitude	equatorial longitude	right ascension
		-	-	RA rate of change
		period of revolution	period of revolution	$\sqrt{\text{(semi-major axis)}}$
		argument of perigee	argument of perigee	Argument of perigee
		-	-	Mean anomaly
		luni-solar term	luni-solar term	-
		time offset	time offset	time offset
		-	-	Frequency offset
Carrier frequency	L1	1598.0625 – 1604.25 MHz	1575.42 MHz	
	L2	7/9 L1	60/77 L1	
Type of PRN codes		ML	GOLD	
No. of code elements	C/A	511	1023	
	P	5110000	$2.35 \cdot 10^{14}$	
Code rate	C/A	0.511 Mbit/s	1.023 Mbit/s	
	P	5.11 Mbit/s	10.23 Mbit/s	
Cross-correlation interference		-48 dB	-21.6 dB	
Navigation message	Rate	50 bit/s	50 bit/s	
	Modulation	BPSK Manchester	BPSK NRZ	
	Total length	2m 30s	12m 30s	

### 3.3 Future of GLONASS

On March 7, 1995, the Russian Government announced a decree "on executing works in use of the GLONASS system for the sake of civil users". The Decree confirms the earlier given commitments concerning a possibility of GLONASS system use by civil users. Four years have elapsed thus far and it seems like the civilian users from the international community are accepting GLONASS as a main element, probably second only to GPS, in the more general Global Navigation Satellite Systems (GNSS). The GNSS is an ambitious vision for a world-wide integrated satellite system which encompasses, besides GPS and GLONASS, some other low-Earth-orbiting (LEO), medium-Earth-orbiting (MEO), geostationary-Earth-orbiting (GEO) communication satellites, such as Inmarsat.

GALILEO, a next generation GPS-GLONASS-like system to be developed by the nations of the European Union (EU) was proposed in February 1999. It is expected that a deployment of 26 to 36 satellites in the Galileo constellation may happen from 2005 to 2007 and the operation would commence in 2008. Some people foresee the GALILEO as a potential threat to the growth and existence of GLONASS if the former is going to be implemented as planned.

Even without the potential threat from GALILEO, the issue of lack of resources for maintaining a full GLONASS constellation has placed some users to some degrees of doubts on the future of the system [Holmes et al., 1998]. However, continued commitments and promises from the Russian authority still give hopes to most people. The performance of GLONASS, in terms of accuracy and coverage, has so far been advantageous to users. This is particularly true in the functionality of complementing the GPS system, and hence enabling GLONASS to maintain to play a key role in the present time.

## CHAPTER FOUR

### ATTITUDE PARAMETERS AND COORDINATE FRAMES

The theory of attitude determination is the main focus in this chapter. Conventional terrestrial, local level and antenna body frames are defined and rotation matrices between these frames are presented. Attitude parameters referenced to these coordinate frames are defined. A direct method to derive the attitude parameters from measurements for twin- and multi-antenna systems is given. It is then followed by a discussion of the error analysis of the estimated attitude parameters.

#### 4.1 Coordinate Systems and Rotation Matrices

The attitude of a moving platform is the orientation of its body frame system with respect to a local reference system that is associated to a global reference system. The attitude parameters can be derived through the rotations, which can be expressed in the form of a rotation matrix. Therefore, the coordinate system and rotation matrix can be viewed as two fundamental elements in defining and estimating a platform attitude.

In order to define the platform attitude precisely so that it can be adapted to various applications, a number of coordinate reference frames are usually used. They are the conventional terrestrial, the local level, the vehicle platform and the antenna body coordinate systems.

### 4.1.1 Conventional Terrestrial System

The conventional terrestrial (CT) system is an ECEF system. The ECEF system, as described in Chapter Three, is fixed to the Earth and rotates with it. Its origin is located at the centre of the mass of the Earth. The  $Z^{\text{CT}}$ -axis points to the North Pole, the Conventional International Origin (CIO) to be exact. The CIO is defined as the mean positions of the movement of the instantaneous pole, due to a 0.002" to 0.003" annual polar motion of the north pole, with respect to the period 1900 to 1905 [Vaníček & Krakiwsky, 1986]. The  $XZ^{\text{CT}}$ -plane contains the mean zero meridian, and the  $Y^{\text{CT}}$ -axis completes a right-handed system.

An ECEF frame rotates with the Earth at a rate of  $7.292 \cdot 10^{-5}$  radians per second. The WGS84 datum, coordinate reference system of GPS, has an ellipsoid associated with it. The GLONASS PZ90, described in Chapter Three, has yet another reference ellipsoid. The semi-major axis and semi-minor axis of the ellipsoid used by WGS84 are as follows [Defense Mapping Agency, 1987]:

$$\begin{aligned} a &= 6378137.0 \text{ metres, and} \\ b &= 6356752.142 \text{ metres.} \end{aligned} \tag{4.1}$$

An arbitrary position on this ellipsoid can be represented by a set of curvilinear coordinates referred to as the geodetic coordinates. The geodetic latitude,  $\phi$ , is the right-handed angle between the plane perpendicular to the  $Z^{\text{CT}}$ -axis and ellipsoid normal measured along a meridian passing through the point of interest,  $p$ . The geodetic longitude,  $\lambda$ , is the right-handed angle from the mean zero meridian to the said meridian, measured in the plane perpendicular to the  $Z^{\text{CT}}$ -axis. The height of point  $p$ ,  $h$ , is measured along the ellipsoid normal and is the distance from the ellipsoid to point  $p$ . Note that as shown in Figure 4.1, the ellipsoid normal does not normally coincide with the centre of the ellipsoid. In the case of attitude determination, point  $p$  is referred to a point, says the location of the primary antenna, on a moving platform. The relationship

between the Cartesian ( $X, Y, Z$ ) and geodetic curvilinear ( $\phi, \lambda, h$ ) coordinates of any ECEF system is given as follows [Vaníček & Krakiwsky, 1986]:

$$\begin{bmatrix} X \\ Y \\ Z \end{bmatrix} = \begin{bmatrix} (N_p + h) \cos \phi \cos \lambda \\ (N_p + h) \cos \phi \sin \lambda \\ \left( \frac{N_p b^2}{a^2} + h \right) \sin \phi \end{bmatrix} \quad (4.2)$$

where  $N_p$  is the prime vertical radius of the curvature at the point of interest,  $p$ , and it is computed from:

$$N_p = \frac{a}{\sqrt{1 - e^2 \sin^2 \phi}} \quad (4.3)$$

where  $e$  is the eccentricity of the ellipsoid and is computed from:

$$e^2 = \frac{a^2 - b^2}{a^2} \quad (4.4)$$

#### 4.1.2 Local Level System

The local level (LL) system is used as a reference frame to measure the attitude of a moving platform. This local level frame is a topocentric coordinate system defined on a best-fitting ellipsoid, for e.g. a WGS84, and the latter rotates with the Earth.

The local level frame is useful when modelling the direction and attitude of a vehicle. The origin of the frame is defined by the phase centre of the primary antenna in a GPS and/or GLONASS attitude system. The  $z^{\text{LL}}$ -axis is normal to the reference ellipsoid,

pointing upwards. The  $y^{LL}$ -axis pointing towards geodetic north. The  $x^{LL}$ -axis completes a right-handed system by pointing east. Figure 4.1 illustrates the local level frame and its relationship to the conventional terrestrial frame.

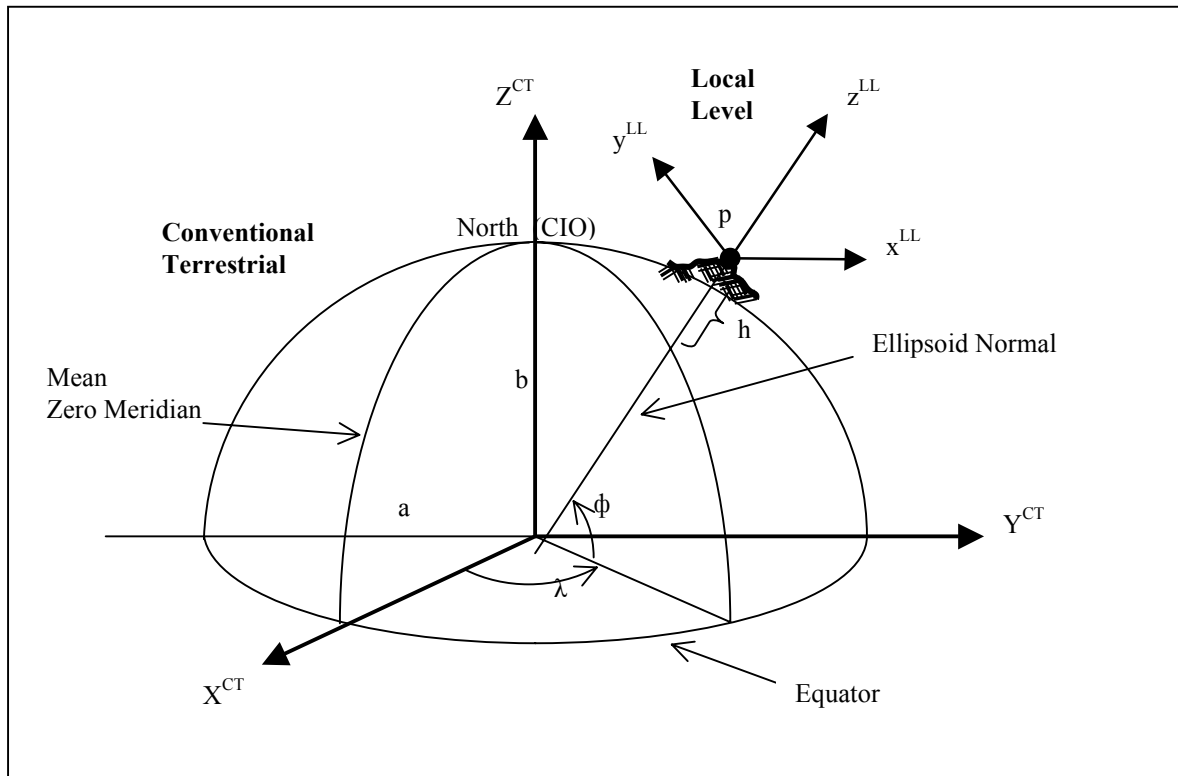


**Figure 4.1: Relationship between the CT Frame and LL Frame**

A baseline vector from a primary antenna to a secondary antenna is determined by GPS and/or GLONASS (after transformation from PZ90) in the WGS84 system. In order to use this baseline vector for attitude determination, it needs to be transformed into the local level system. The origin of the local level system is at the primary antenna whose location, for instance  $(\phi, \lambda, h)$ , is determined usually by pseudorange measurements in single point positioning mode.

The transformation of a baseline vector  $\mathbf{r}$  from a LL frame to the CT frame is accomplished using the equation:

$$\mathbf{r}^{\text{CT}} = \mathbf{R}_{\text{LL}}^{\text{CT}} \cdot \mathbf{r}^{\text{LL}} + \mathbf{r}^{\text{CT}_0} \quad (4.5)$$

where,

$\mathbf{r}^{\text{CT}}$  is the baseline vector expressed in the CT frame,

$\mathbf{R}_{\text{LL}}^{\text{CT}}$  is the rotation matrix to transform the baseline vector from LL frame to CT frame,

$\mathbf{r}^{\text{LL}}$  is the baseline vector expressed in the LL frame, and

$\mathbf{r}^{\text{CT}_0}$  is the LL frame origin,  $\mathbf{o}$ , expressed in the CT frame.

The rotation matrix  $\mathbf{R}_{\text{LL}}^{\text{CT}}$  is given by Wong [1988] as follows:

$$\mathbf{R}_{\text{LL}}^{\text{CT}} = \mathbf{R}_3\left(-\lambda - \frac{\pi}{2}\right) \cdot \mathbf{R}_1\left(\phi - \frac{\pi}{2}\right) \quad (4.6)$$

where,

$\mathbf{R}_1$  is the rotation matrix about the x-axis, and

$\mathbf{R}_3$  is the rotation matrix about the z-axis.

Expanding the above equation yields

$$\mathbf{R}_{\text{LL}}^{\text{CT}} = \begin{bmatrix} -\sin \lambda & -\cos \lambda \sin \phi & \cos \lambda \cos \phi \\ \cos \lambda & -\sin \lambda \sin \phi & \sin \lambda \cos \phi \\ 0 & \cos \phi & \sin \phi \end{bmatrix} \quad (4.7)$$

Therefore, the rotation matrix for transforming a baseline vector,  $\mathbf{r}$ , from the CT system to the LL system can be formed by transposing  $\mathbf{R}_{\text{LL}}^{\text{CT}}$ . The equation is as follows:

$$\mathbf{r}^{\text{LL}} = \begin{bmatrix} -\sin \lambda & \cos \lambda & 0 \\ -\cos \lambda \sin \phi & -\sin \lambda \sin \phi & \cos \phi \\ \cos \lambda \cos \phi & \sin \lambda \cos \phi & \sin \phi \end{bmatrix} \cdot (\mathbf{r}^{\text{CT}} - \mathbf{r}^{\text{CT}_0}) \quad (4.8)$$

Alternatively, Eq. (4.8) can also be expressed implicitly as follows:

$$\mathbf{r}^{\text{LL}} = \mathbf{R}_{\text{CT}}^{\text{LL}} \cdot (\mathbf{r}^{\text{CT}} - \mathbf{r}^{\text{CT}_0}) = \mathbf{R}_{\text{CT}}^{\text{LL}} \cdot \Delta \mathbf{r}^{\text{CT}} \quad (4.9)$$

where,

$$\mathbf{R}_{\text{CT}}^{\text{LL}} = \begin{bmatrix} -\sin \lambda & \cos \lambda & 0 \\ -\cos \lambda \sin \phi & -\sin \lambda \sin \phi & \cos \phi \\ \cos \lambda \cos \phi & \sin \lambda \cos \phi & \sin \phi \end{bmatrix} \quad (4.10)$$

A more detailed description of the transformation from the CT system to a LL system for a baseline vector, as well as its associated covariance matrix, is given in [Torge, 1980].

### 4.1.3 Wander Frame

The wander frame is usually used in high latitude areas. The y-axis of the local level frame is always pointing towards geodetic north. At very high latitudes, a large rotation about the z-axis is necessary to maintain the orientation of the local level frame whenever the longitude of the origin changes [Wong, 1988]. The wander frame is used in this case to avoid the y-axis from being dependent on the geodetic north. Instead, the y-axis wanders off north at a pre-defined rate. The wander angle,  $\alpha$ , is defined as the angle between the y-axis of the wander frame and geodetic north and is equal to the meridian convergence at the startup location. The rate of change of the wander angle is given as follows:

$$\dot{\alpha} = -\dot{\lambda} \sin \phi \quad (4.11)$$

Within the scope of this thesis, the wander angle mechanization is not used for attitude determination. However, it should be considered for any potential application in polar regions.

#### 4.1.4 Vehicle Platform Coordinate System

The vehicle platform coordinate system is usually defined by the users. This is the platform whose attitude parameters are of interest. The heading direction of the centre line of the moving platform is the y-axis, which lies in the plane of the platform. The x-axis is perpendicular to the centre line pointing to the right of the origin and it also lies on the same plane. The z-axis then completes a right-handed system by pointing upwards and it is normal to the plane of the platform. The attitude components are then the rotation angles of this platform system with respect to the local level system. Figure 4.2 illustrates the definitions of attitude parameters in a vehicle platform coordinate system.

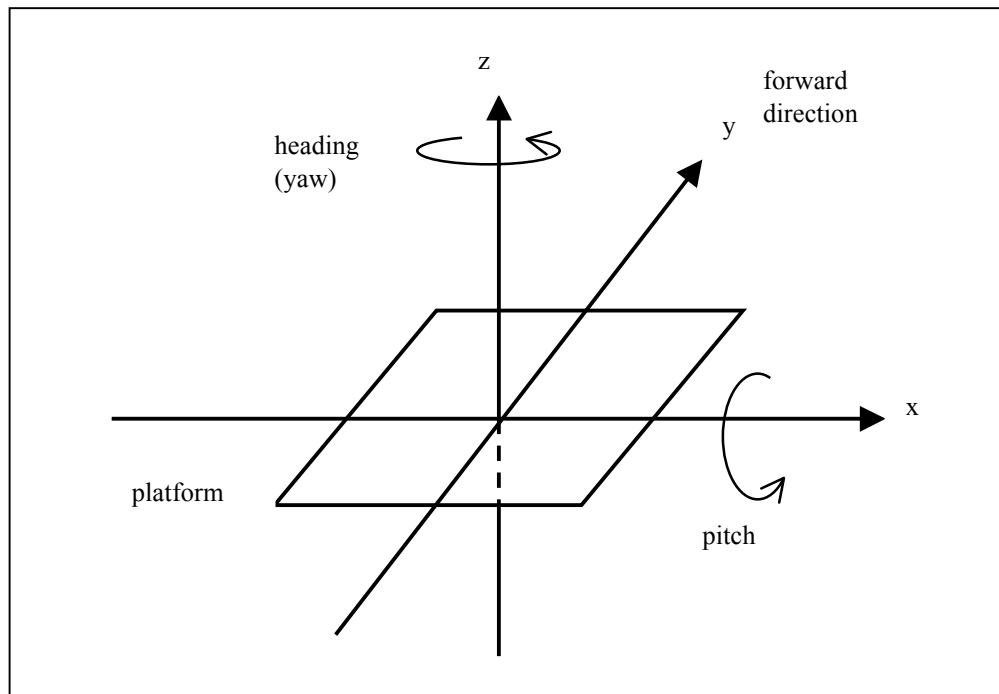


**Figure 4.2: Defining Heading and Pitch in a Vehicle Platform Coordinate System**

As shown in Figure 4.2, heading is the rotation angle about the z-axis, counter-clockwise being positive. Pitch is the rotation angle about the rotated x-axis, upward being positive. In a twin-antenna system, both the heading and the pitch components are defined by the baseline vector formed between the two antennas.

#### **4.1.5 Antenna Body Coordinate System**

The antenna body (AB) frame, or simply known as the body frame, is an idealized orthogonal frame related to the sensors of a GPS and/or GLONASS navigation system. It is considered idealized because it is free of manufacturing inaccuracies associated with the antenna array. The antenna body frame coordinate system is considered a rigid body frame and this implies that the relative positions between the antennas are fixed during all kinematic movements. The orientation and origin of an antenna body system are arbitrary and normally defined by the design of the navigation system. In a twin-receiver system, the origin of a body frame is at the primary antenna, which also corresponds to the origin of the local level frame. The  $x^{AB}$ -axis and  $y^{AB}$ -axis lie on an imaginary plane approximately level with the plate mounting the two antennas. The  $y^{AB}$ -axis points in the forward direction of the plate, while the  $z^{AB}$ -axis points upwards, normal to the imaginary plane passing through the primary antenna. The  $x^{AB}$ -axis completes the right-handed system by pointing to the right of the plate. A graphical representation of the antenna body frame of a twin-antenna attitude system is shown in Figure 4.3.

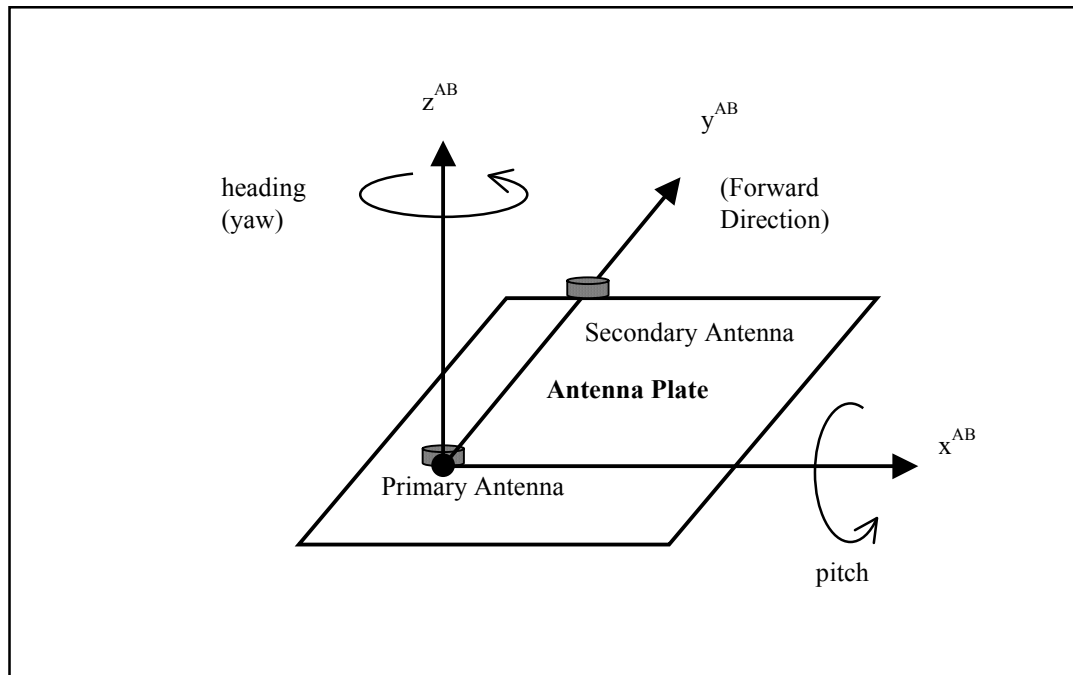


**Figure 4.3: Antenna Body Frame of a Twin-antenna System**

Two methods can be used to measure the GPS antennas in the body frame coordinates. The first one is often called a self-survey method. Static or on-the-fly kinematic GPS measurements are used to calculate the relationship between the two antennas. Some other conventional means are then used to establish the relationship between the twin-antenna system and the moving platform. The second method involves using conventional measurements to establish both the relationships between the antennas and between the twin-antenna and the one between the antennas and the moving platform. These antenna coordinates are only needed to be determined once for a rigid body configuration since it can be held fixed in later applications.

In some instances, the baseline vector formed by two antennas is exactly parallel to the true heading direction of the vehicle. The GPS determined heading is equal to the heading of the platform if this is the case. In most cases, however, it is very difficult to set up the GPS antennas such that they are exactly parallel to the vehicle's heading direction. Therefore, a misalignment angle between the two headings needs to be determined and taken into account in the computations to give a correct heading

information for the vehicle platform. If the GPS antennas are mounted rigidly on a vehicle or ship, the misalignment angles between the vehicle platform and the antenna body frame will be constant. The measurement errors of the body frame usually cause these misalignment errors and this results in a non-orthogonal frame. These measurement errors of the body frame coordinates should be minimized and the measurement technique should be designed with the ultimate use of the attitude system in mind.

By using a GPS twin-or multi-antenna system, the attitude of the GPS antenna body frame with respect to the local level frame can be precisely computed at each observation epoch. These attitude values can then be rotated into the defined vehicle platform coordinate system if the misalignment angles between the two platforms are known. Therefore, the remaining problem is to determine the attitude parameters in the body frame using GPS observations.

To describe the relationship between the body frame and the local level frame, the parameterization of the platform attitude is of concerns. A baseline vector  $\mathbf{r}$  is transformed from the local level coordinate frame to the body frame using the formulae of rudimentary vector algebra (e.g. [Torge, 1980]). Since the body and local level frames theoretically share the same origin and scale, the relationship between the two becomes:

$$\mathbf{r}^{\text{AB}} = \mathbf{R}_{\text{LL}}^{\text{AB}} \cdot \mathbf{r}^{\text{LL}} \quad (4.12)$$

where,

$\mathbf{r}^{\text{AB}}$  is the baseline vector expressed in the AB frame,

$\mathbf{R}_{\text{LL}}^{\text{AB}}$  is the rotation matrix to transform the baseline vector from the LL frame to the AB frame, and

$\mathbf{r}^{\text{LL}}$  is the baseline vector expressed in the LL frame.

The rotation matrix  $\mathbf{R}_{LL}^{AB}$  can be described in terms of quaternion form or in terms of the Euler angles of yaw (heading), pitch, and roll. Using primitive direction cosine matrices, the relationship between the Euler angles and the direction cosine matrix can be described in a number of different ways. The usual practice for the transformation from the local level frame to the body frame is accomplished first by a rotation about the  $z^{AB}$ -axis by the yaw angle, then about the  $x^{AB}$ -axis by the pitch angle and finally about the  $y^{AB}$ -axis by the roll angle, yielding the following equation:

$$\mathbf{R}_{LL}^{AB} = \mathbf{R}_2(\varphi)\mathbf{R}_1(\theta)\mathbf{R}_3(\psi) = \mathbf{R}_{312}(\psi, \theta, \varphi) \quad (4.13)$$

where,

$$\mathbf{R}_1(\theta) = \begin{bmatrix} 1 & 0 & 0 \\ 0 & \cos\theta & -\sin\theta \\ 0 & \sin\theta & \cos\theta \end{bmatrix} \quad (4.14)$$

$$\mathbf{R}_2(\varphi) = \begin{bmatrix} \cos\varphi & 0 & \sin\varphi \\ 0 & 1 & 0 \\ -\sin\varphi & 0 & \cos\varphi \end{bmatrix} \quad (4.15)$$

$$\mathbf{R}_3(\psi) = \begin{bmatrix} \cos\psi & -\sin\psi & 0 \\ \sin\psi & \cos\psi & 0 \\ 0 & 0 & 1 \end{bmatrix} \quad (4.16)$$

A rotation sequence of 3-1-2 is shown in Eq. (4.13). This particular rotation sequence multiplies the position vector  $\mathbf{r}$  by  $\mathbf{R}_3$  (rotation about the z-axis), then  $\mathbf{R}_1$  (rotation about the rotated  $x'$ -axis), and lastly  $\mathbf{R}_2$  (rotation about the rotated-rotated  $y''$ -axis). This sequence of rotations is adopted because it has been the most commonly used form in the photogrammetry applications in geomatics engineering. This is due to the fact that the heading (azimuth) rotation about the z-axis is usually the largest angle, and hence should

be first taken care of. The rotation sequence is then followed by the usually second largest pitch component and the smallest roll component.

In total, there are 12 possible axes rotation sequences to align one coordinate system with another [Wertz et al., 1978]. For example, the rotations can be made first about the x-axis, then about the rotated y'-axis and lastly about the rotated-rotated z''-axis. This sequence is denoted commonly by 1-2-3 sequence and the overall rotation matrix which aligns the two coordinate systems is the matrix dot product of  $\mathbf{R}_1 \cdot \mathbf{R}_2 \cdot \mathbf{R}_3$  and the three rotation angles are known as the Euler angles. A detailed description of Euler rotations can be found in [Wertz et al., 1978]. Any overall rotation matrix which aligns two Cartesian coordinate systems will fix the orientation of one coordinate system with respect to the other completely in a specific sequence. For this reason, the overall rotation matrix is also called an attitude matrix. Besides the Euler angles used and described in this thesis, the direction cosine matrix and the quaternion parameters are also widely used in attitude determination [Schleppe, 1996].

## **4.2 Deriving the Heading and Pitch Parameters**

GPS and GLONASS are basically two independent ranging systems that provide position, velocity, and time information to users. By determining the precise relative positions of at least two points in space, two of the three attitude parameters of the platform associated with these points can be computed. Attitude determination using non-dedicated GPS/GLONASS receivers relies on (due to the GLONASS's FDMA) either the SD (instead of DD) carrier phase model or the SD (instead of DD) interferometry model (for e.g. [van Grass & Braasch, 1991]).

If two or more GPS or GLONASS antennas are properly mounted on a platform and the measurements are simultaneously collected, the baseline vector from the primary antenna to other secondary antenna can be determined. The orientation of the antenna platform

defined by these antennas can then be computed from the derived baseline vector. Usually, the baseline vector of the antennas obtained by GPS and/or GLONASS (after transformation from PZ90) are in the WGS84. Then, the baseline vector is transformed into the local level coordinate system with the origin at the primary antenna.

#### 4.2.1 Twin-Antenna System

To compute attitude parameters using a twin-receiver (or twin-antenna) system, two sets of coordinates are needed for a baseline vector. One set is in a local reference frame, the other set is in an antenna body frame. The reference frame coordinates are derived by GPS and/or GLONASS measurements for each epoch in a local level frame with the origin at the primary antenna. The antenna body frame coordinates, on the other hand, are assumed to have been determined through an initialization process and remain unchanged in all kinematic movements. In this section, the attitude of a GPS antenna platform computed directly using only the local level coordinates derived by GPS is derived. The body frame coordinates of the antennas are not indeed needed explicitly as some of the body frame coordinate components take zero values [Lu, 1995].

Assume that a GPS antenna platform coordinate system or body frame is defined as in Figure 4.3 based on two antennas. The primary antenna is the origin of the coordinate system and the baseline from the primary antenna to the secondary antenna defines the y-axis. The body frame coordinates for the secondary antenna are, says,  $\mathbf{b} (0, L, 0)^T$ , where  $L$  is the baseline length between the primary and secondary antennas. The corresponding GPS derived coordinates in the local level frame for the secondary antenna is  $\mathbf{u} (x_2, y_2, z_2)^T$ . Mathematically, the local level coordinates for the secondary GPS antenna should be rotated into the corresponding body frame coordinates by the attitude matrix, i.e.,

$$\mathbf{b} = \mathbf{R}_{312}(\psi, \theta, \varphi) \cdot \mathbf{u} \quad (4.17)$$

where  $\psi$ ,  $\theta$ , and  $\phi$  are vehicle's heading, pitch, and roll, respectively. Using orthogonality of the attitude matrix  $\mathbf{R}_{312}(\psi, \theta, \phi)$  as shown in Eq. (4.13), the formulae for computing heading and pitch are immediately obtained as follow:

$$\psi = \arctan \frac{\Delta E}{\Delta N} \quad (4.18a)$$

and

$$\theta = \arctan \frac{\Delta Up}{\sqrt{\Delta E^2 + \Delta N^2}} \quad (4.19a)$$

where  $\Delta N$ ,  $\Delta E$  and  $\Delta Up$  are the three components of the baseline vector between two antennas determined from GPS in north, east and vertical direction in the local level frame respectively. Since  $\psi \in (0, 2\pi)$  and  $\theta \in (-\pi, \pi)$ , Eq. (4.18a) and Eq. (4.19a) carry within them an uncertainty of  $\pi$ . It is thus sometimes preferable to use the equivalent equations of a half-angle,

$$\psi = 2 \cdot \arctan \frac{\Delta E}{\Delta N + \sqrt{\Delta E^2 + \Delta N^2}} \quad (4.18b)$$

and

$$\theta = 2 \cdot \arctan \frac{\Delta Up}{\sqrt{\Delta E^2 + \Delta N^2} + \sqrt{\Delta Up^2 + \Delta E^2 + \Delta N^2}} \quad (4.19b)$$

which are unequivocal [Vaniček & Krakiwsky, 1986].

In the case that a third antenna in a multi-antenna system is available, the roll component of the moving platform can also be derived. This will be discussed in the following subsection.

#### 4.2.2 Multi-Antenna System

As mentioned previously, a full set of attitude parameters, namely heading, pitch, and roll, can be derived in a multi-antenna system of three antennas or more. The roll,  $\phi$ , is the rotation angle about the  $y$ -axis, left-side up being positive. It can be seen from (4.18) and (4.19) that the baseline vector between the primary antenna and the secondary antennas actually determines the heading and pitch of the antenna platform.

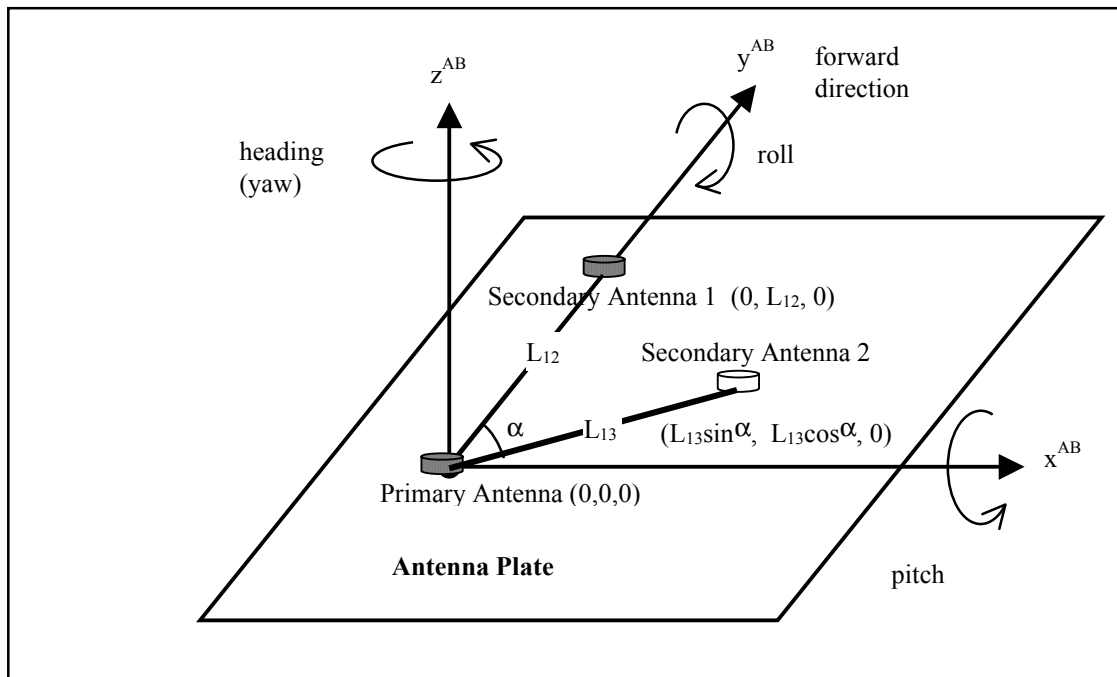


**Figure 4.4: Antenna Body Frame of a GPS/GLONASS Multi-antenna System**

From Figure 4.4, it can be seen that the body frame coordinate for the primary antenna is  $(0, 0, 0)^T$ . The two secondary antennas coordinates are  $b_2 (0, L_{12}, 0)^T$  and  $b_3 (L_{13}\sin\alpha, L_{13}\cos\alpha, 0)^T$ . The local level coordinates for the primary antenna is made to coincide

with its origin, i.e.  $\mathbf{u}_1 (x_1, y_1, z_1)^T = (0, 0, 0)^T$ . The corresponding GPS derived local level coordinates for the two secondary antennas are given by  $\mathbf{u}_2 (x_2, y_2, z_2)^T$  and  $\mathbf{u}_3 (x_3, y_3, z_3)^T$ . As in the case of a twin-antenna system, the local level frame and the antenna body frame in multi-antenna system share the same origin at the location of the primary antenna.

Once the estimates of heading  $\psi$  and pitch  $\theta$  are obtained as in Eq. (4.18) and Eq. (4.19), a couple of rotations need to be carried out prior to determining the roll angle  $\phi$ . The local level coordinates  $\mathbf{u}_3 (x_3, y_3, z_3)^T$  of the third antenna is first rotated about the local level  $z^{\text{LL}}$ -axis by an amount  $\psi$ , and then rotated again about the rotated local level  $x^{\text{LL}'}$ -axis by  $\theta$ . The resulting coordinates of the third antenna after these two rotations are denoted  $\mathbf{u}_3'' (x_3'', y_3'', z_3'')^T$ . A third rotation,  $\mathbf{R}_2(\phi)$ , rotates the local level coordinates  $\mathbf{u}_3'' (x_3'', y_3'', z_3'')^T$  to its body frame coordinates  $\mathbf{b}_3 (L_{13}\sin\alpha, L_{13}\cos\alpha, 0)^T$ , as follows:

$$\begin{bmatrix} L_{13} \sin \alpha \\ L_{13} \cos \alpha \\ 0 \end{bmatrix} = \begin{bmatrix} \cos \phi & 0 & -\sin \phi \\ 0 & 1 & 0 \\ \sin \phi & 0 & \cos \phi \end{bmatrix} \begin{bmatrix} x_3'' \\ y_3'' \\ z_3'' \end{bmatrix} \quad (4.20)$$

Expanding Eq. (4.20) and from the third row, the roll angle  $\phi$  can be computed as follows:

$$\phi = -\arctan \frac{z_3''}{x_3''} \quad (4.21a)$$

or in the unequivocal form:

$$\phi = -2 \cdot \arctan \frac{z_3''}{x_3'' + \sqrt{(z_3'')^2 + (x_3'')^2}} \quad (4.21b)$$

Shown in Eq. (4.18), Eq. (4.19), and Eq. (4.21) three equations are the direct computation formulae for the heading and pitch components (in a twin-antenna system) as well as the roll component (if a multi-antenna system is available). These derivations only use GPS-derived local level coordinates from two or three GPS antennas to define the platform. Therefore, the attitude parameters do not depend on the *a priori* body frame coordinates. This property is very useful in some situations where the antenna body frame coordinates are not known or in the initialization stage where the antenna body frame coordinates actually need to be determined precisely from GPS measurements [Lu, 1995].

Also seen from the above derivations, the direct computation method for attitude determination can only use one or two baseline vectors at a time. If two or more baseline vectors are available in a multi-antenna system, the baseline information can only be utilized by a rather cumbersome combination of attitude solutions for various vector-pairs. Therefore, the direct computation method is sub-optimal in a sense that only some, but not all, direction angles provided by the available baseline vectors are used. Obviously, there is a total of three independent equations that can be used in Eq. (4.20) to derive the pitch angles. Using only the simplest third equation as in Eq. (4.21) has left the information carried by the other two abandoned.

Alternatively, attitude parameters can also be estimated by an implicit least-squares model [Lu, 1995]. Compared to the direct computation method, the least-squares estimation of the attitude parameters is optimal since all the baseline information contained in the attitude determination system is used. The accuracy of the estimated attitude parameters is obtained through the diagonal elements of the inverse of the normal equation matrix. Another advantage of least-squares estimation over the direct computation is that the least-squares solution is less dependent on the measurements from a single antenna since the solution is made by the best fit over all antenna positions. For a twin-antenna system, the least-squares estimation yields a result identical to the direct computation method because the two methods use all available information.

The underlying problem of attitude determination using GPS and/or GLONASS, as can be clearly seen above, is to find the rotation matrix or the orientation parameters. In a GPS multi-antenna system configuration, the vector measurements or equivalently, the differential carrier phase measurements with ambiguities resolved, are used. Several other existing methods for attitude estimation from vector observations can be found in, for e.g., [Cohen, 1992] and [Lu, 1995].

The estimation of the attitude parameters using a direct computation method is presented. The following section discusses the accuracy, namely the covariance elements, associated with the three attitude components.

### 4.3 Accuracy of the Attitude Parameters

As shown in Figures 4.1 and 4.2, the origin of the local level coordinate system is defined at the position  $(\phi, \lambda, h)$  of the primary antenna in a twin- or multi-antenna system. This position is often computed at each epoch by a single point solution with pseudorange measurements from usually the primary GPS antenna. From Eq. (4.8), it can be seen that the local level coordinates  $(x^{LL}, y^{LL}, z^{LL})$  derived from the global geocentric baseline vector  $(\Delta X^{CT}, \Delta Y^{CT}, \Delta Z^{CT})$  are related to the latitude and longitude of the local level origin,  $o$ . Thus, a shift or change of the origin  $o$  may cause an error in the derived local level coordinates that are explicitly or implicitly used for platform attitude computations. The error relationship between the LL frame and the horizontal position  $(\phi, \lambda)$  of the origin  $o$  in the CT frame can be obtained by differentiating Eq. (4.9) as follows:

$$dx^{LL} = -(\cos\lambda \Delta X^{CT} + \sin\lambda \Delta Y^{CT}) \cdot d\lambda \quad (4.22)$$

$$dy^{LL} = -(\cos\phi \cos\lambda \Delta X^{CT} + \cos\phi \sin\lambda \Delta Y^{CT} + \sin\phi \Delta Z^{CT}) \cdot d\phi + (\sin\phi \sin\lambda \Delta X^{CT} - \sin\phi \cos\lambda \Delta Y^{CT}) \cdot d\lambda \quad (4.23)$$

$$dz^{LL} = -(\sin\phi \cos\lambda \Delta X^{CT} + \sin\phi \sin\lambda \Delta Y^{CT} - \cos\phi \Delta Z^{CT}) \cdot d\phi + (\cos\phi \sin\lambda \Delta X^{CT} - \cos\phi \cos\lambda \Delta Y^{CT}) \cdot d\lambda \quad (4.24)$$

To investigate the effect of position errors on the origin  $o$  in attitude accuracy, an example is illustrated. Under SA, the single point positioning accuracy with C/A-code pseudorange measurements is about 100 metres horizontally at two-dimensional RMS. In that case, the worst value for  $\sigma_\phi$  or  $\sigma_\lambda$  would be 71 metres. Suppose that  $\Delta X^{CT} = \Delta Y^{CT} = \Delta Z^{CT} = 2$  metres (i.e., a 2.8 metres baseline length) and  $d\phi = d\lambda = 71$  metres. The errors for  $dx^{LL}$ ,  $dy^{LL}$ , and  $dz^{LL}$  would be at the sub-millimetre level for,  $\phi = 51^\circ$  E and  $\lambda = 114^\circ$  W, the location of Calgary. For the errors to reach 1 millimetre, the baseline would have to be at least 100 metres in length, which is not a reasonable proposition in most applications. These errors are negligible compared to the effects of the carrier phase multipath which can reach centimetres level.

#### 4.3.1 Deriving DOP for Attitude Parameters

From [Schwarz & Krynski, 1992], the covariance transformation from the Cartesian coordinates (X, Y, Z) to the corresponding geodetic coordinates ( $\phi$ ,  $\lambda$ , h) is, in unit of metres, as follows:

$$\begin{bmatrix} d\phi \\ d\lambda \\ dh \end{bmatrix} = \begin{bmatrix} -\cos\lambda \sin\phi & -\sin\lambda \sin\phi & \cos\phi \\ -\sin\lambda & \cos\phi & 0 \\ \cos\lambda \cos\phi & \sin\lambda \cos\phi & \sin\phi \end{bmatrix} \cdot \begin{bmatrix} \Delta X \\ \Delta Y \\ \Delta Z \end{bmatrix} \quad (4.25)$$

The above equation is identical to Eq. (4.9). Based on the relatively short baseline length(s) in a twin- or multi-antenna system, the variance of the local level coordinates are then equal to the variances of the latitude, longitude, and height of a point of interest from a differential positioning solution (relative to the origin  $o$ ) [Lu, 1995], namely,

$$\sigma_y^2 \cong \sigma_\phi^2 \quad (4.26)$$

$$\sigma_x^2 \cong \sigma_\lambda^2 \quad (4.27)$$

$$\sigma_z^2 \cong \sigma_h^2 \quad (4.28)$$

The accuracy of the computed heading, pitch, and roll by direct computation formulas can be derived based on laws of error propagation. For instance, by differentiating Eq. (4.18a) and knowing the fact that

$$(\Delta E, \Delta N, \Delta Up) = (x_2, y_2, z_2)^T - (x_1, y_1, z_1)^T = \mathbf{u}_2 - \mathbf{u}_1 \quad (4.29)$$

with  $\mathbf{u}_1 = (0, 0, 0)^T$ , the error in the heading component becomes:

$$d\psi = \frac{y_2 dx_2 - x_2 dy_2}{x_2^2 + y_2^2} \quad (4.30)$$

Neglecting the correlation among the coordinate components, the standard deviation of the heading component is obtained as follows:

$$\sigma_\psi = \frac{\sqrt{\sigma_{x_2}^2 \cos^2 \psi + \sigma_{y_2}^2 \sin^2 \psi}}{L_{12} \cos \theta} \quad (4.31)$$

As can be seen in Eq. (4.26), Eq. (4.27), and Eq. (4.28), the variance of local level coordinates point  $(x_2, y_2, z_2)^T$  are known to equal the variance of longitude, latitude, and height of the secondary antenna, i.e.,

$$\sigma_{x_2} \cong \sigma_\lambda = \sigma_{\text{measurement}} \text{REDOP} \quad (4.32)$$

$$\sigma_{y_2} \cong \sigma_\phi = \sigma_{\text{measurement}} \text{RNDOP} \quad (4.33)$$

$$\sigma_{z2} \cong \sigma_h = \sigma_{\text{measurement}} \text{RVDOP} \quad (4.34)$$

where REDOP, RNDOP, and RVDOP are the relative DOP (RDOP) of the longitude or easting, the latitude or northing, and the height components, respectively. DOP, as described in Chapter Two, is commonly used to describe the impact of the geometric distribution of the satellites on the accuracy of a navigation solution.  $\sigma_{\text{measurement}}$  is the standard deviation of the measurements, be it raw, SD, or DD of the carrier phase. In a GPS/GLONASS twin-antenna attitude system,  $\sigma_{\text{measurement}}$  is the standard deviation of the SD carrier phase measurements. The accuracy of the solution is given by the product of the accuracy of measurement and the respective DOP. The accuracy of the heading component is as follows:

$$\sigma_\psi = \frac{\sigma_{\text{measurement}}}{L_{12} \cos \theta} \cdot \text{ADOP} \quad (4.35)$$

where ADOP is known as the azimuth DOP. ADOP has been commonly used as a figure of merit in assessing the impact of satellite geometry and baseline orientation on the determination of the heading component. Relating Eq. (4.31) through Eq. (4.35) four equations, ADOP can be obtained as follows:

$$\text{ADOP} = \sqrt{\text{REDOP}^2 \cos^2 \psi + \text{RNDOP}^2 \sin^2 \psi} \quad (4.36)$$

In a similar manner, applying the error propagation law by differentiating Eq. (4.19) and neglecting the correlation among the coordinate components, the standard deviation of the pitch component can be obtained as follows:

$$\sigma_\theta = \frac{\sqrt{\sigma_{h_2}^2 \cos^2 \theta + \sigma_{y_2}^2 \sin^2 \psi \sin^2 \theta + \sigma_{x_2}^2 \sin^2 \theta \cos^2 \psi}}{L_{12}} \quad (4.37)$$

The accuracy of the pitch solution can also be given by the product of the accuracy of the measurements and the DOP that describes the pitch component, i.e.,

$$\sigma_{\theta} = \frac{\sigma_{measurement}}{L_{12}} \cdot EDOP \quad (4.38)$$

where EDOP is known as the elevation DOP. Similar to ADOP, EDOP has been commonly used as a figure of merit in assessing the impact of satellite geometry and baseline orientation on the determination of the pitch component. EDOP can be obtained by relating equations from Eq. (4.32) to Eq. (4.38) as follows:

$$EDOP = \sqrt{RVDOP^2 \cos^2 \theta + ADOP^2 \sin^2 \theta} \quad (4.39)$$

Having the above formulae, it is often convenient to utilise them to estimate the anticipated accuracy of the attitude determination system in the design or planning stage.

### 4.3.2 Error Sizes and Other Impacts

To have a rough estimate of the magnitude of the errors on the attitude components, one may substitute the maximum errors anticipated in the measurements into the equations in the previous sub-section. For instance, substituting  $\sigma_{x_2}$  and  $\sigma_{y_2}$  with  $\sigma_{max}$  in Eq. (4.31), one obtains that for the heading component:

$$\sigma_{\psi} \leq \frac{\sigma_{max}(x_2, y_2)}{L_{12} \cos \theta} = \frac{\sigma_{max}(\phi, \lambda)}{L_{12} \cos \theta} \quad (4.40)$$

Through similar derivations the approximate accuracy estimation during planning stages for pitch and roll can be found as follows:

$$\sigma_{\theta} \leq \frac{\sigma_{h_2}}{L_{12}} = \frac{\sigma_{\text{measurement}} RVDOP}{L_{12}} \quad (4.41)$$

$$\sigma_{\phi} \leq \frac{\sigma_{\max}(x_3'', y_3'')}{L_{13} \cos \alpha} \quad (4.42)$$

It is apparent that the heading, pitch, and roll estimation accuracy is inversely proportional to the heading direction baseline length  $L_{12}$  and  $L_{13}$  when the positioning accuracy  $\sigma_{\max}$  is fixed. The accuracy of the height component is usually found to be poorer than those of the horizontal components. Therefore, the pitch accuracy is also usually found to be poorer than the heading accuracy. Results from Chapter Six confirm that the above statement is indeed true.

As described earlier, the attitude parameters of a moving platform are computed using the baseline vector formed by the antennas. Depending on the satellite geometry and the antenna configuration, the computed attitude parameters and the accuracy vary. The user does not have much control over the GPS and/or GLONASS geometry. Fortunately, with the combined constellation of the satellites offered by the two systems, ADOP and EDOP are normally less than three with six to eight satellites visible. The work to be done during at the planning stage of setting up a twin- or multi-antenna system is to properly select the antenna configuration to minimize the impact of errors on attitude estimation.

In a twin-antenna system, the best and probably the least complicated configuration is to align the two antennas as close as possible to the centre line of its moving platform. This is to avoid taking into consideration later the misalignment angle that exists between the heading computed from the system and true heading of the moving platform. As shown in Eq. (4.40), the accuracy of the estimated attitude parameters is inversely proportional to the inter-antenna distance. Therefore, the distance between the two antennas in the system should be as large as possible. The impact on the accuracy of attitude determination due to the antenna configuration in a multi-antenna system is discussed in [Lu, 1995].

## CHAPTER FIVE

### ATTITUDE DETERMINATION USING GPS/GLONASS

In Chapter Three, a SD and a DD solutions are briefly introduced to account for the GLONASS FDMA problem. This chapter discusses the technique of SD for the GPS/GLONASS carrier phase measurements to a greater extent. It first presents an overview of the SD technique. It is then followed by a discussion of the modified SD carrier phase ambiguity resolution in an attitude system. The problem faced with SD, namely the existence of a bias residual, is addressed. A solution, namely the use of a common oscillator with a filter estimate, is subsequently given. The results of several tests, including a shadow test and a clock test, are presented to validate the SD carrier phase approach. The effect of multipath from a GPS/GLONASS attitude system is also investigated and presented.

#### 5.1 SD Carrier Phase

Carrier phase measurements are essential in heading and pitch determination using GPS and/or GLONASS. In order to achieve highest possible accuracy in attitude determination, it is necessary to resolve correctly the integer ambiguities for the SD carrier phase measurements. The carrier phase measurements could give a solution of millimetre level accuracy provided the ambiguities are resolved correctly and fixed at all time. Therefore, the process of carrier phase integer ambiguity resolution plays a key role in high precision GPS applications including attitude determination.

For an attitude determination system used on a moving platform for real-time application, fast and reliable on-the-fly ambiguity resolution, i.e., ambiguity resolution while the platform is in motion, is very much needed. The term on-the-fly has been coined to generally cover a wide range of techniques used to determine ambiguities within many kinematic systems. Many of these techniques were originally developed for rapid static and kinematic differential carrier phase positioning operations such as land surveying. These include the Hatch's least-squares ambiguity search technique (LSAST), the ambiguity function method (AFM), the fast ambiguity resolution approach (FARA), and the fast ambiguity search filter (FASF) (e.g. [Chen, 1994] and [Weisenburger, 1997]).

In this chapter, modifications and improvements of these techniques are discussed to accommodate special conditions in a twin-receiver GPS/GLONASS attitude system. In particular, the SD carrier phase is used as the main observable for ambiguity resolution. The utilization of *a priori* information from the attitude system is studied.

From Eq. (2.2) and Eq. (2.3), observation equations for the carrier phase measurements and the between-receiver SD measurements are given as follows:

$$\Phi = \rho + d\rho + \lambda N + cdt - cdT + lb - dIon + dTrop + \varepsilon \quad (2.2)$$

$$\Delta\Phi = \Delta\rho + \Delta d\rho + \lambda\Delta N - c\Delta dT + \Delta lb - \Delta dIon + \Delta dTrop + \Delta\varepsilon \quad (2.3)$$

In a twin-receiver attitude system, the orbital and atmospheric errors practically cancel out due to its relatively short inter-antenna distance. The satellite clock error term,  $cdt$ , in Eq. (2.2) is eliminated. However, SD operation does not eliminate the receiver clock offset term,  $cdT$ , and the line bias term,  $lb$ , as in the case of DD operation. It also does not eliminate the integer ambiguity term,  $N$ , as in the case of between-epoch differencing. The sum of the random errors,  $\varepsilon$ , which includes multipath and receiver measurement noise cannot be reduced. In contrast, using SD operation theoretically increases the noise

by a factor of  $\sqrt{2}$ . The increase is smaller when comparing to the case of DD operation which doubles the magnitude of the noise.

Rearranging the single difference equation to solve for  $\lambda\Delta N$ , one obtain:

$$\lambda\Delta N = \Delta\Phi - \Delta\rho - \Delta d\rho + c\Delta dT - \Delta lb + \Delta dIon - \Delta dTrop - \Delta\epsilon \quad (5.1)$$

where,

$\Delta\Phi$  is the carrier phase measurement from a GPS receiver,

$\Delta\rho$  can be computed,

$\Delta d\rho$ ,  $c\Delta dTrop$ , and  $c\Delta dIon$  are negligible for a short baseline, but the  $c\Delta dT$  and  $\Delta lb$  have to be modelled or accounted for.

By re-arranging the terms and neglecting the errors that are cancelled out in Eq. (5.1), the following is obtained:

$$\lambda\Delta N = \Delta\Phi - \Delta\rho + c\Delta dT - \Delta lb - \Delta\epsilon \quad (5.2)$$

As described previously, the  $c\Delta dT$  term cannot be cancelled with a SD operation. The magnitude of the  $c\Delta dT$  could be quite large and must be accounted for prior to solving the integer ambiguity of the carrier phase measurements. To account for this remaining error in Eq. (5.2), a number of solutions are available. One obvious solution is to have the  $cdT$  term in each of the two receivers determined independently and hence the  $c\Delta dT$  term can be calculated. However, the current receiver technology is not quite capable of handling the job by determining the  $cdT$  to a satisfactory level of accuracy for the carrier phase ambiguity resolution. The other solution, which is the one proposed herein, is to have the two receivers in the twin-antenna system to be time-and-frequency-referenced by one common clock. This can be done, in practice, by having an external oscillator to give time and frequency signal to the two receivers simultaneously using a splitter.

Having a common clock used to generate frequency and time standard (FTS) for the two receiver clocks, the  $cdT$  terms of the two receivers experience the same degree of drift. For a good quality time and frequency generator, such as a Rubidium, the slope of the drift is small with only little variations about the slope. It does not however imply that the values of the  $cdT$  term from the two receivers are identical. It does not either imply that the  $c\Delta dT$  term takes on zero value.

The reasons are that the tracking loops in the two receivers are not synchronized with each other and the common clock is not synchronized with the GPS system time, GPST. Therefore, the  $cdT$  term of each receiver is still different from the other despite the fact that both of them are experiencing the same degree of drift. Differencing two different values with identical drift rate  $cdT$  terms obviously yield a constant  $c\Delta dT$  term at all time. This can also be understood in a different context. The common clock only provides the two GPS receivers with a stream of pulses with no absolute time tag. One could decompose the  $cdT$  term into two parts: the first part being an absolute initial bias from GPST and the second part being the drift over time. Driving two receivers with a common oscillator only ensures that the second part is identical, but there is no guarantee that the first part is the same for both receivers. In obvious conclusion, the  $c\Delta dT$  term is indeed a non-zero constant term.

The  $c\Delta dT$  term does not cancel out after GPS SD carrier phase measurements. Similarly, the  $c\Delta dT_{GLONASS}$  in GLONASS observations does not vanish after SD for the same reason. The  $c\Delta dT_{GLONASS}$  is the clock offset term, referenced to GLONASST, after the between-receiver SD operation with the use of a common clock. The difference between the GPST and GLONASST can be accounted, as described in Chapter Three, by an additional satellite measurement. In a combined GPS/GLONAS attitude system therefore, the receiver clock error term for GPS satellites and for GLONASS satellites should be the same after the system-time-difference is corrected. The relationship between them can be shown as follows:

$$c\Delta dT = c\Delta dT_{\text{GPS}} = c\Delta dT_{\text{GLONASS}} + \text{STD}_{\text{GPS-GLONASS}} \quad (5.3)$$

where,

- $c\Delta dT$  is the SD clock offset (with a common clock) for the GPS/GLONASS system,
- $c\Delta dT_{\text{GPS}}$  is the SD clock offset (with a common clock) for GPS,
- $c\Delta dT_{\text{GLONASS}}$  is the SD clock offset (with a common clock) for GLONASS, and
- $\text{STD}_{\text{GPS-GLONASS}}$  is the system-time-difference between the GPST and the GLONASST.

Due to the fact that all three terms on the right-hand side of Eq. (5.3) are all constant over time, naturally, the SD clock offset term,  $c\Delta dT$ , in a combined GPS/GLONASS attitude system should also be a constant bias with unknown magnitude. With the system-time-difference taken into consideration, this  $c\Delta dT$  term should be identical for each and every GPS and GLONASS satellite.

The SD line bias term in Eq. (5.2),  $\Delta lb$ , is mainly due to the different cable lengths between the two antennas and the hardware biases between the two receivers. Therefore, it cannot usually be cancelled out after single difference. The contribution of the hardware biases between the two receivers is usually negligible considering the size of the difference in antenna cable lengths. Therefore, the magnitude of this  $\Delta lb$  term is generally equal (or somewhat equal due to the different propagation speed of the cable) to the difference in cable length between the two units. Therefore, the  $\Delta lb$  term should also be constant giving the fact that the factors affecting the bias do not usually change over time. Moreover, the  $\Delta lb$  term should be identical for all GPS and GLONASS satellites.

The clock offset term and line bias term can then be combined as follows:

$$\Delta_{\text{comb}} = c\Delta dT + \Delta lb \quad (5.4)$$

Before going deeper in exploring the characteristics and the effect of the  $\Delta_{\text{comb}}$  term, the theory of ambiguity resolution needed to be understood. The following section studies the integer ambiguity resolution using SD technique in an attitude system.

## 5.2 SD Carrier Phase Ambiguity Resolution in an Attitude System

Since a receiver can only measure the beat carrier phase, the integer number of whole cycles in the carrier,  $N$ , in Eq. (2.2), is unknown for all phase measurements. It is absolutely necessary to solve for this unknown integer ambiguity term, in float or in integer (fixed) mode, for the measurements to make actual sense. For a 1-metre level baseline, a float ambiguity solution typically yields centimetre level accuracy in the position domain. A fixed ambiguity solution with the same baseline, on the other hand, could give an accuracy at the millimetre level. Attitude determination of sub-degree accuracy generally requires the carrier phase ambiguity to be resolved as integer numbers at all time.

The ultimate goal an ambiguity resolution technique aims for, especially for real time attitude application, is to determine the correct set of ambiguities in the shortest period of time possible with a minimum load of computation. An ambiguity resolution technique intended for attitude determination should strive to achieve the following properties:

- correct ambiguities are consistently selected;
- incorrect ambiguities are never selected; and
- computations should not take longer than one measurement epoch (desirable but not essential).

These properties could be conflicting with each other and hence a trade-off decision has to be made in designing the algorithm of an ambiguity resolution technique. Here lies the difficulty in achieving reliable and robust but yet fast and effective ambiguity resolution.

One advantage for satellite-based attitude system is that the inter-antenna distance between the antennas is rigidly held fixed in most cases. The inter-antenna distance can be measured *a priori* and can be used as a constraint to improve the performance in the ambiguity resolution process. The other advantage, as described earlier, is that the differenced carrier phase measurements, be it SD or DD, over a short baseline found in attitude application essentially cancels all the spatially correlated orbital, ionospheric, and tropospheric errors.

In general, all ambiguity resolution strategies involve the following three basic steps, namely:

- defining the ambiguity search space/volume;
- selecting the ambiguity candidates; and
- distinguishing the correct ambiguity.

As mentioned above, a starting point for the ambiguity search is to locate the search position and to determine the search dimension. This is usually based on the knowledge from either a carrier phase smoothed code solution [Lachapelle et al., 1992] or a Kalman filter float solution [Ford & Neumann, 1994]. This involves the estimation of the position, velocity and the float ambiguity states using either a least-squares method or a Kalman filtering method. In order to achieve the best and simplest solution of an over-determined problem in a static case, least-squares estimation is usually used [Weisenburger, 1997]. Kalman filtering can be thought of as an extension of the least-squares method from a static problem to a kinematic one. Thus, the Kalman states are no longer assumed to be constant as in the case of least-squares, but are allowed to change over time according to a certain pre-defined dynamic pattern [Maybeck, 1994]. In an attitude system where *a priori* baseline information is available, it is to locate a search space, equivalent to an approximate position of the secondary antenna with respect to the primary antenna within a given uncertainty. As can be seen later, the size of a search space affects both the speed and the reliability of the ambiguity resolution process.

The second step is to search through all of the possible ambiguity combinations and to select the ones that are feasible. The ambiguity search can be performed either in the position or ambiguity domain. Recent algorithms have focused on searching in the ambiguity domain. This is because when searching in the position domain, a very fine grid of points must be searched and the number of points to be searched within a typical search volume can be very large, thus making the computation load heavy. Several different search procedures have been developed. These include the AFM in the position domain; and the Hatch's LSAST, the FARA, and the FASF in the ambiguity domain.

The final step is to distinguish the correct ambiguity set out of many candidate sets selected from the previous step. There are several methods in existence and all methods use a test, or combination of tests, to isolate the correct ambiguity set. Tests that are too conservative may lengthen the time to resolve the ambiguity, while too optimistic tests may reduce the reliability of the results.

The speed and reliability of the carrier phase ambiguity resolution method selected depend on, aside from parameters used in the three steps described above, a number of other factors. These factors include the carrier phase measurement noise, multipath effects, satellite geometry and, in the case of attitude determination, the accuracy of the pre-determined baseline length. Generally speaking, the smaller the effects of noise and multipath are, the faster the resolution of the ambiguity is. More satellites in view and a better-determined baseline length, on the other hand, determine the ambiguity more reliably. The following sub-sections will discuss the three main steps of the ambiguity resolution more in depth.

### **5.2.1 Defining the Ambiguity Search Space/Volume**

The concept of ambiguity search space determination in the integer ambiguity resolution process for an attitude system can be shown in Figure 5.1. The coordinates at the primary

antenna (or monitor station) are usually held fixed. An approximate carrier phase smoothed code, Kalman filter float phase, or raw code solution provides the location of the centre of the search space. The accuracy provided by the carrier smoothed code and Kalman Filter float phase solution is usually good to about sub-metre level, considering the short inter-antenna distance in an attitude system. The one using raw code solution is typically about one order of magnitude worse than the other two.

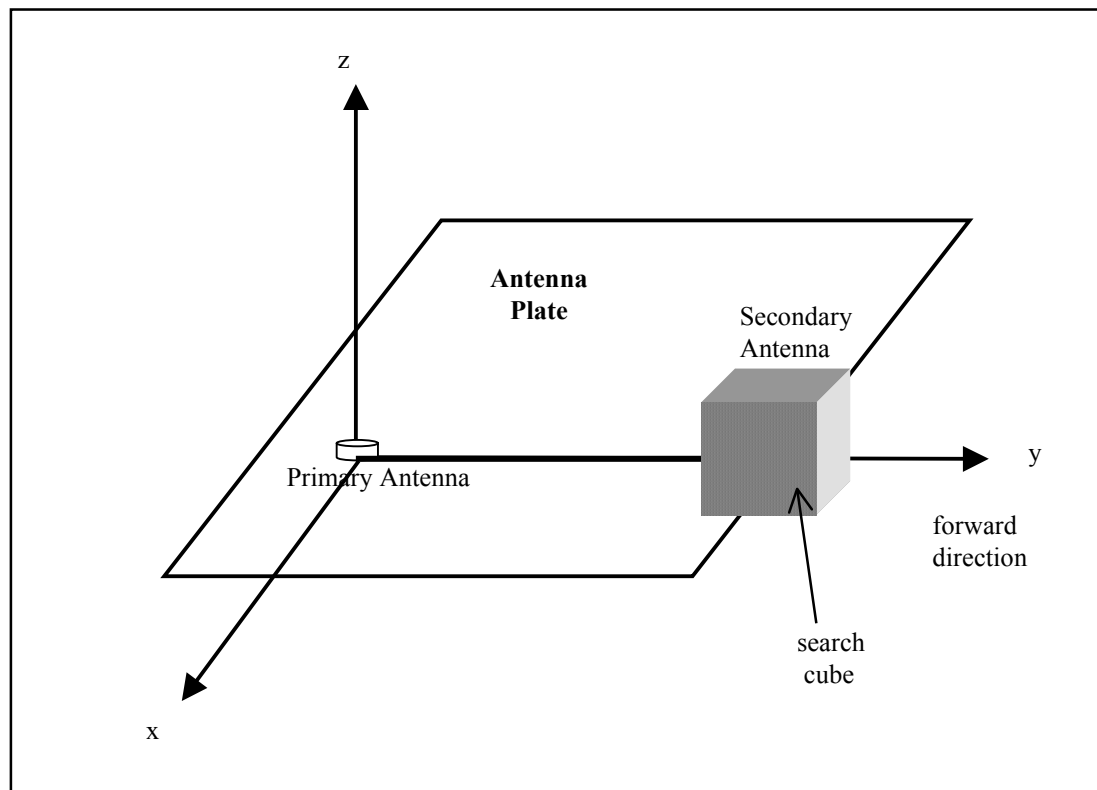


**Figure 5.1: Ambiguity Baseline Constraint Cube Search Concept**

The shape of the search volume, on the other hand, also varies with the application. A cube, ellipsoid, and sphere can be used as ambiguity search volumes [Chen, 1994]. A cube search volume, for instance, is shown in Figure 5.1. For attitude determination, the sphere shape with its origin at the primary antenna has advantages when used in a twin- or multi-antenna attitude system featuring rigidly mounted antennas. Since the baseline length between the primary and secondary antennas is fixed, the potential position solution for the remote antenna corresponding to the trial of an ambiguity combinations

must lie on the surface of a sphere. The radius of this sphere should be equal to the baseline length formed by the primary and secondary antennas. Using this technique, it is only necessary to search those combinations whose solutions fall on the surface of the sphere. It is not necessary to search those combinations whose solutions fall inside of the sphere. This advantage certainly reduces the number of search combinations and computation load, thereby increasing the speed of the ambiguity resolution process.

For attitude determination, the extent of the search volume on the sphere is usually based on the attitude estimates and corresponding variances from the approximate solution. Therefore, the size of the search volume is usually a function of the accuracy of the approximate solution. The attitude estimates give the initial orientation of the search volume. Its size is determined using the standard deviation of the estimated attitude parameters and multiplying the standard deviation by an expansion factor.

If one could assume that the estimated attitude parameters are only subject to errors of random nature, i.e. a Gaussian distribution of errors [Maybeck, 1994], the choice of an expansion factor at one standard error level (expansion factor of unity) have a 68.2% probability of containing the correct ambiguity combination. Increasing the expansion factor to two or three will increase the confidence level to 95.4% or 99.7%, respectively. However, systematic errors can contaminate the observations from which the approximate parameters are estimated. This makes the selection of an expansion factor a subjective one.

If the factor is set to give a small search volume, the ambiguity search will be completed faster, but there is an increased risk that systematic errors will cause the correct ambiguity set to fall outside the search volume. If a large expansion factor is selected, the search volume has a very good chance of containing the correct ambiguity combination.

Since the search area must contain the correct but yet unknown solution, the dimensions of the search area can be set at as many as five times the estimated standard deviation [Chen, 1994]. The larger the initial search cube, the higher is the number of potentially correct integer ambiguity solution to calculate and test, and thus the longer is the computation time required for ambiguity resolution.

One advantage for attitude system, beside the baseline constraint, is the use of pitch (and roll) constraint in the ambiguity search process [Harvey, 1998]. This can be shown in Figure 5.2. With a pitch constraint, the search area can then be confined to those areas of the sphere within maximum possible pitch angle about the local horizon. This will enhance the search algorithm and reduce the search time.

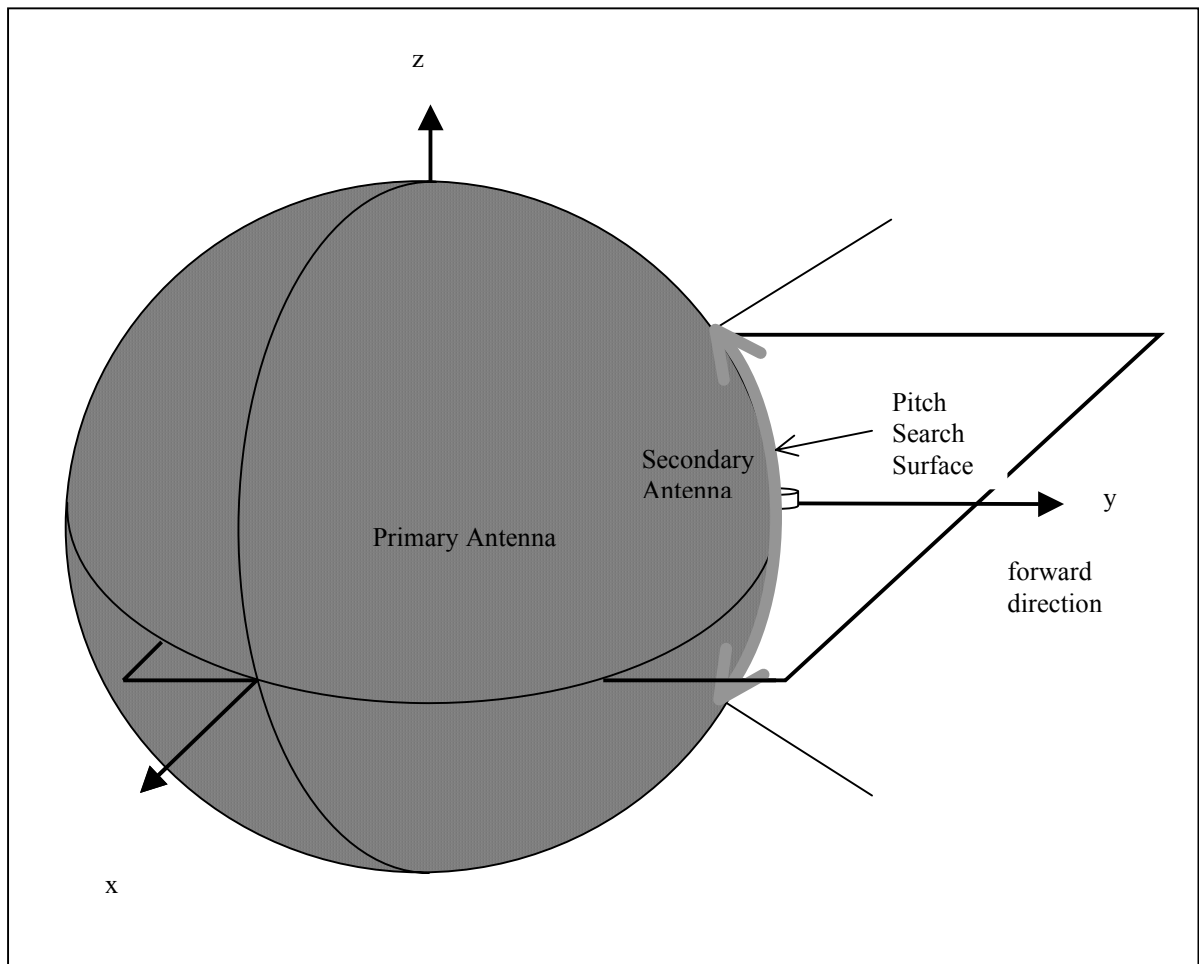


**Figure 5.2: Ambiguity Pitch Constraint Spherical Surface Search Volume Concept**

The other advantage that may be applicable to a kinematic system is the forward constraint. In cases where the vehicle is aligned with the heading axis of the attitude system and speed is relatively constant, the GPS course over ground can also be used to aid the ambiguity search by providing an initial orientation. Unfortunately, this will not work if the dynamic of the platform is relatively high or if the trajectory of the platform is unpredictable. Due to the above limitations, the forward constraint is seldom used in attitude determination.

### 5.2.2 Selecting the Ambiguities Candidates

Once the search volume is defined, the selection process begins. There are a number of commonly used ambiguity search methods. Most of them make use of an important property in ambiguity resolution: only three of the differenced carrier phase ambiguities is independent [Lachapelle et al., 1992]. This means once three differenced carrier phase ambiguities are correctly determined, the position of the moving receiver can be determined precisely, and therefore the ambiguities of the remaining satellites can be fixed. Using a GPS/GLONASS combined system however, requires an additional measurement for the determination of the system-time-difference, STD in Eq. (5.3), between GPS and GLONASS. Therefore, four *primary* satellite measurements with at least one from either GPS or GLONASS are needed. Typically, with the current status of GPS and GLONASS constellations, three GPS and one GLONASS satellites are used as the primary satellites.

The measurements from the primary satellite are used to generate an entire set of potential solutions, which are computed based on different trials of differenced carrier phase ambiguities. Each potential solution, which corresponds to a specific ambiguity set of the primary satellites, is checked using observations from the remaining *secondary* satellites. At potentially correct solutions, the computed observations for the secondary satellites should be very close to the corresponding measured observations. The

agreement can be quantified using an estimated variance factor or an ambiguity function. A large disagreement between the computed and measured observations means the solution tested is not the correct one and can be rejected.

The single difference ambiguities of the secondary satellites can be calculated by the equation:

$$\Delta N_{\text{calc}} = \text{int}\left[\frac{\Delta\Phi_{\text{obs}} - \Delta\Phi_{\text{calc}}}{\lambda}\right] \quad (5.5)$$

where,

$\Delta N_{\text{calc}}$  the calculated ambiguity of a secondary satellite,

$\text{int}[\bullet]$  the nearest integer operator,

$\Delta\Phi_{\text{obs}}$  the observed SD carrier phase measurements of the secondary satellite in unit of length, and

$\Delta\Phi_{\text{calc}}$  the corresponding calculated SD carrier phase observable of the secondary satellite in unit of length.

Once the integer ambiguity ambiguities of all the satellites have been determined, the measurement residual,  $v$ , from a satellite computed through a least-squares adjustment is as follows:

$$v = \Delta\Phi_{\text{obs}} - \Delta\Phi_{\text{calc}} - \Delta N_{\text{calc}} \quad (5.6)$$

The residuals from all the satellites then provide the basis for the testing discussed in the following sub-section.

The two criteria for choosing the primary satellites are satellite elevation and satellite geometry. Generally speaking, the highest satellite and three other mid-elevation satellites in three different directions will be picked. The position DOP (PDOP) of the

four primary satellites should be no larger than 15.0. Hatch [1990] reported that as the number of secondary satellites increases to three or more, dual-frequency observations at a single epoch could eliminate all the false potential solution except the correct one. This leads to the possibility of on-the-fly instantaneous ambiguity resolution. If more than one potential solution pass the acceptance test at a certain epoch, the ambiguity sets corresponding to these potential solutions are retained and further tested at the following epochs. As more epochs are used, all the false ambiguity sets of the primary satellites will be rejected except the correct one. The more satellites are available, the less will the computation time be for resolving the ambiguities.

### **5.2.3 Ambiguities Distinguishing Testing**

This step involves, if necessary, the determination of the correct ambiguity set out of many other potential candidate sets which is perhaps the greatest challenge to ambiguity resolution. There are several methods in existence and all methods use a test (or combination of tests) to try to isolate the correct ambiguity set. In general, tests that are too conservative may lengthen the time to resolve the ambiguities, while too optimistic tests may reduce the reliability of the results.

There are typically three commonly used ambiguity testing mechanisms in a software algorithm of an attitude system, namely:

- the variance factor test;
- the baseline constraint test; and
- the ratio test.

#### **5.2.3.1 Variance Factor Test**

The variance factor test is usually the first and sometimes the only test used in selecting the correct ambiguity set. The least-squares method, in particular, always makes use of the estimated variance factor,

$$\hat{\sigma}^2 = \frac{\mathbf{v}^T \mathbf{C}^{-1} \mathbf{v}}{n_s - 4} \quad (5.7)$$

where,

- $\hat{\sigma}^2$  is the estimated variance factor,
- $\mathbf{v}$  is the vector of residuals for all satellites calculated as in Eq. (5.6),
- $\mathbf{C}$  is the covariance matrix of the measurements, and
- $n_s$  is the total number of satellites.

At the potentially correct solution, the estimated variance factor should be a minimum. Taking the observation noise and other biases into account, only those potential solutions at which the estimated variance factor  $\hat{\sigma}^2$  is less than a predetermined threshold can be the correct potential solutions and are retained for further testing at subsequent epochs [Lachapelle et al., 1992]. If the ambiguities are fixed correctly, the least-squares residuals can be expected to be normally distributed and the estimated variance factor  $\hat{\sigma}^2$  has a chi-squares distribution. The criterion to accept the potential solution could therefore be formulated as follows:

$$\hat{\sigma}^2 < \left(\frac{\sigma^2}{df}\right) \chi_{df, 1-\alpha}^2 \quad (5.8)$$

where,

- $\sigma^2$  is the variance factor,
- $\chi_{df, 1-\alpha}^2$  is the chi-squares percentile,
- $df$  is the degree of freedom which is equal to  $(n_s - 4)$ , and
- $\alpha$  is the parameter for significance level  $(1 - \alpha)$ .

The variance factor statistics,  $\sigma^2$ , is given *a priori* for the testing of the potential primary ambiguity sets and it can be further classified into a *local* variance factor and a *global*

variance factor. The local variance factor is calculated using a single epoch of observation. Since the number of satellites from a single epoch is limited, the degree of freedom of the local variance factor is often small, e.g., less than four. From a statistical point of view, when the number of redundant observations is small, the calculated variance factor may change a lot from one kinematic epoch to another, due to the influence of the receiver or multipath noise. The global variance factor, however, overcomes this problem by accumulating the degrees of freedom over multiple epochs of observations from the kinematic mode. Therefore, a relatively loose threshold should usually be assigned to the local variance factor and a more stringent threshold could thus be applied to the global variance testing [Lachapelle et al., 1992].

If no ambiguity sets of the primary satellites pass the variance factor test, the whole search procedure has then to be restarted at the next epoch when new measurements come in. If cycle slips occur on the primary satellites during the search period, the procedure is also restarted at the next epoch.

More satellite measurements available usually allow false ambiguity sets of the primary satellites within the search volume to be rejected, resulting in faster ambiguity resolution.

### **5.2.3.2 Known Baseline Constraint Test**

In a twin-receiver system, additional information becomes available and this information can be used, not just in distinguishing the correct ambiguity set, but to speed up the whole ambiguity resolution process and to improve quality control (for e.g. in cycle slip detection) [Weisenburger, 1997]. The concept of a fixed baseline constraint is based upon the fact that the inter-antenna distance of the twin-receiver system on a moving vehicle can be known *a priori*. A constraint in the baseline length, utilized in ambiguity distinguishing test, is to ensure the final fixed ambiguity set results in the given known baseline and therefore discarding other potential ambiguity sets that give otherwise. A detailed discussion in using this test can be found in, for e.g., [Lu, 1995].

### 5.2.3.3 Ratio Test

If the above test still cannot distinguish the correct ambiguity set from other in one epoch, the ratio test has to be used. Over time, the estimated variance factors of the incorrect ambiguity sets will increase as the effect of the random errors causes the distribution of the measurement residuals to drift from the normal distribution due to the change of satellite geometry. At one point, the minimum summed variance factor can be compared to the second minimum. The test quantity is the sum of squared residuals,  $\Omega$ , and can be calculated as follows:

$$\Omega = \sum_{i=1}^{n_e} \mathbf{v}_i^T \mathbf{C}_i^{-1} \mathbf{v}_i \quad (5.9)$$

where  $n_e$  is the total number of epoch used, typically about 10 seconds. This straight summation of the consecutive variance factor is possible if the measurements are assumed to be uncorrelated between epochs.

There is a number of ratio testing mechanisms available. One commonly used is a comparison of the smallest sum of squared residuals to the second smallest, i.e.,

$$\frac{\Omega_2}{\Omega_1} > \text{threshold} \quad (5.10)$$

where,

$\Omega_1$  is the smallest sum of squares of the residuals in metre<sup>2</sup>,

$\Omega_2$  is the second smallest sum of squares of the residuals in metre<sup>2</sup>.

A threshold of three is usually suggested and implemented, though this may be somewhat optimistic for many kinematic operational environments, such as attitude determination (e.g. [Chen, 1994] and [Harvey, 1998]).

Another test used by Chen and Lachapelle [1994] is:

$$\frac{\Omega'_2}{\Omega'_1} > \text{threshold} \quad (5.11)$$

with

$$\Omega' = (\mathbf{N}_{\text{float}} - \mathbf{N}_{\text{int}})^T \mathbf{C}_N^{-1} (\mathbf{N}_{\text{float}} - \mathbf{N}_{\text{int}}) \quad (5.12)$$

where,

- $\mathbf{N}_{\text{float}}$  is a vector of the floating ambiguity states,
- $\mathbf{N}_{\text{int}}$  is a vector of the potential ambiguity states, and
- $\mathbf{C}_N$  is the covariance matrix for the float ambiguity states.

There are some similarities between the Eq. (5.10) and Eq. (5.11) with the only difference being the constant factor, i.e. the float sum of squared residuals, added to the numerator and denominator in Eq. (5.11). This means that if identical thresholds were used for both tests, Eq. (5.10) would be slightly more conservative than Eq. (5.11). One of the advantages of using Eq. (5.11) is that the sum of squared residuals can be computed recursively [Chen, 1994].

Figure 5.3 summarize some of the key procedures in a typical integer ambiguity resolution process.

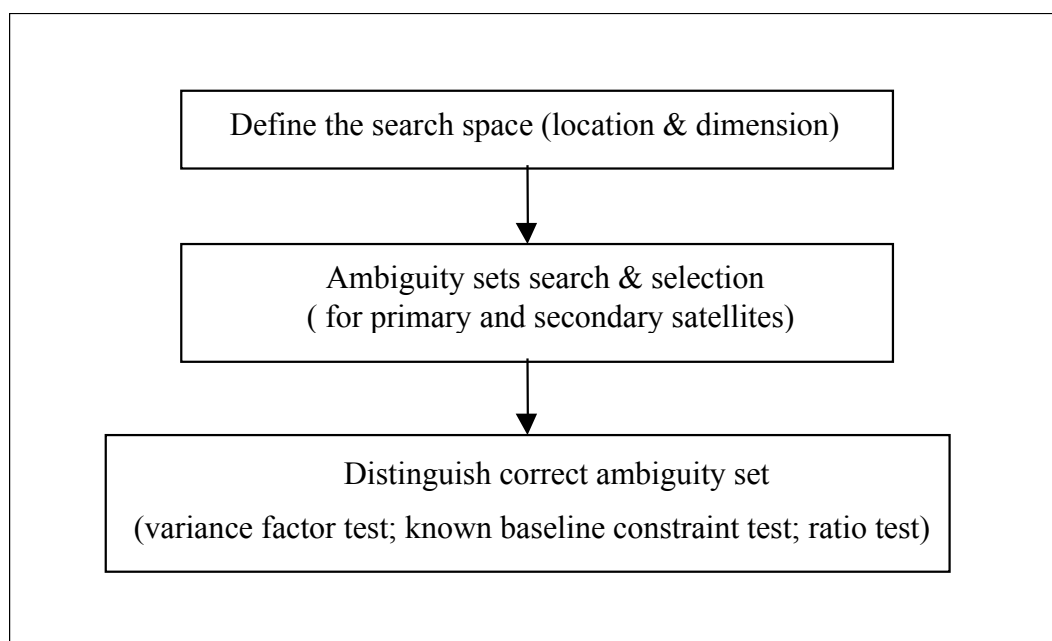


**Figure 5.3: Key Procedures in a typical Integer Ambiguity Resolution Process**

An ambiguity resolution technique is usually based on the assumption that the observations are free of blunders and biases [Weisenburger, 1997]. Unfortunately, this may not be true in the case of a GPS/GLONASS attitude system. The existence errors and system biases cause effectiveness of the process to be reduced. The previous section discusses the existences of bias in the SD measurements of GPS/GLONASS measurements. The following section is going to discuss the solution for estimating and removing the bias such that the ambiguity resolution process would be minimally affected.

### **5.3 SD Clock Offset and Line Bias Residuals**

From Section 5.1, it is found that both the effects of the clock offset and the line bias are constant and their combined effect is of a random bias nature. A random bias can be of any value prior to its determination. However, after system initialization, the value does not drift over time [Maybeck, 1994].

The combined effect of the clock error and the line bias can reach the metre level. However, this bias will not be shown in the residuals. This is because both of the effects (and hence the combined effect) are constant over time. The fact that they are constant makes the multiple of L1 wavelength (19.03 cm) part of the combined term  $\Delta_{\text{comb}}$  absorbed by the  $\lambda\Delta N$  term in the ambiguity resolution process. Therefore, only the remaining fractional part (always smaller than  $\frac{1}{2}$  of 19.1 cm) of the  $\Delta_{\text{comb}}$  term shows up as a constant bias in the SD residuals. In fact, any unmodelled error between the two receivers which is constant over time will combine with the  $\Delta_{\text{comb}}$  term and have its fractional part shown up in the residuals.

The theoretical maximum of the combined effect should therefore be no larger than half of one wavelength, which is 9.51 cm for L1. This residual bias should be common and identical to all satellites. This can be shown in Figure 5.4 where there is a  $-0.15$  cycle bias for the four satellites.

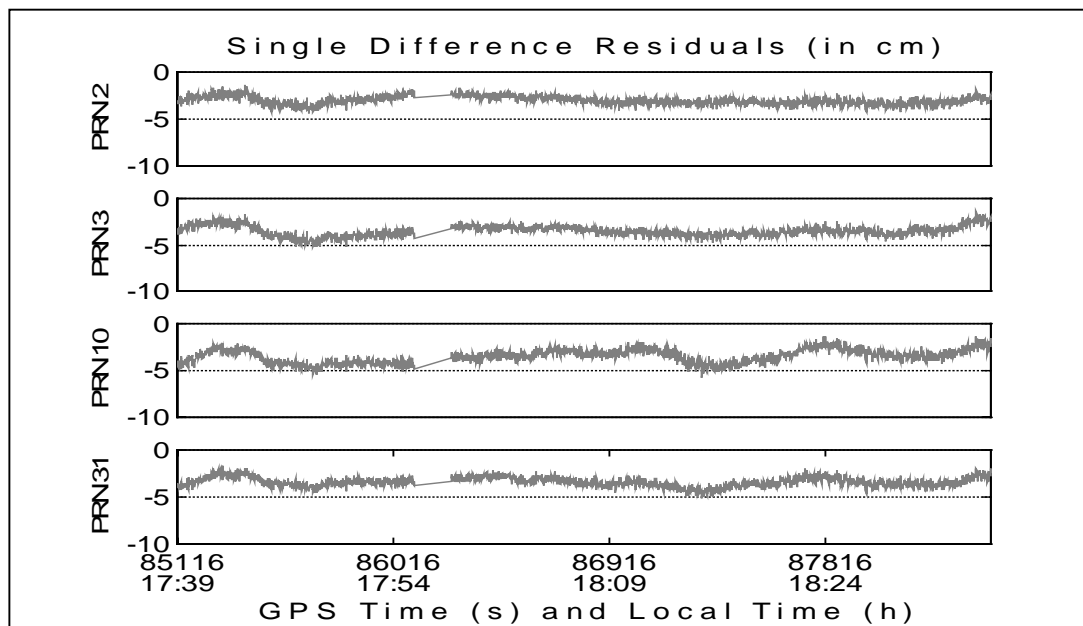


**Figure 5.4: Residuals for Selected GPS SVs**

### 5.3.1 Estimating the SD Biased Residuals

The fractional part of the bias, of magnitude typically at the centimeter level, can be disastrous for integer ambiguity fixing if not being accounted for. It must be estimated and removed from the carrier phase measurements. Given the fact that the residuals are constant over time, the bias can be estimated using a low pass filter.

The equation to estimate the bias in residuals can be written as follows:

$$\text{Res} = [\Delta\rho - \Delta\Phi - \text{“}\lambda\Delta N\text{”}] \quad (5.13)$$

where the “ $\lambda\Delta N$ ” is simply the closest integer and not the  $\lambda\Delta N$  estimated from the ambiguity resolution process. If the Res term is larger than 1 cm, it is fed back to the system at the subsequent epoch. The Res term is subtracted from the carrier phase measurements of all satellites at one of the two antennas, say the primary antenna.

The equation for residual bias estimation using an averaging low-pass filter is as follows:

$$\text{est}_i = \frac{i-1}{i} \text{est}_{i-1} + \frac{1}{i} \text{Res}_i \quad (5.14)$$

where est is the estimate of the residual bias and Res is the residual bias and i is the counter. The estimates of the residual biases for the four satellites shown in Figure 5.4 are found to agree among each other within 1 cm, or 0.05 cycle, after the averaging filter converges to a steady state. It typically takes around 10 minutes for the filter to come to a steady state. These can be seen in Figure 5.5.

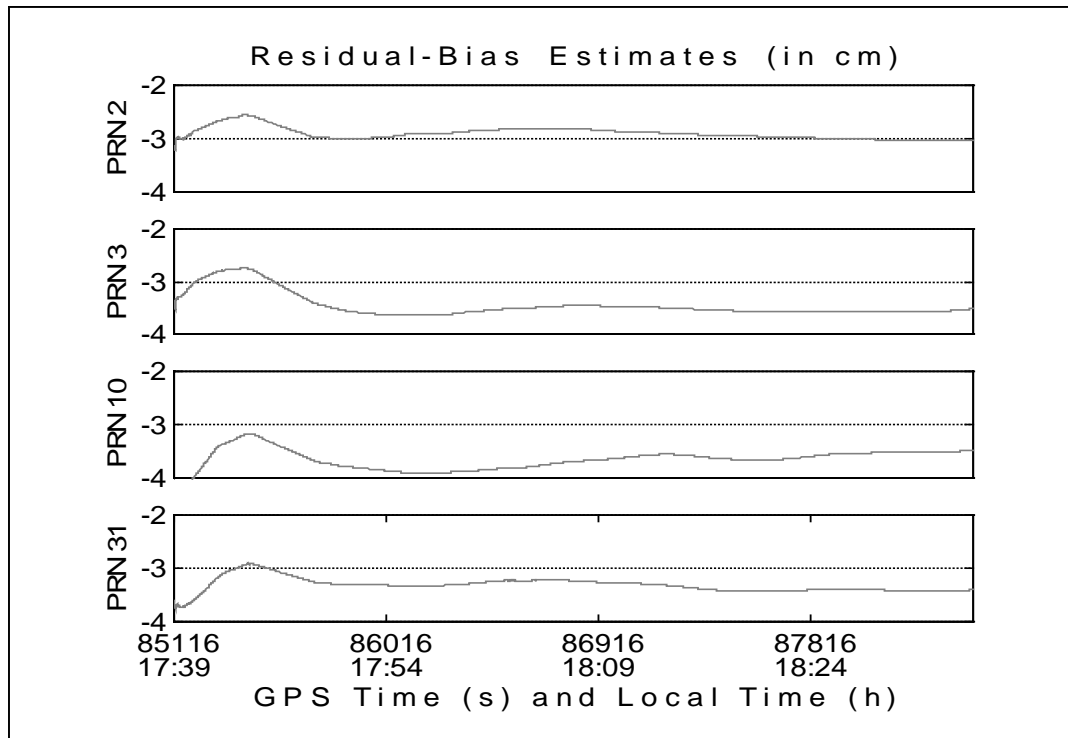


**Figure 5.5: Residual Bias Estimates for Four SVs**

Once the biases are estimated and fed back to the carrier phase measurements, a zero-mean should be obtained. This can be seen in Figure 5.6. The 1-cm noise is typically the magnitude of multipath, which does not cancel out. During the convergence phase of the filter, the estimated attitude parameter accuracy will be initially lower than once the filter has converged. In addition, the residual bias estimates are affected by multipath and some other errors. Estimated errors will increase the SD carrier phase observable noise and this will further degrade the estimated attitude parameter accuracy. The accuracy given by the SD approach is therefore expected to be somewhat lower than the corresponding accuracy derived using a standard DD approach in the case of GPS.

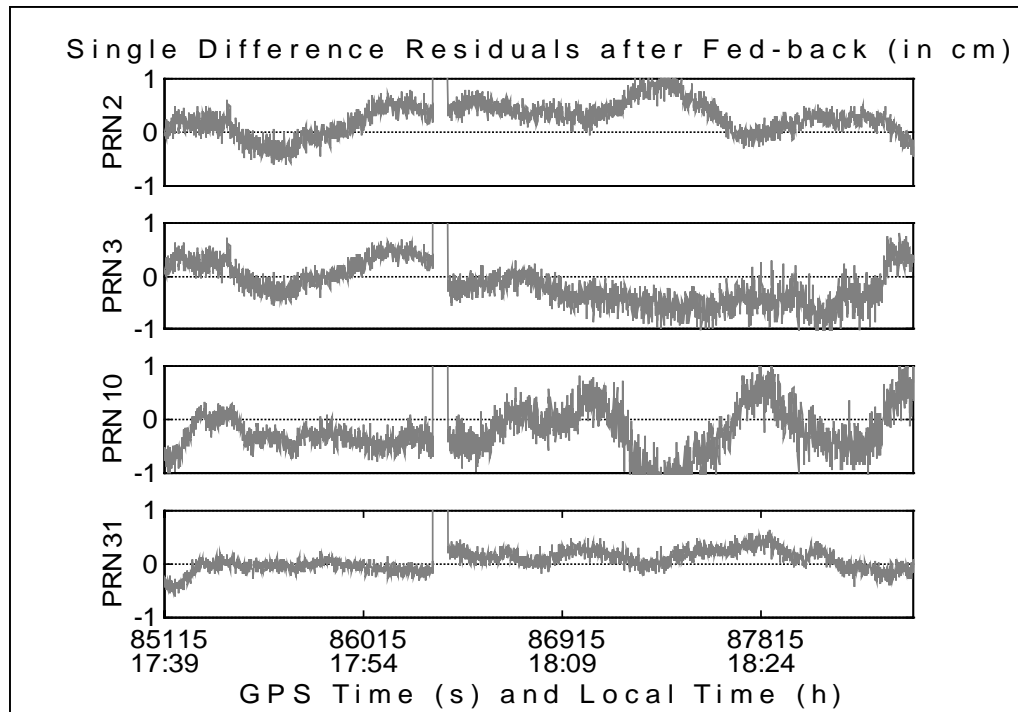


**Figure 5.6: SD Residuals after Bias Estimate Feedback**

### 5.3.2 Shadow Test

An averaging low-pass filter may only be used to estimate the residuals if the residuals are constant over time. But it is also crucial to verify that the residuals are indeed constant over time even when no satellite is tracked. A static “shadow test” was conducted for this purpose. The antenna baseline vector was 12 metres and a 2-hour data set was collected. One of the antennas was shaded for about 10 minutes in the middle of the test interval so that no satellite could be tracked during the shading period. The estimated heading and pitch were  $89.80^\circ$  and  $-0.46^\circ$ , respectively. The heading and pitch estimates with the 2-sigma bounds as obtained by the filter are plotted in Figure 5.7.

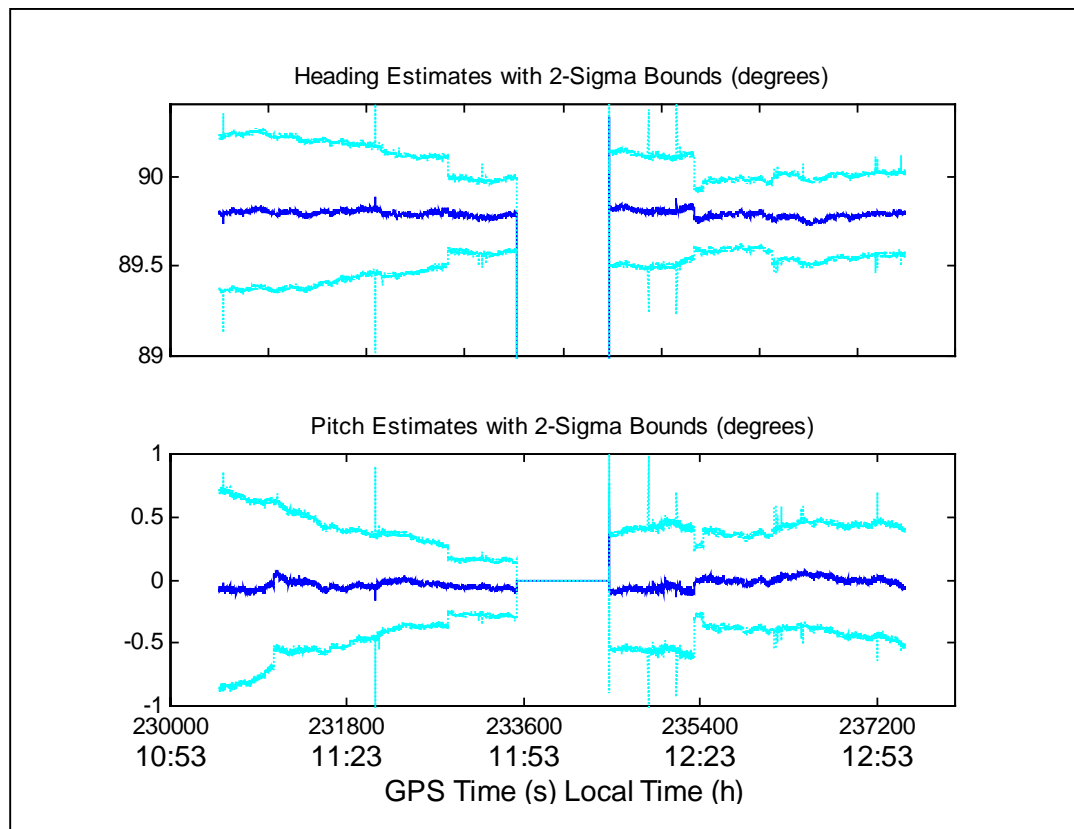


**Figure 5.7: Heading and Pitch Estimates with 2-Sigma Bounds**

The residuals from a satellite before and after the bias removed are showed in Figure 5.8. The ones with bias are shown in the upper plot of Figure 5.8. It is obvious that there is a +4.5 cm (+0.23 of a  $L_1$  cycle) bias in this case. Other satellites (not shown) also contain biases of +4 to +5 cm. Using Eq. (5.13) and Eq. (5.14), the estimated residual bias for PRN15 is found to be +4.56 cm and is plotted in the middle of Figure 5.8. This estimated bias is then fed back to the carrier phase measurements and zero-mean residuals are obtained. The residuals after bias removed are then plotted in the lower part of Figure 5.8. This slow varying 1-cm noise is a typical characteristic of multipath. Receiver noise is more random and has an amplitude of a few millimetres. The results of this test show that the effect of the  $\Delta_{\text{comb}}$  term is indeed constant.

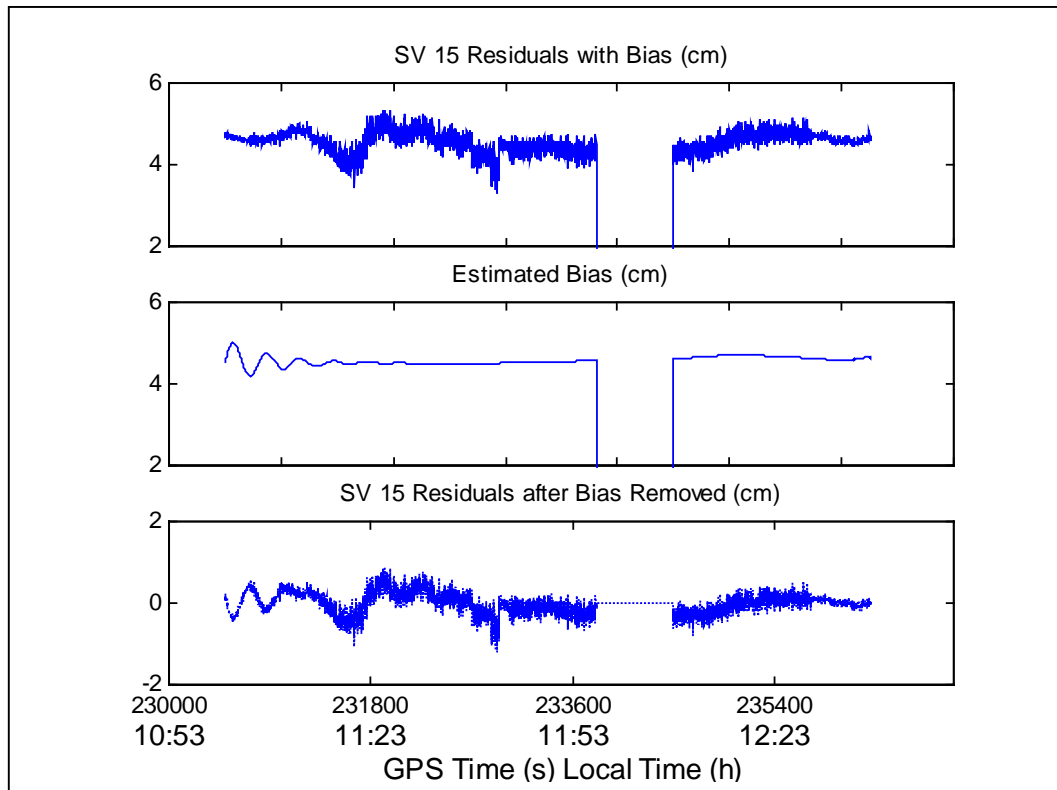


**Figure 5.8: SD Residuals, before and after Bias Removal**

### 5.3.3 Clock Test: Rubidium vs. OCXO

In the shadow test, it was found that the residual bias stays constant through out the period even when no satellite is tracked. This is made possible by an expensive and high quality Rubidium as a common oscillator to simultaneously provide the two receivers with time and frequency. The advantage of a Rubidium over a low cost time and frequency standard (FTS) is its superior stability. In this case however, this advantage is marginal since the only important point is for the two receivers to have a common drift. Therefore, it cannot be justified if the random bias property of the residual bias is dependent upon the quality of the FTS. The consistency of the residual bias is crucial to the realization of attitude determination using a GPS/GLONASS twin-receiver system. The expensive Rubidium has proven to have long term stability and is suitable for GPS clock aiding [Zhang, 1997]. A clock test was conducted to investigate if a lower cost

FTS, such as a high quality oven-controlled crystal oscillator (OCXO), is capable of maintaining the random bias property of the residual bias.

Errors in a FTS usually are due to the aging of the clock material and the environment. The errors from environment, mostly temperature, can be kept minimal by having the oscillator controlled in an “ovenized” environment so that a constant temperature is maintained [Lachapelle, 1997].

There are the primary and secondary FTS. The primary ones are the FTS which require no other reference for calibration. There are two types of primary FTS and both of them are atomic types. The Hydrogen Masers provide the highest stability and accuracy for both short and long period of time, at a few parts in  $10^{14}$ . They are very sensitive but, to date, can only be used under laboratory conditions. The Cesium clocks provide also high accuracy and high short- and long-term stability. The Cesium clocks are approximately one order of magnitude less stable than the Hydrogen Maser. Cesium clocks are the FTS used in both the space and control segments of GPS and GLONASS.

There are many secondary FTS which require a reference, such as a primary FTS, for calibration.. Rubidium clocks are the best secondary FTS, being only one order of magnitude less stable and less accurate than the Cesium clocks, i.e., a few parts in  $10^{12}$ . Rubidium clocks, moreover, are very portable and they are much less expensive than the two primary FTS. They can be made commercially available for less than \$10,000. Used together with the Cesium clocks, Rubidium clocks can be found in the GPS control segments and onboard the GPS satellites to realize the time base in the GPS system. The much lower cost Quartz (or Crystal) clocks usually come at less than \$1000. They have an excellent short term stability for time period less than 100 seconds. Quartz oscillators are those usually found in most commercial GPS receivers.

The frequency of a FTS is not strictly constant. The behavior of the frequency can be modelled and the parameters of the model can be estimated through the comparison with

other FTS. The relative frequency errors show a typical behavior for different types of atomic FTS. A suitable measure for the relative frequency errors in the time or frequency domain is the so-called Allan variance.

The Allan Variance is a statistical measure of the FTS stability in the time or frequency domain. The Allan Variance converges for all noise processes observed in precise oscillators. The Allan Variance can be interpreted as half of the (biased) variance of the difference in slope of the FTS error, computed by points separated several seconds apart. A bias will not affect the Allan Variance since it will cancel in the computation of the slope.

A “clock test” was conducted to investigate the effect of the quality of a common clock on the accuracy of the heading and pitch components. The same GPS/GLONASS receivers were used during two one-hour periods separated by eight days in order to reproduce the same multipath environment. A Ball Efratom Rubidium oscillator, model FRK-LLN, and a Vectron OCXO, model CO-330 series, were used in the test. The Rubidium is a compact, voltage-controlled oscillator which provides a pure and stable sinusoidal signal of 10 MHz with a long term drift of several parts in  $10^{12}$  [Ball, 1993]. The OCXO, on the other hand, is also capable of providing signal of 10 MHz with short term (tens to hundred of seconds) drift of several parts in  $10^{12}$  and aging rate of one part in  $10^{10}$  a day. Aging is the change in signal frequency with time due to the internal changes in the oscillator while the external factors in the environment are kept constant. Drifting, on the other hand, is the change in signal frequency due to aging and other external factors from the environment with time that one observes in an application [Ball, 1993].

In this clock test, the Rubidium was used as the common oscillator on the first day, while the OCXO was used on the ninth day. The inter-antenna distance was three metres and the masking angle was  $10^\circ$ . The epoch-to-epoch heading and pitch solutions (shifted by  $+1^\circ$ ) for both days are shown in Figure 5.9.

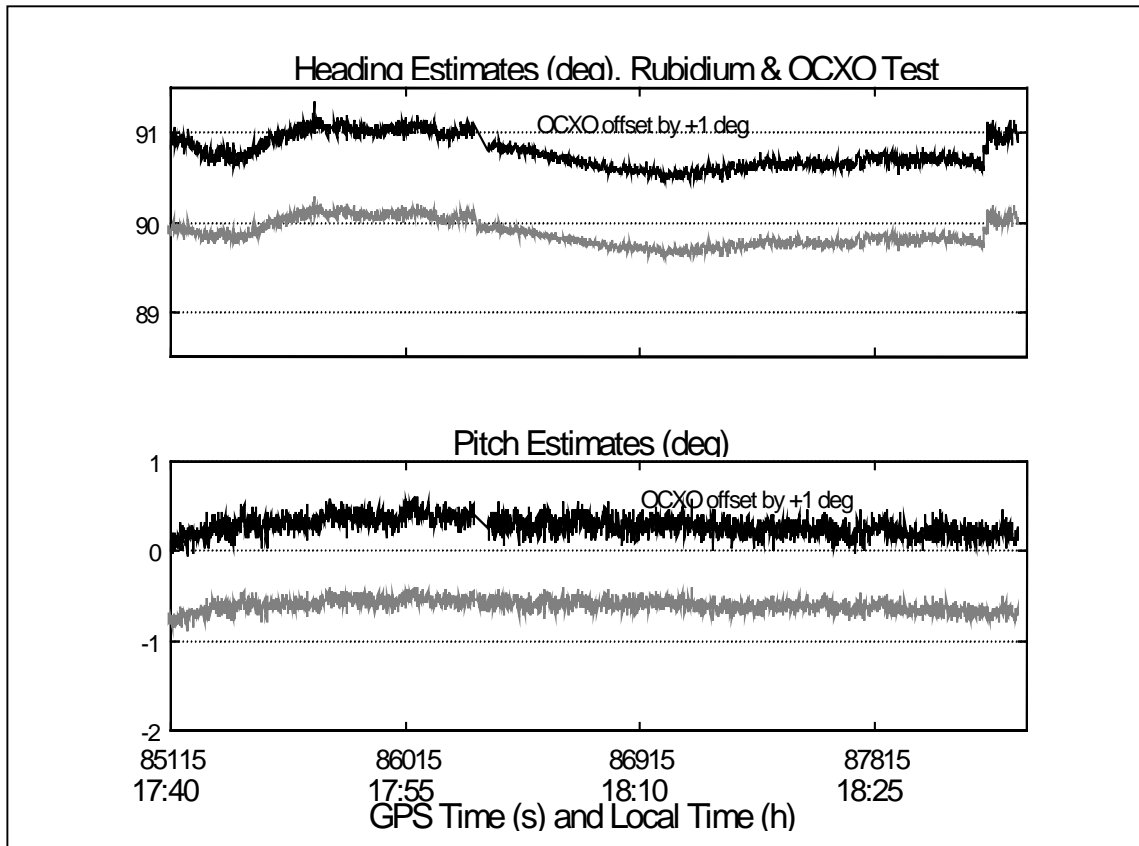


**Figure 5.9: Heading and Pitch using Rubidium and OCXO as Common FTS**

The heading RMS differences are  $0.157^\circ$  for the OCXO and  $0.149^\circ$  for the Rubidium, while the corresponding pitch RMS differences are  $0.195^\circ$  and  $0.186^\circ$ , respectively. The slightly better results with the Rubidium are due to a lower phase noise. As can be clearly seen in Figure 5.9, the Rubidium and OCXO results are strongly correlated and are still dominated by common multipath, which remains the dominant error source.

### 5.3.4 Multipath in SD GPS/GLONASS

One message conveyed in Figures 5.6, 5.8 and 5.9 is that multipath is indeed a dominant error source in an attitude system. In order to illustrate the effect of GPS and GLONASS carrier phase multipath on platform attitude estimation, another static repeatability test was performed on the lower roof of the Engineering Building of the University of

Calgary, as shown in Figure 5.10. The multipath environment was moderate. The inter-antenna separation was 12 metres. Since the antennas were stationary, the estimated heading and pitch of the platform should be constant from epoch to epoch. Time series analysis thus provides a way to analyse multipath effects on the estimated heading and pitch components. It should be noted that, compared to multipath, receiver noise only causes small random changes in the estimated attitude parameters while multipath tends to repeat itself over a certain period of time.

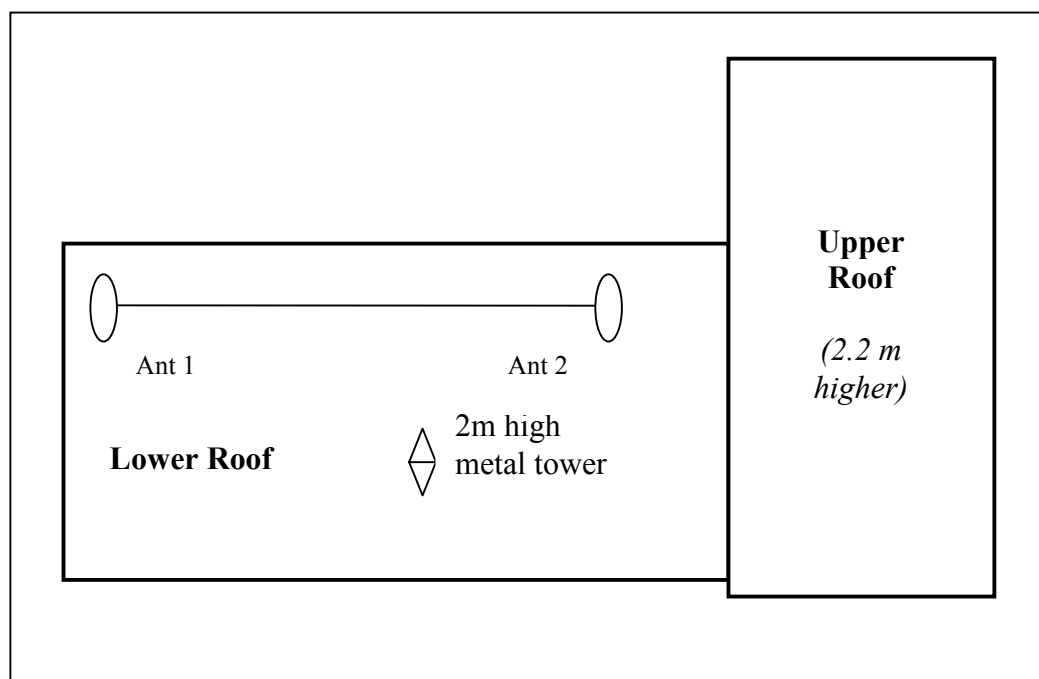


**Figure 5.10: Site of Static Roof Test for Multipath**

To investigate the effect of multipath, one has to find out the exact repeat period of the multipath. The orbital period of GPS satellites is about 718 minutes and their ground tracks repeat every two orbits, i.e., one solar day less four minutes. It is hence a common practice to investigate the effect of multipath of a site using data observed over two consecutive days, with the second day moved back four minutes in time. On the other hand, GLONASS satellites have the same nominal orbital period of 675.7 minutes, but their orbits produce ground tracks that repeat every 17 orbits or every 8 solar days less 32 minutes [Daly & Misra, 1996]. Therefore, the GPS/GLONASS satellite-reflector-

receiver geometry is theoretically identical after about eight days. In a fixed static environment, multipath errors from GPS/GLONASS will repeat themselves after about eight days.

Shown in Figure 5.11 are the heading and pitch components estimated using GPS/GLONASS measurements from epoch to epoch on the first day and the ninth day. The results from the ninth day are shifted upward by  $0.2^\circ$  for clarity. Centred at  $89.5^\circ$  in the upper plot and  $0.4^\circ$  in the lower plot are the heading and pitch differences between the two days (plotted in lighter colour). The reference heading is  $89.79^\circ$  and the reference pitch is  $-0.05^\circ$ . There was no chokering ground plane used in the experiment and there was no elevation mask angle limit used.

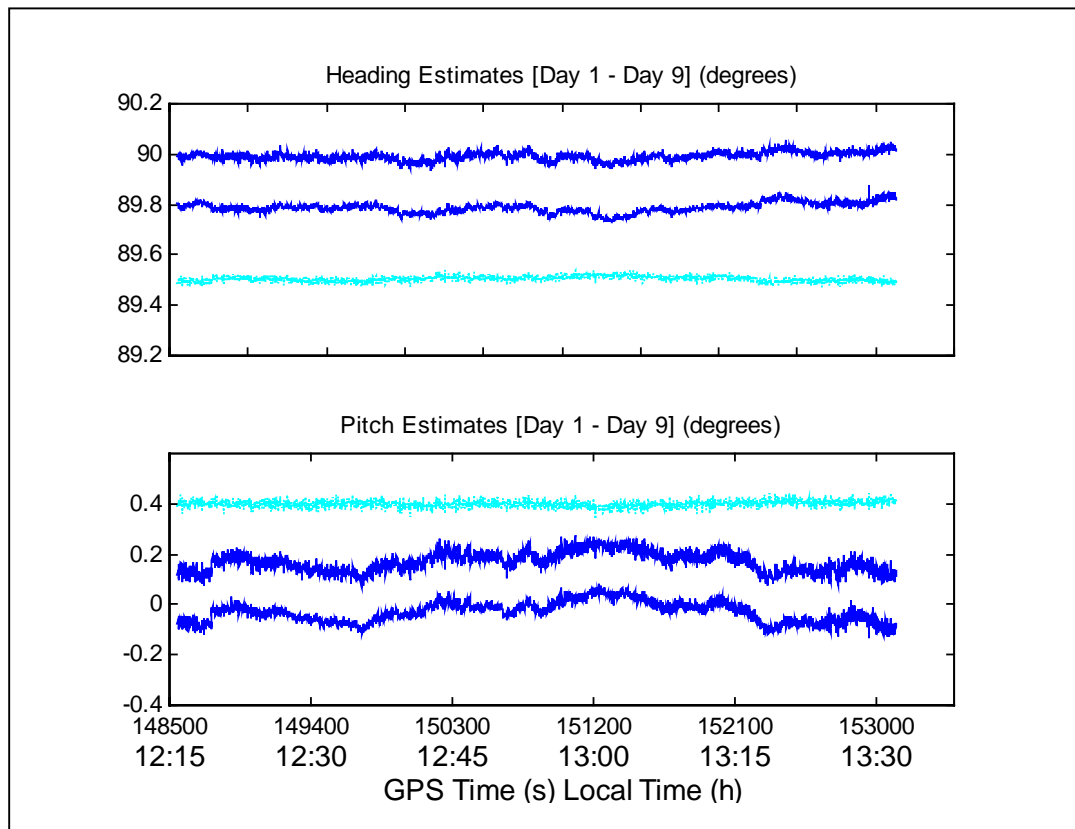


**Figure 5.11: Heading and Pitch Estimates from Day 1 and Day 9**

It can be seen, especially from the lower plot of Figure 5.11, that the variation pattern of the estimated heading and pitch parameters for the ninth day is quite similar to that of the first day. The long-term variations due to multipath have been eliminated. The statistics of the above results can be found in Table 5.1.

**Table 5.1: Statistics for Heading and Pitch Estimates for Day 1 and Day 9 – Static Multipath Test**

<b>Heading</b>	<b>Day1</b>	<b>Day9</b>	<b>Day1 – Day9 Difference</b>
<b>Mean</b>	$-89.789^{\circ}$	$-89.798^{\circ}$	$0.003^{\circ}$
<b>Standard Deviation</b>	$0.010^{\circ}$	$0.011^{\circ}$	$0.008^{\circ}$
<b>Pitch</b>	<b>Day1</b>	<b>Day9</b>	<b>Day1 – Day9 Difference</b>
<b>Mean</b>	$-0.051^{\circ}$	$-0.054^{\circ}$	$-0.004^{\circ}$
<b>Standard Deviation</b>	$0.029^{\circ}$	$0.027^{\circ}$	$0.012^{\circ}$

The computed *a posteriori* standard deviation in this test is  $0.01^{\circ}$  for heading and  $0.03^{\circ}$  for pitch. The relative baseline positioning accuracy, translated from the above computed standard deviation for attitude parameters, is about two to six millimetres using an inter-antenna separation of 12 metres. This level of accuracy is within the expected accuracy range of carrier phase positioning in a moderate multipath environment. The computed *a posteriori* standard deviation of the difference is about  $0.01^{\circ}$  for both heading and pitch and it translates to about 2 mm. Since the residuals have been differenced (between Day 1 and Day 9) once, the relative baseline positioning accuracy is about 1.4 mm. This level of accuracy is also within the expected accuracy range of carrier phase noise with low or no multipath.

The jump in the pitch component at epoch 148768 s in Figure 5.11 is caused by a change in satellite constellation. The loss of a low elevation satellite causes a noticeable jump in the pitch component but very little effect in the heading component. Depending on the relative geometry between the satellites and baseline vector, the effect of losing or

gaining a satellite on heading and pitch estimates may be different. Usually, the low elevation satellites significantly strengthen the satellite geometry but these satellites are more affected by multipath [Lu, 1995]. In order to achieve the highest possible accuracy in attitude determination, multipath should be reduced as much as possible.

If the environment and equipment can be controlled, methods used to reduce the effect of multipath are to have a careful site selection, to use ground planes such as chokering [Lu, 1995], and/or to use narrow-correlator-based receiver multipath reduction techniques [van Nee et al. 1994]. If the above conditions are beyond the control of the users which is more likely the case in attitude determination, mathematical modelling of multipath signatures may be an option. Efforts have been made by several research groups to study and mitigate the errors generated from carrier phase multipath. Georgiadou & Kleusberg [1988] uses L1 - L2 measurements to estimate the carrier phase multipath by making use of the relationship between the frequency of the carrier phase multipath error and the carrier wavelength. Axelrad et al. [1994] has exploited the signal-to-noise (SNR) information from the receiver in post mission, along with the antenna gain patterns, to estimate multipath. Ray et al. [1998] more recently has been investigating the spatial correlation of carrier phase multipath and developed a system to reduce the effect using multiple closely-spaced antennas. The technique estimates the parameters of the composite multipath signal in a Kalman filter and removes the errors due to all multipath signals in static mode.

## CHAPTER SIX

### SYSTEM ARCHITECTURE, TEST RESULTS AND ANALYSIS

A twin-receiver GPS/GLONASS attitude system with test results and analysis are presented in this chapter. Prior to presenting these, the hardware installation and software implementation of the system are first described. The results from several tests, including one static and two kinematic tests, conducted to validate the SD approach are also presented. The results are compared against the results obtained using a standard GPS DD approach.

#### 6.1 System Architecture

Following the approach proposed in the previous chapter, the next requirement is to assemble the hardware and software to realize a GPS/GLONASS heading and pitch determination system.

##### 6.1.1 Hardware

The hardware of the proposed heading and pitch attitude system consists of a pair of non-dedicated, off-the-shelf, Ashtech GG24<sup>TM</sup> GPS/GLONASS receivers, each equipped with a GPS/GLONASS antenna. An external and common FTS is required. A splitter is used such that the two receivers can share the signal output from the common FTS. Two laptop computers are used to capture the data streams from the two receivers using their

COM data ports. Other minor accessories include a source of power supply, the antenna cables, the download cables, the splitter cables, etc.

The Ashtech GG24<sup>TM</sup> receivers have tracking capability of 12 channels L1 GPS code and carrier and 12 channels L1 GLONASS code and carrier. The receivers are able, as stated in Magellan [1998], to provide solutions with accuracy as a function of mode, as summarized in Table 6.1.

**Table 6.1: Accuracy of Ashtech GG24<sup>TM</sup> as a Function of Mode at 95%**

Positioning Mode	GPS+GLONASS	GPS-only	GLONASS-only
Real-Time Stand-alone	16 metres	100 metres	20 metres
Real-Time Code Differential	0.75 metre	0.90 metre	1.0 metre
Real-Time Carrier (Float)	< 0.1 metre	< 0.1 metre	N.A.
Real-Time Carrier (Fixed)	0.02 metre	N.A.	N.A.

The common FTS used in these tests was a Rubidium oscillator (model FRK-LLN), a Ball Efratom product. It is a compact and portable device. Its atomic resonance-controlled oscillator provides a pure and stable sinusoidal signal of 10 MHz. The output signal is obtained from a 10 MHz frequency generator, whose frequency is referenced and locked to the atomic “resonance frequency” of Rubidium, Rb<sup>87</sup>. This Rubidium oscillator generally requires five to ten minutes warm-up initialization period to obtain a drift stability of several parts in  $10^{12}$  [Ball, 1993].

The splitter used in the system is a two-way splitter, capable of splitting the signal simultaneously from a FTS output to two different outputs. It is specifically designed to work with signals in the 5-10 MHz bandwidth. Theoretically, the two output signals should have the same SNR and power levels.

The hardware installation of the GPS/GLONASS heading and pitch determination system used in this study is shown in Figure 6.1.

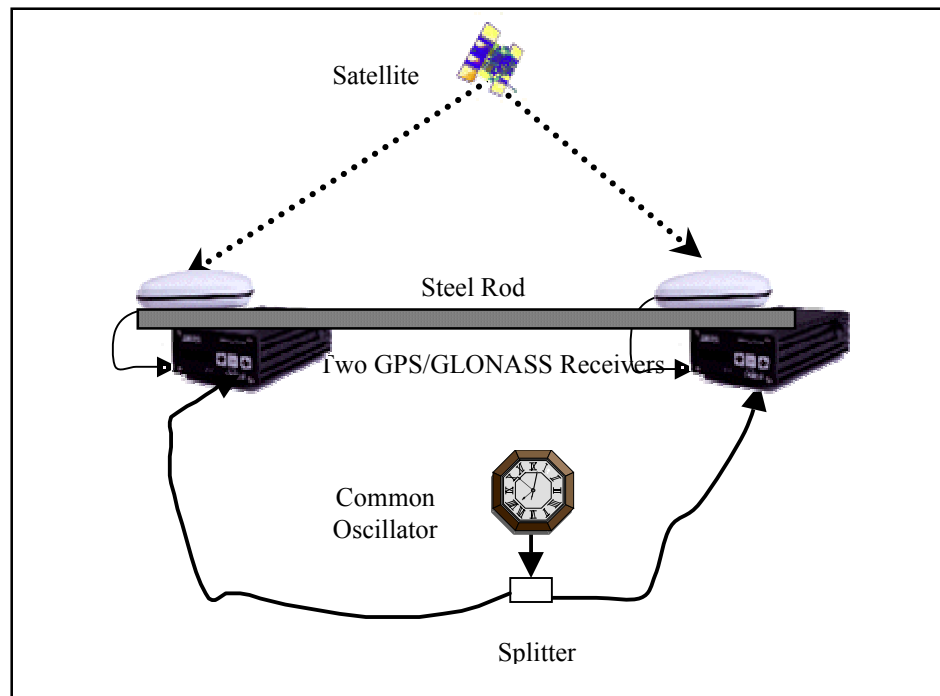


**Figure 6.1: Hardware Installation for GPS/GLONASS Attitude System**

Several factors should be considered when installing the GPS/GLONASS antennas of an attitude system. The antenna locations, the inter-antenna distance, and the stability of the antenna mounts could have influence on the performance of the system. Each antenna location should strive to be clear from obstruction objects which can have severe effect for attitude determination. This is for two reasons. First, it prevents satellite signal interruption and hence has a better view of the sky. Second, it minimizes the multipath influence which may induce significant amount of errors. The distance between the antennas affects the accuracy of the estimated platform attitude parameters. The longer the length, the better the accuracy. This is true provided the platform is free from distortions due to motion, temperature gradients, and etc, which are harder to maintain with longer baseline. The stability of the antenna mounts is also critical to the accuracy of the estimated attitude parameters. Since the platform is considered a rigid body platform, a movement of the antennas is transformed into a variation of attitude

parameters through the estimation process thereby degrading the performance of the system.

When installing the system, the direction from the primary antenna to the secondary antenna defines the heading of the platform. Therefore, the direction from the primary antenna to the secondary antenna should be close to vehicle's physical heading direction as much as possible. In some cases, the baseline formed by two antennas may be parallel to the true heading direction of the vehicle. If this is the case, the heading estimates derived from the GPS/GLONASS attitude system is equal to the true heading of the platform. In most cases, however, it is very difficult to have the set up that the antenna vector is exactly parallel to the vehicle's heading direction. Therefore, a misalignment angle between the two headings needs to be determined and taken into account.

### **6.1.2 Software**

The software implementation of the SD GPS/GLONASS approach was realized by modifying the University of Calgary HEAD<sup>TM</sup> software [Sun et al., 1997]. The original version of HEAD<sup>TM</sup> uses a standard DD GPS approach to resolve integer ambiguity for heading and pitch determinations. The software was modified by the author to accommodate the SD technique described in Chapter Five and to take into considerations of all the GPS/GLONASS differences described in Chapter Three. The new software is called HEADG<sup>2TM</sup>.

The SD carrier phase integer ambiguities are resolved using a least-squares on-the-fly ambiguity resolution technique. The method employed is the one described by Lachapelle et al. [1992]. Modifications are also made to incorporate the known baseline and the pitch constraint from the two antennas, as described in Chapter Five. Figure 6.2 shows a flowchart of the ambiguity resolution process. The speed and reliability of the carrier phase ambiguity resolution depend on the carrier phase noise, multipath effects, satellite geometry and the accuracy of the baseline constraints. The smaller the noise and

multipath effects the faster the resolution of the ambiguities. Also, the higher the number of satellites observed and the more accurate the baseline length, the more reliable are the ambiguities.

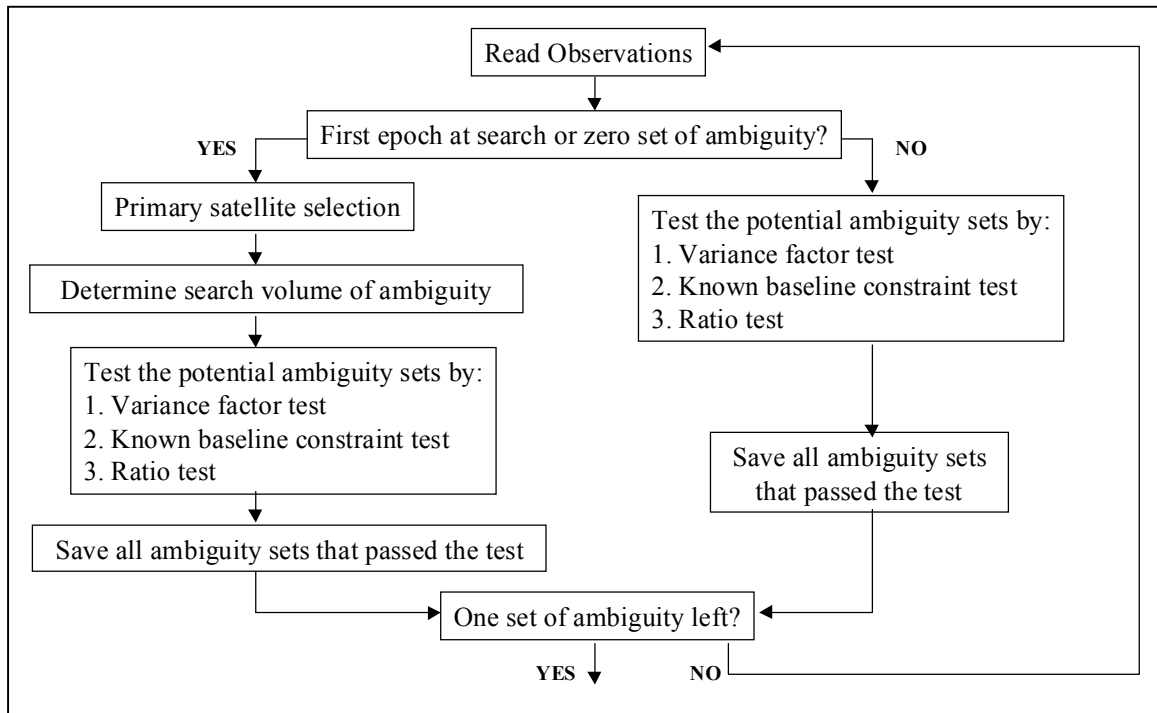


**Figure 6.2: Flowchart of the Ambiguity Resolution Process in HEADG<sup>2</sup>™**

A minimum of four satellites, including at least one from the two systems, is required to initialize the ambiguity search process. Four satellite measurements yield four pairs of SD observations, in which three are used for ambiguity resolution and one is for solving the STD, system-time-difference between GPS and GLONASS. Once the ambiguities are resolved, a minimum of four satellites (GPS, GLONASS, or GPS/GLONASS) is required to estimate heading and pitch.

Cycle slips in the carrier phase measurements cause positions to drift and they degrade the estimated heading and pitch of the platform. Therefore, cycles slips must be taken into considerations. A cycle slip is a sudden jump in the carrier phase observable by an integer number of cycles [Leick, 1995]. The fractional part of the carrier phase is not

affected by this discontinuity in the observation sequence. Cycle clips are caused by the loss of the phase lock loops. Loss of lock may occur briefly between two epochs, or may last several minutes or more if the satellite signals cannot reach the antenna.

Currently, there are two methods implemented in the ambiguity resolution software for cycle slip detection. One is the phase rate prediction and the other one is the precise baseline length check between the two antennas. The method of cycle slip detection using phase rate prediction is as follows:

$$\hat{\Phi}_k = \Phi_{k-1} + \frac{\dot{\Phi}_k + \dot{\Phi}_{k-1}}{2} \delta t \quad (6.1)$$

where,

$\hat{\Phi}_k$  is the predicted phase measurement at  $t_k$  (cycles),

$\Phi_{k-1}$  is the phase measurement at  $t_{k-1}$  (cycles),

$\dot{\Phi}_k$  is the phase rate measurement, Doppler, at  $t_k$  (Hz),

$\dot{\Phi}_{k-1}$  is the phase rate measurement, Doppler, at  $t_{k-1}$  (Hz), and

$\delta t$  is the time difference between the current and previous epochs (second).

The predicted phase measurement is then compared to the measured phase:

$$\left| \hat{\Phi}_k - \Phi_k \right| < \tau_c \quad (6.2)$$

where  $\tau_c$  is the tolerance criterion for cycle slip detection capability of the phase rate method. The numerical value of the tolerance criterion depends on the data interval, phase rate accuracy and the dynamics of the vehicle. In land and marine kinematic mode with one second data intervals, a 10 to 15 cycle tolerance will be suitable in most cases.

In a twin-antenna system, the baseline length between the antennas is precisely determined before a mission. If cycle slips occur in the phase measurements and are not corrected, the computed baseline length will gradually drift away from the known true baseline length [Lachapelle et al., 1992]. Therefore, the computed (estimated) baseline lengths are compared to the known baseline lengths at every epoch to detect cycle slips:

$$|\hat{L} - L| < \tau_d \quad (6.3)$$

where,

- $\hat{L}$  is the estimated baseline length,
- $L$  is the known baseline length, and
- $\tau_d$  is the tolerance criterion in unit of length.

If the above equation is not satisfied for any three consecutive epochs, the ambiguities related to this baseline are set to invalid and are re-initialized by the search process. The tolerance criterion  $\tau_d$  is a function of the accuracy of the known baseline length, carrier phase multipath effects and measurement noise. It should not be less than two centimetres in order to absorb the multipath effects on the GPS/GLONASS computed baseline length, even if the known baseline is very precise, such as better than one centimetre.

Chapter Five describes the necessity for having a residual feedback system to estimate the bias in the SD residuals. The flowchart of the residual feedback system is shown in Figure 6.3.

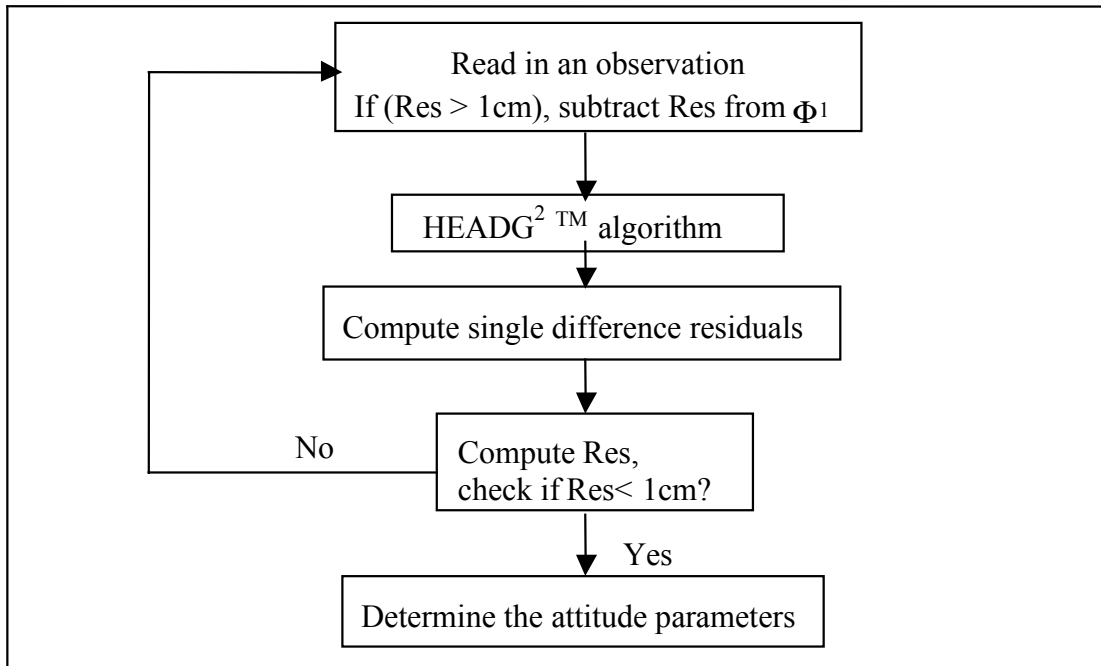


**Figure 6.3: Flowchart of the Residuals Feedback System**

A bias in the SD residuals is computed using the Eq. (5.13) and Eq. (5.14) as described in the previous chapter. If the numerical value of the bias-residuals is found to be larger than one centimetre, which is about 0.05 of a L1 cycle, a correction of that value will be fed back to the observation in the next epoch. After the feedback algorithm, the fractional part of the  $\Delta_{\text{comb}}$  term in Eq. (5.4) is removed and the correct SD integer ambiguity can then be correctly resolved.

## 6.2 Static Test I

A static test was first conducted on the roof of the Engineering building at the University of Calgary. An one-hour data set was collected. The antenna baseline vector was formed by two pillars separated by approximately three metres. The three-dimensional baseline coordinates were determined beforehand to an accuracy of two millimetres during a previous campaign. Using a GPS standard DD approach with fixed integer ambiguity, the estimated heading and pitch were found to be  $89.817^\circ$  and  $-0.458^\circ$ , respectively.

### 6.2.1 $10^\circ$ Elevation Mask

The results of the test reveal that the geometry of the satellites was fairly good. For a  $10^\circ$  elevation mask, which is commonly used in practice to reduce the effect of multipath, the number of GPS satellites was seven, while the number of GLONASS satellites varied from two to four. The ADOP of the GPS/GLONASS (GG) constellation is not much better than that of GPS alone, and both are always less than one. The EDOP, affected also by the RVDOP, are in the range of one to two.

The number of satellites, ADOP and EDOP for the solutions from GPS and GG are shown in Figure 6.4. The ones from GPS-only solution are plotted in blue (darker) colour, whereas, the ones from GG solution are plotted in red (lighter) colour. The results from heading and pitch estimates, together with their statistics, are shown in Figure 6.5 The plots for GPS are shifted by  $1^\circ$  for clarity. The statistic  $d_{\text{mean}}$  denotes the difference in the mean values of the SD solution from the referenced solution, and RMS is the squares-root of the quadratic sum of  $d_{\text{mean}}$  and standard deviation of the solution.

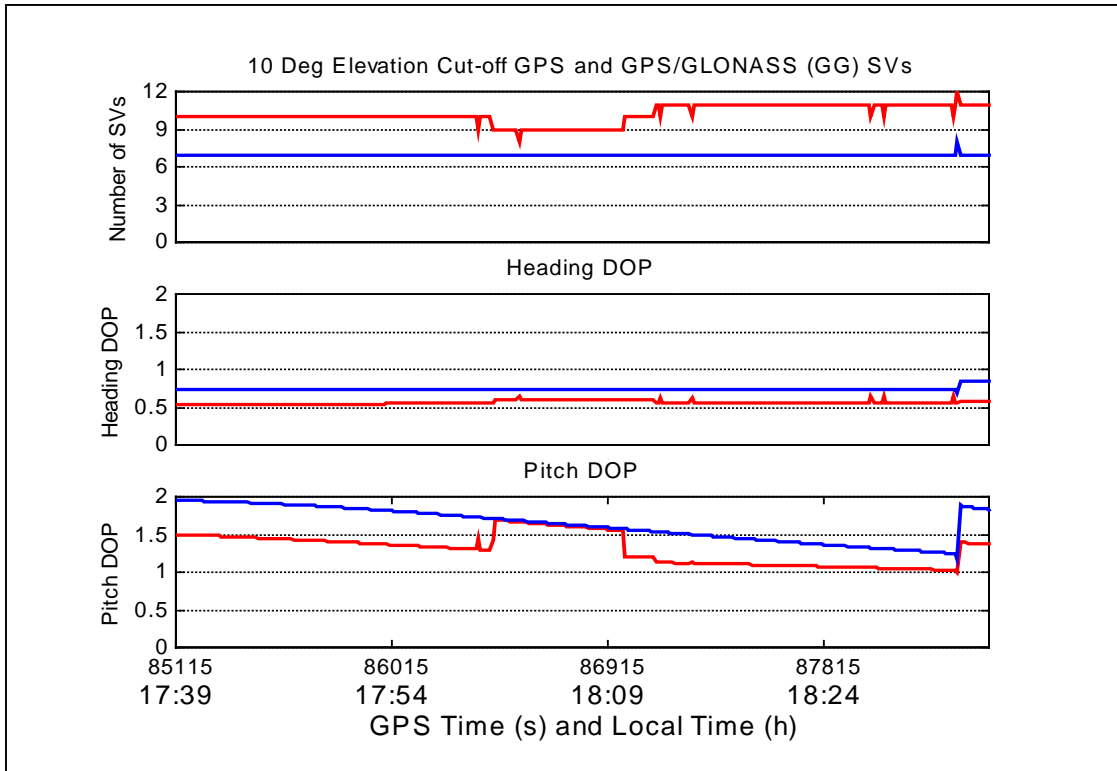


**Figure 6.4: Number of SVs, ADOP, and EDOP for 10° Elevation Mask – Static Test**

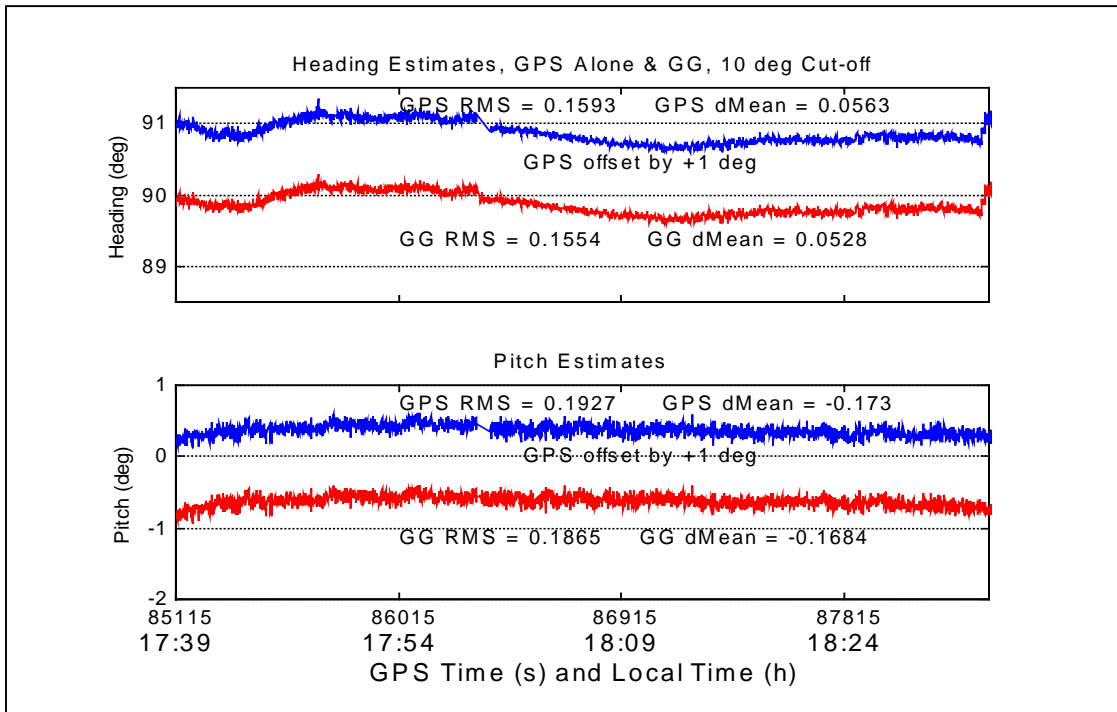


**Figure 6.5: GPS and GG Heading and Pitch Estimates for 10° Elevation Mask – Static Test**

It can be seen from Figure 6.5 that the heading and pitch estimates from the GPS and GG solutions are not significantly different from each other. The heading RMS differences from the reference values, denoted by  $d_{\text{mean}}$ , are  $0.1593^\circ$  for GPS and  $0.1554^\circ$  for GG. The corresponding RMS differences in pitch are  $0.1927^\circ$  and  $0.1865^\circ$  for GPS and GG, respectively. A noticeable difference of the two sets of results in Figure 6.5 is that, at epochs 86305 to 86395, the computed residuals exceed the limit. Thus, the software re-initialized the ambiguity search process and initially obtained wrong estimates for a few epochs. Quickly, the software found the error and a correct set of ambiguities were found and used. With the addition of two GLONASS satellites, the software was able to prevent the wrong set of ambiguities from being selected. This shows that more satellites are good for speed and reliability of ambiguity fixing.

### **6.2.2 35° Elevation Mask**

In order to show the performance of GLONASS augmentation under signal masking or reduced visibility condition, an isotropic wall was simulated with a  $35^\circ$  elevation mask angle. As can be seen in Figure 6.6, the number of GPS satellites jumps from three to four at epoch 86800. The number of GLONASS satellites stays at two for the entire period of time with occasional loss of lock. The ADOP is two to three when the number of GPS satellites is three and it is around one when the number of GPS satellites is four. There is not much difference in the ADOP when adding the two GLONASS satellites. The EDOP increases dramatically from three to eight when the number of GPS satellites is at three, this is probably due to the change of satellite over time. The EDOP reduces immediately to three after the fourth GPS satellite becomes available and it reduces further to one with the GLONASS augmentation. Figure 6.7 shows the heading and pitch estimates, together with statistics, under the  $35^\circ$  signal masking for GPS and GG.

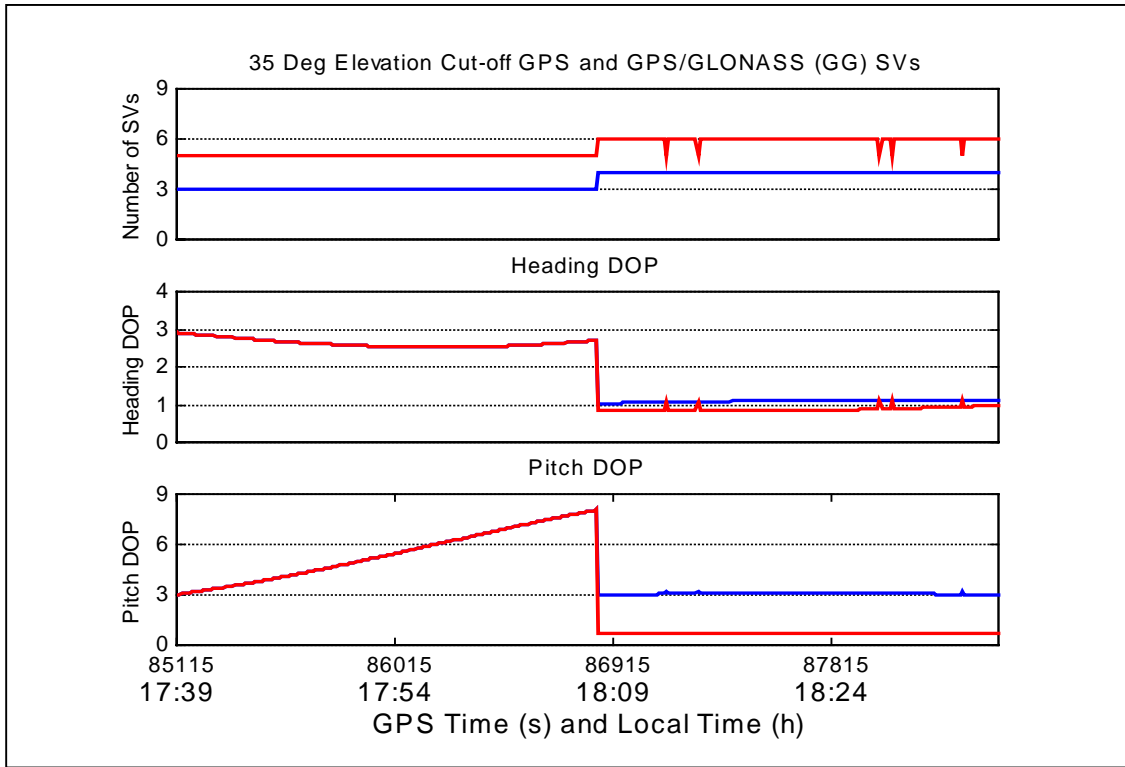


Figure 6.6: Number of SVs, ADOP, and EDOP for 35 ° Elevation Mask – Static Test

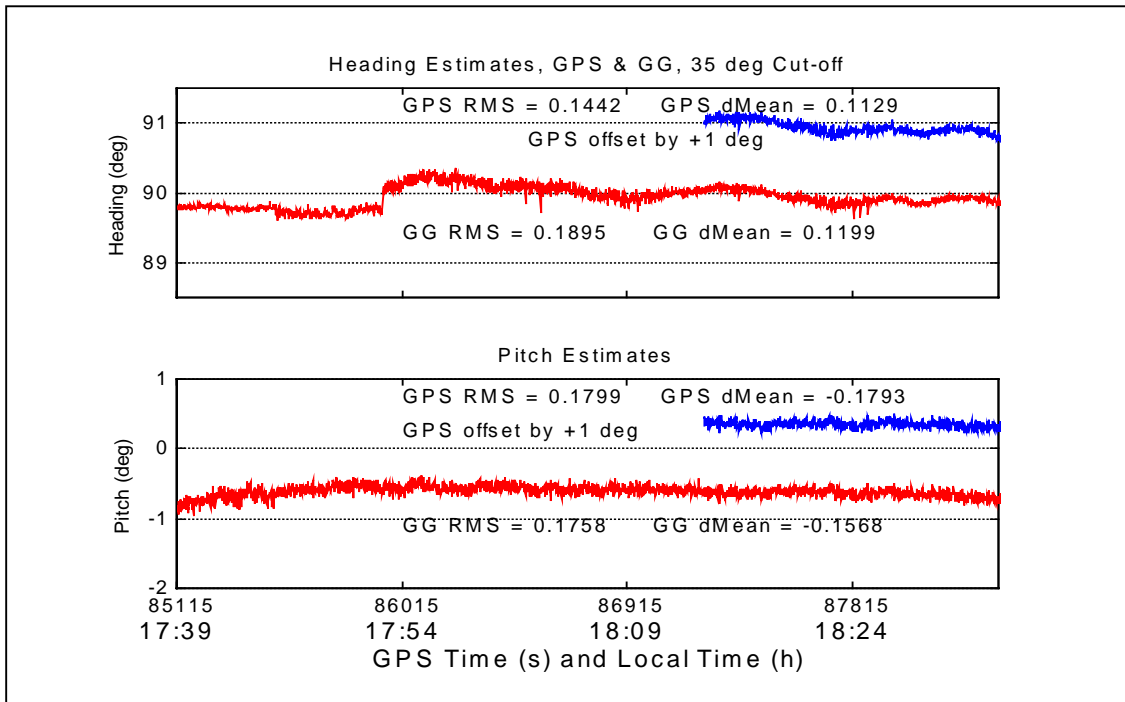


Figure 6.7: GPS and GG Heading and Pitch Estimates for 35° Elevation Mask – Static Test

The advantage of GLONASS augmentation is quite obvious. With GPS alone, estimates are only available for 35% of the time. The use of GG results in close to 100% availability. Again, no conclusion as of the inferiority or superiority in accuracy performance of the GLONASS augmentation can be concluded.

Therefore, the static test shows that the combined GPS/GLONASS SD solution for heading and pitch determination is compatible with the corresponding standard GPS DD results. The RMS differences of GPS and GG are quite similar.

### **6.3 Kinematic Test I**

After obtaining some satisfactory results from the static test, a kinematic test was conducted in an unobstructed area to validate the SD approach in a normal operating environment. The data was collected for about 1.5 hours on September 6, 1998. The system described at the beginning of the chapter was installed on a steel rod mounted on the roof of a vehicle. The equipment used in the static test was used. The length of the baseline is 0.9 metre. The vehicle speed ranged from 25 km/h to 55 km/h. The pitch angle variation ranged from  $-10^\circ$  to  $+10^\circ$ . The reference heading and pitch estimates, shown in Figure 6.8, were obtained using the standard fixed ambiguity GPS DD technique.

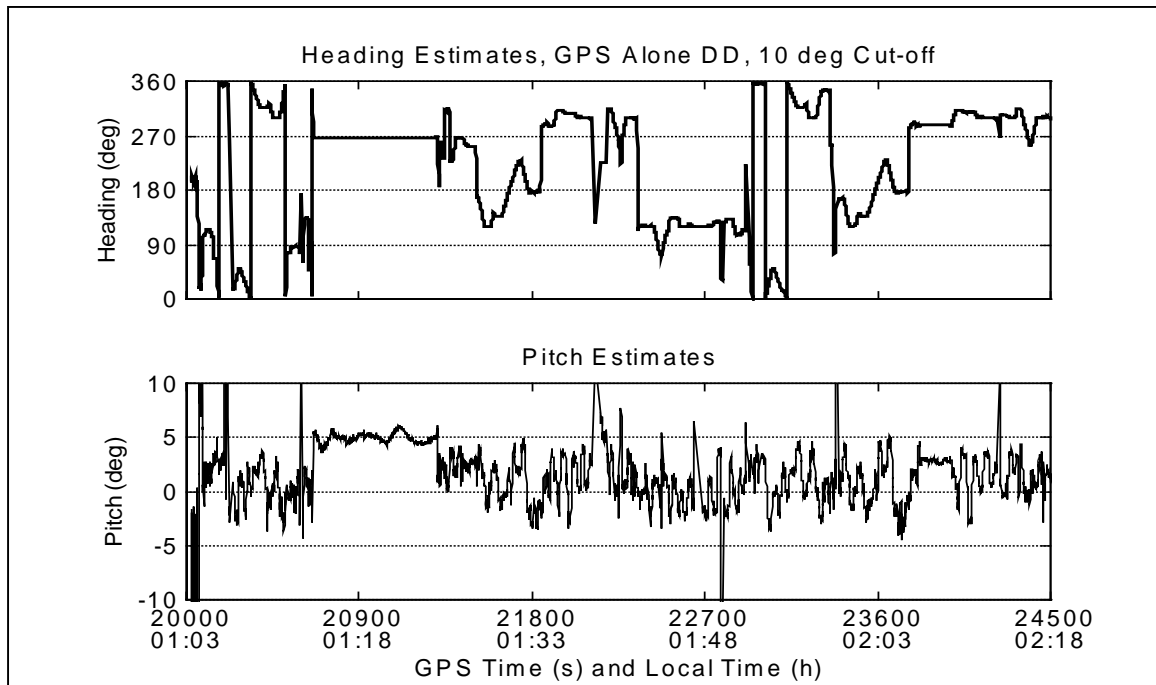


**Figure 6.8: Reference Estimates of Heading and Pitch from Standard GPS DD Technique – Kinematic Test I**

### 6.3.1 10° Elevation Mask

Again, a 10° elevation mask was used to reduce the effect of multipath. There were about six to seven GPS satellites available throughout the test interval. The number of GLONASS satellites varied from two to three from time to time. The ADOP of the combined GG solution was not much better than that of GPS and both were less than one. GLONASS augmentation however did improve the EDOP. The combined GG solution reduced the EDOP to 1.5, comparing to having a value of two with GPS-only solution. This shows the satellite geometry may have a significant impact in one solution but not in the other. The number of satellites together with ADOP and EDOP are shown in Figure 6.9. The ones from GPS-only solution are plotted in blue (darker) colour, whereas, the ones from GG solution are plotted in red (lighter) colour. The heading and pitch estimates from GPS-only and combined GG solutions can be seen in Figure 6.10. The GPS/GLONASS estimates are offset by 3° for heading and 6° for pitch.

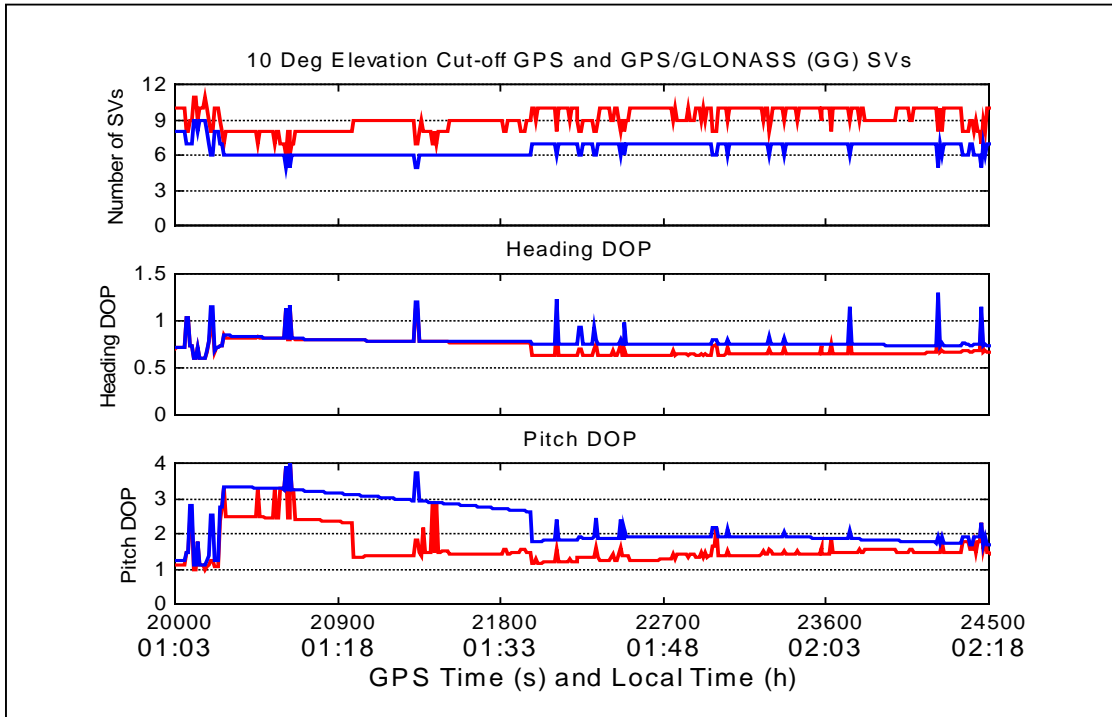


**Figure 6.9: Number of SVs, ADOP, and EDOP for 10° Elevation Mask – Kinematic Test I**

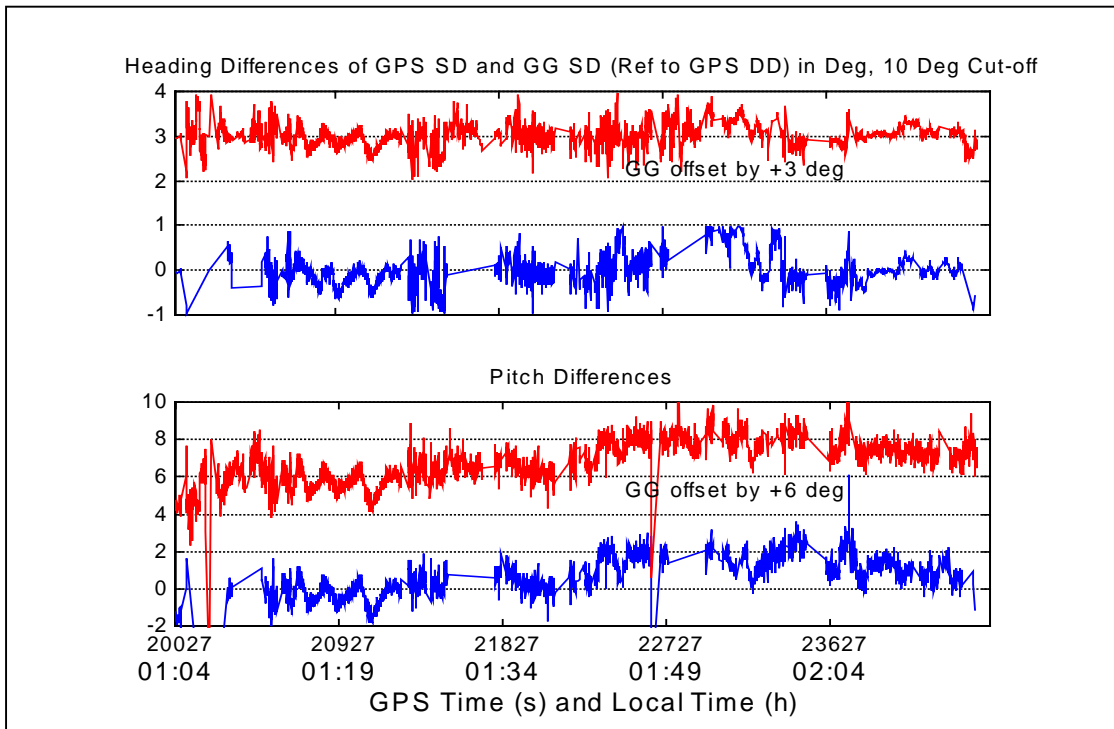


**Figure 6.10: Differences in SD Heading and Pitch Estimates with respect to (w.r.t.) GPS DD for 10° Elevation Mask – Kinematic Test I**

GLONASS augmentation increased availability by 6%. In the gaps where no heading and pitch were estimated due to ambiguity fixing failure, GLONASS augmentation resulted in faster recovery due to the addition of two to three satellites. A blunder is defined as an estimated value being different from the reference value by a magnitude of more than three times the standard sigma, giving a confidence level of 99.7%. Blunders are mainly caused by having incorrect ambiguity fixes during the ambiguity resolution algorithm. Thus, the number of blunders can be used as a reliability measure. The percentage of blunders is significantly reduced from 7.5% to 1.5% with GLONASS augmentation. The GPS and GG mean and RMS differences for both heading and pitch estimates are statistically similar. A summary of the statistics of the results is given in Table 6.2.

### 6.3.2 30° Elevation Mask

As in the case for the static test, a 30° isotropic signal masking angle was introduced to investigate the system performance under signal masking conditions. Figure 6.11 shows the number of satellites and the associated ADOP and EDOP for both GPS-only and combined GG solutions. The number of GPS satellites is at five throughout the first two-third of the period of the test interval and gradually decreases to three towards the end, whereas the number of GLONASS satellites varies from one from two. The ADOP of the combined GG solution is not much better than that of GPS. Both of them are around one during the first two-third period, and the one from the GPS-only solution increases to three and above in the last one-third period whereas that from the GG solution is at two. GLONASS augmentation however does improve the EDOP. The combined GG solution reduces the EDOP to three from five and then to five from eight, compared to the GPS-only solution. The heading and pitch estimates from GPS-only and combined GG solutions can be seen in Figure 6.12. The GPS/GLONASS estimates are offset by 3° for heading and 6° for pitch. Statistics of the results are summarized in Table 6.2.

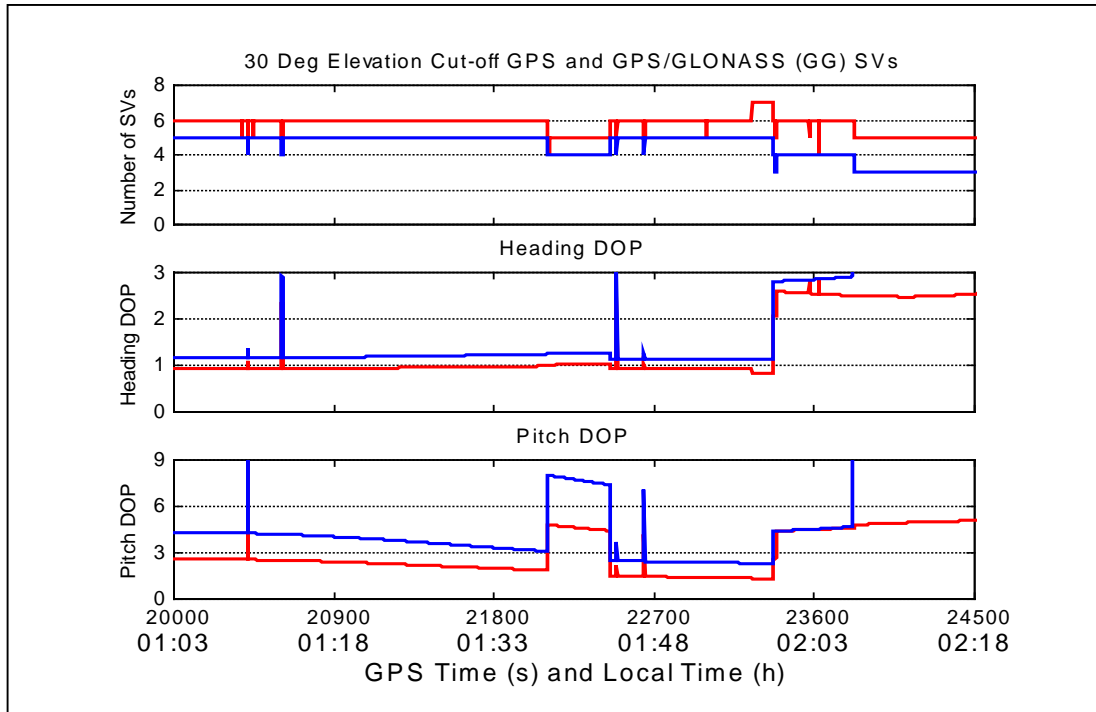


**Figure 6.11: Number of SVs, ADOP, and EDOP for 30° Elevation Mask – Kinematic Test I**

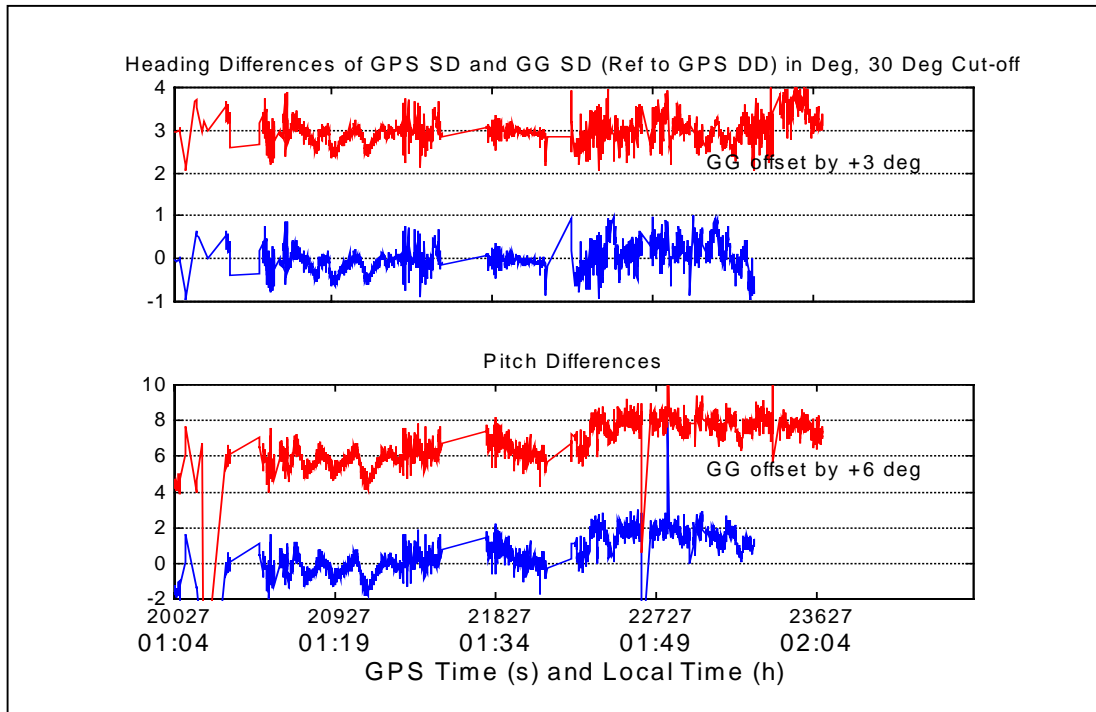


**Figure 6.12: Differences in SD Heading and Pitch Estimates w.r.t. GPS DD for 30° Elevation Mask – Kinematic Test I**

**Table 6.2: Statistics of GPS and GLONASS Augmentation for 10° and 30° Elevation Mask – Kinematic Test I**

	Mean/ RMS $\psi$	Mean/ RMS $\theta$	Availability	Blunder Percentage
GPS	-0.04°	0.56°	85%	7.5%
10° mask	0.34°	1.15°		
GG	-0.15°	0.66°	91%	1.5%
10° mask	0.25°	1.26°		
GPS	0.01°	0.57°	60%	9.2%
30° mask	0.30°	1.17°		
GG	-0.02°	0.77°	71%	7.8%
30° mask	0.30°	1.39°		

Statistics for the 30° elevation mask shown in Table 6.2 reveal that availability is improved by 11% with GLONASS augmentation, whereas blunders are reduced by 1.4%. Similar to the 10° elevation mask case, no improvement in RMS or mean differences with the GLONASS augmentation occurs.

#### 6.4 Kinematic Test II

The next kinematic test conducted to test the SD approach consists of data from two parts, one from an unobstructed open-sky area and the other from a less open residential area. The two data sets were collected in mid February 1999. The same system described earlier was installed on the roof of a vehicle. The length of the baseline was 1.1 metre. The vehicle speed ranged from 20 km/h to 80 km/h. The pitch angle of the platform varied from +8° to -8°. Reference heading and pitch estimates, shown in Figure 6.13, were obtained using the GPS measurements with the standard DD approach.

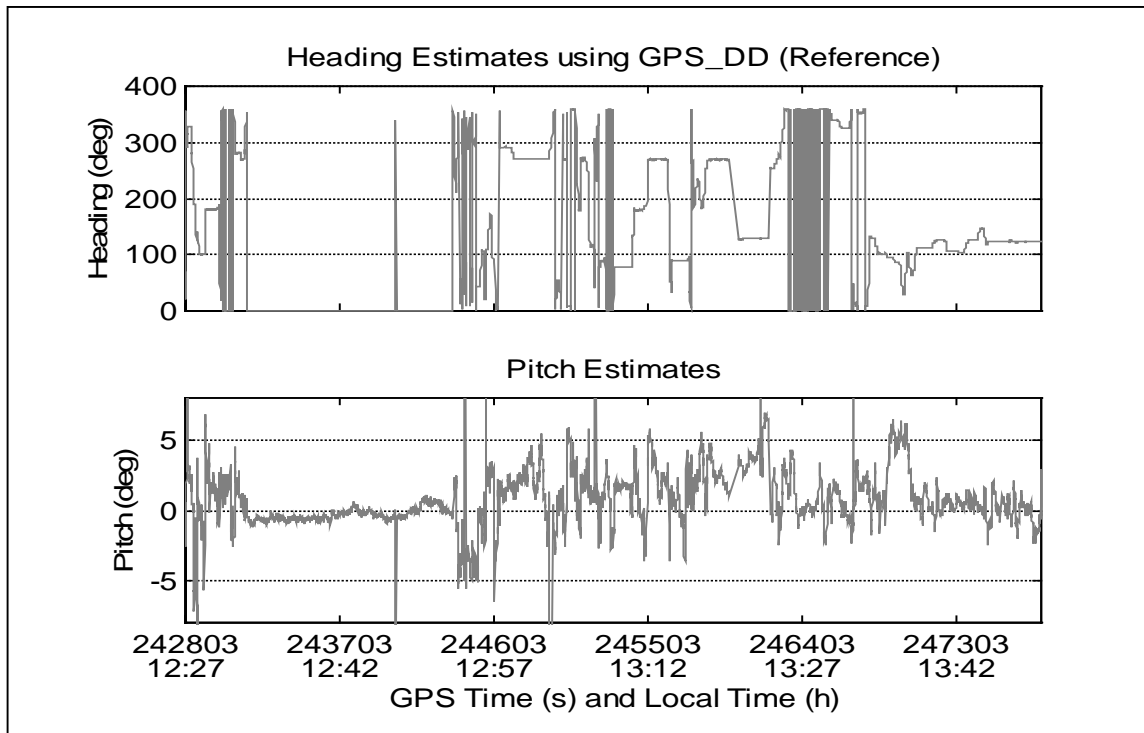


**Figure 6.13: Reference Estimates of Heading and Pitch using a Standard GPS DD Technique – Kinematic Test II**

#### 6.4.1 Open Sky Area

The data set was collected in an open sky area in the northwest quadrant of Calgary and was about 1.5 hour long. Again, a typical  $10^\circ$  elevation masking angle is used. The number of GPS satellites ranged from seven to eight, whereas the number of GLONASS satellites stayed at four throughout the period. The ADOP of the combined solution was not much better than that of GPS and both were less than one most of the time. GLONASS augmentation however did improve the EDOP (Elevation or pitch DOP). During the interval between 244300 s and 246050 s, the combined GG solution reduced the EDOP to about 1.2, from about 1.8 with the GPS-only solution. The number of satellites, ADOP, and EDOP from both solutions are shown in Figure 6.14. The ones from GPS-only solution are plotted in lighter colour, whereas, the ones from GG solution are plotted in darker colour. Figure 6.15 shows the heading and pitch estimates from the two solutions. The GG solution is offset by  $5^\circ$  for heading and pitch for clarity.

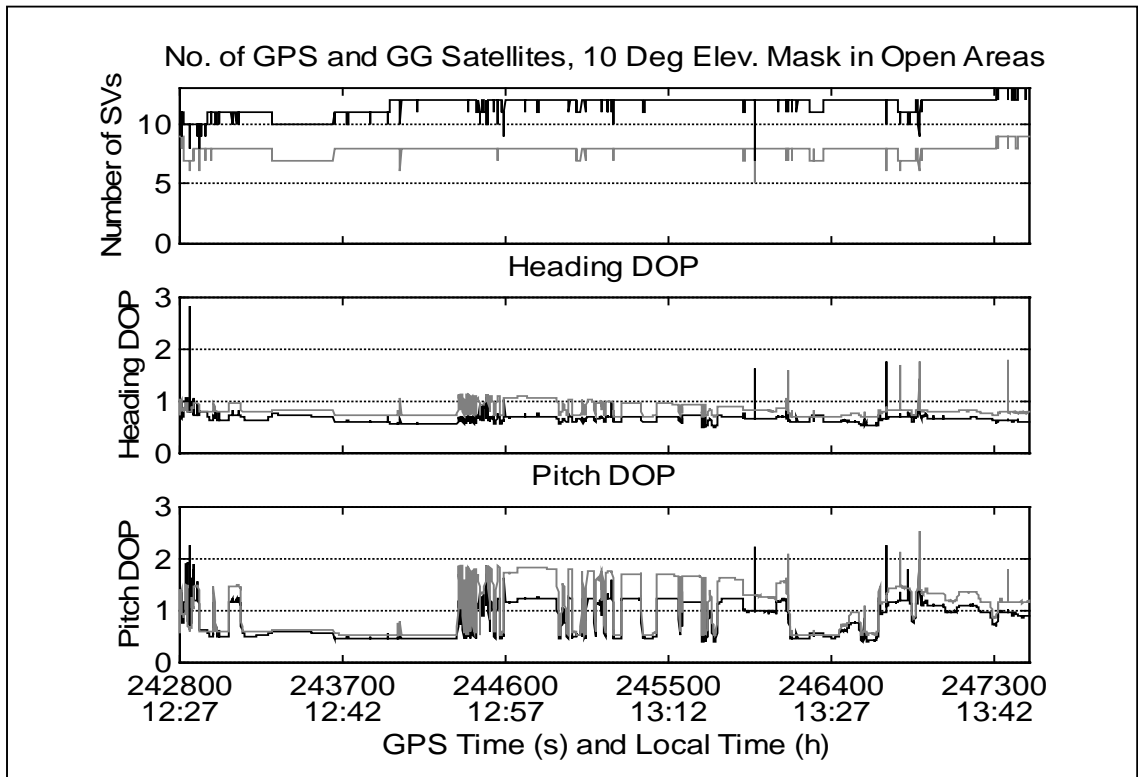


**Figure 6.14: Number of SVs, ADOP, and EDOP for Open Sky – Kinematic Test II**

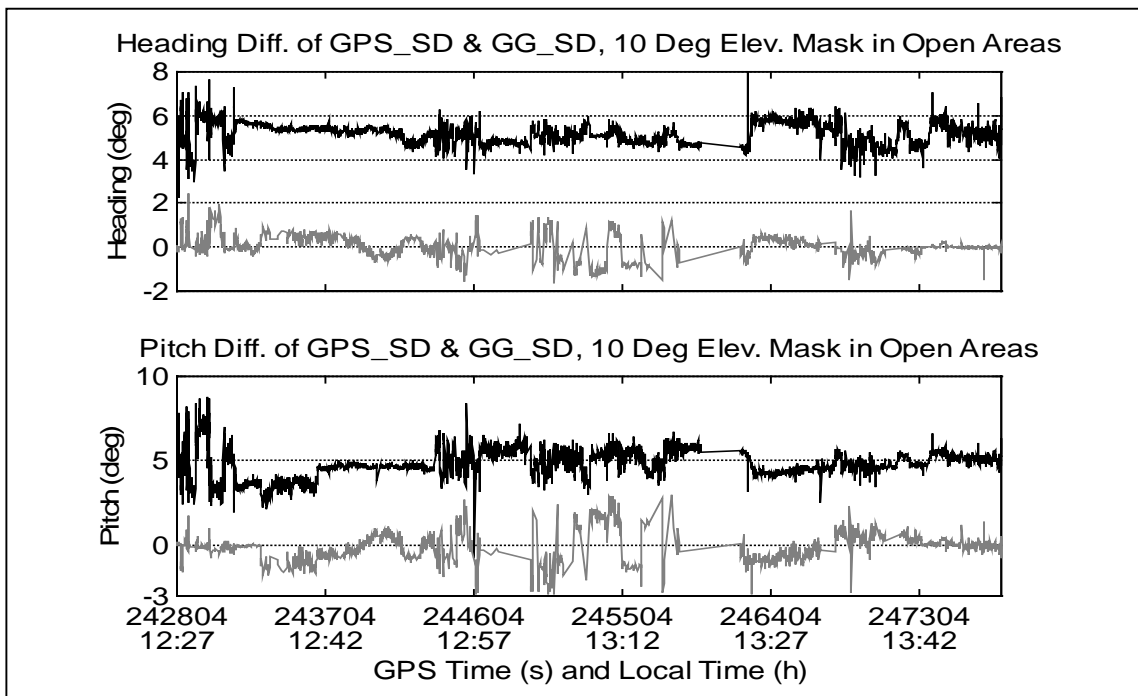


**Figure 6.15: Differences in SD Heading and Pitch Estimates w.r.t. GPS DD for Open Sky – Kinematic Test II**

Again, both solutions are obtained with the SD method while the reference solution is obtained with the DD method as described earlier. The agreement between the two solutions provides a measure of compatibility of the two approaches since they are both based on the same measurements. The statistics are summarized in Table 6.3. GLONASS augmentation increases availability by about 3%. In the gaps where no heading and pitch were estimated due to ambiguity fixing failure, the augmented GLONASS solution again resulted in faster recovery. The percentages of blunders were about the same with and without GLONASS augmentation. The GPS and GG mean and RMS differences for both heading and pitch estimates are quite statistically similar.

#### **6.4.2 Residential Area**

Another data set, lasting about an hour, is collected from a less open residential area in the City of Calgary. The purpose of collecting this data set was to investigate the performance of the system under true reduced visibility conditions.

To reduce the effect of multipath, a  $10^\circ$  elevation masking angle was used. Only four to six GPS satellites were available during the first three-fourth period of the test interval and another satellite appeared in the last quarter. The number of GLONASS satellites stayed mostly at two (with occasional jumps to three) throughout the period. The ADOP and EDOP from the combined GG solution is about 0.5 better than the corresponding values from the GPS-only solution.

Figure 6.16 shows the number of satellites and the associated ADOP and EDOP for the two solutions. The ones from GPS-only solution are plotted in lighter colour, whereas, the ones from GG solution are plotted in darker colour. The heading and pitch estimates from GPS-only and combined GG solutions are shown in Figure 6.17. The GG estimates again are offset by  $5^\circ$  for heading and pitch for clarity.

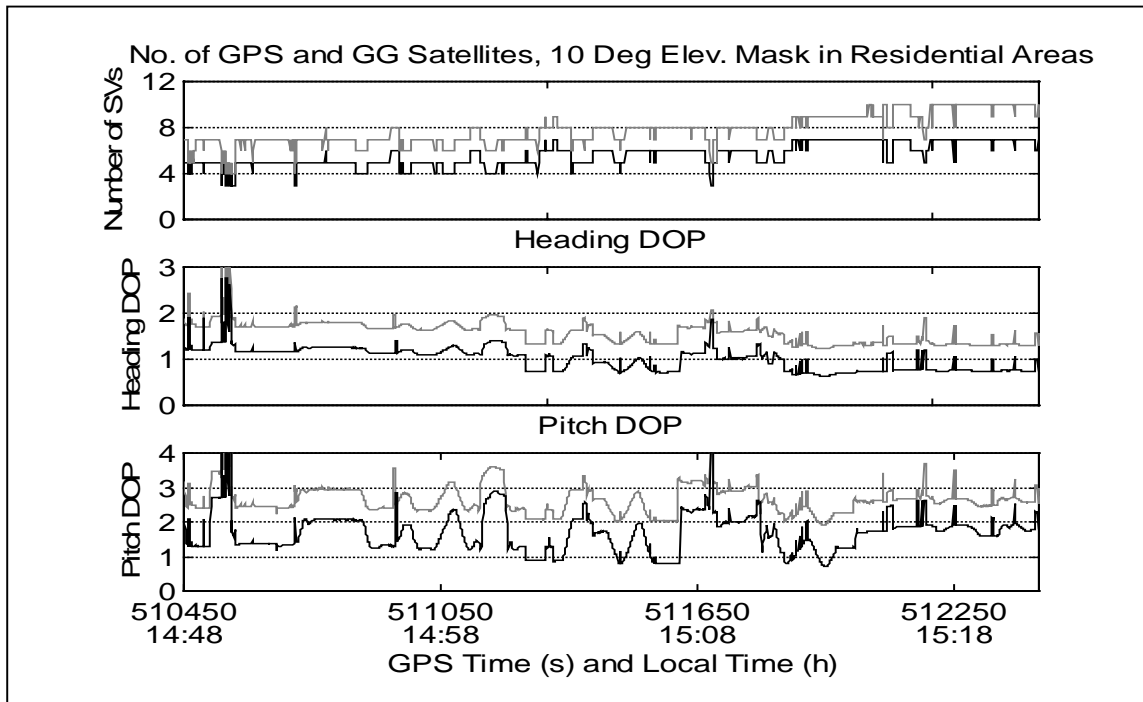


**Figure 6.16: Number of SVs, ADOP, and EDOP for Residential Area – Kinematic Test II**

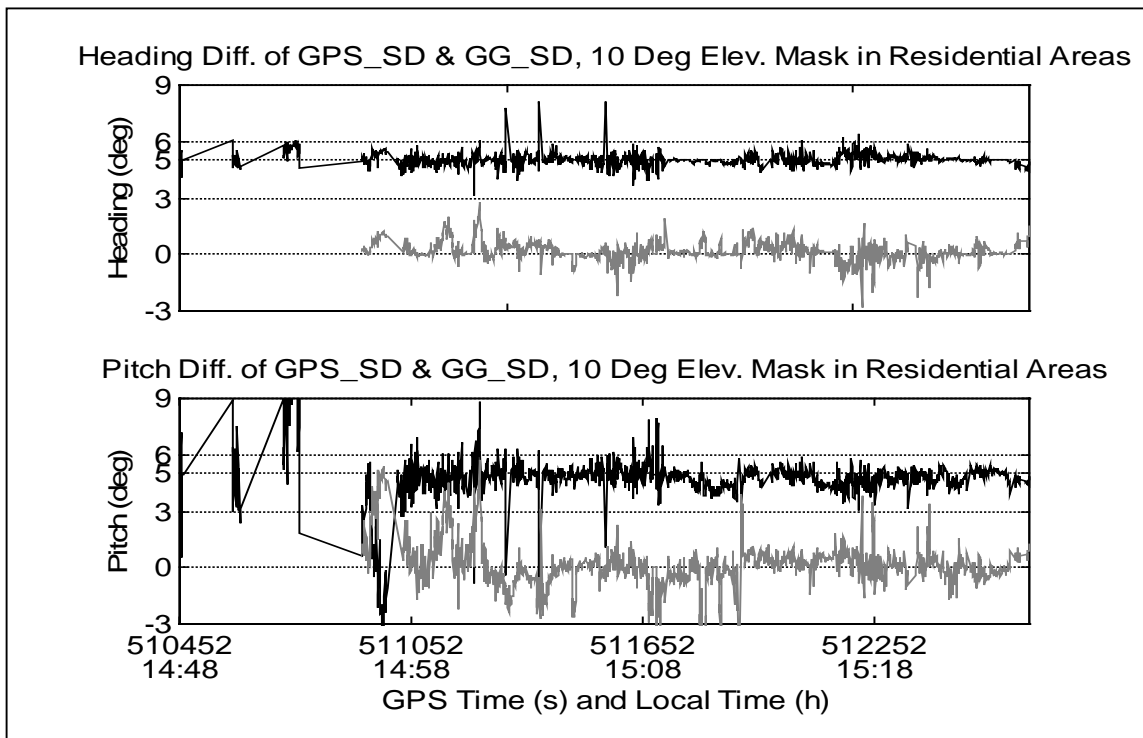


**Figure 6.17: Differences in SD Heading and Pitch Estimates w.r.t GPS DD for Residential Area – Kinematic Test II**

The statistics of the results are also summarized in Table 6.3. An improvement in availability by an amount of 8% is reported when GLONASS measurements are augmented to the measurements of GPS. However, the percentage of blunders also increased, namely by 2.9%. The cause of this is likely due to either a filter tuning problem or the additional noise in the GLONASS measurements. Another possibility for this cause is the temperature effects on frequency differences (for e.g. [Dodson et al 1998]). Under signal masking conditions, the use of the combined solution is still advantageous to improve availability.

**Table 6.3: Statistics of GPS and GLONASS Augmentation for Open Areas and Residential Areas – Kinematic Test II**

	Mean/ RMS $\psi$	Mean/ RMS $\theta$	Availability	Blunder Percentage
GPS open sky	0.02°	-0.06°	89%	1.8%
	0.46°	0.80°		
GG open sky	0.15°	-0.16°	91%	2.2%
	0.50°	0.84°		
GPS Residential	0.17°	0.20°	71%	7.2%
	0.53°	1.26°		
GG residential	0.04°	-0.25°	79%	10.1%
	0.33°	1.38°		

The results show that GLONASS augmentation improves the availability of the heading and pitch attitude determination system. This is especially true under reduced visibility conditions. The ADOP and EDOP obtained from the combined GG solutions are always better than those from the GPS-only solutions.

With the addition of GLONASS satellites, the system is able to prevent some wrong set of ambiguities from being selected. This shows the advantage of having more satellites in speed and reliability in ambiguity fixing. Also, in some occasions where no heading and pitch were estimated due to ambiguity fixing failure, GLONASS augmentation resulted in faster recovery than the GPS-only solution.

The improvement in availability, however, comes at a cost of a slightly lower heading and pitch accuracy. This is due to the limits of the single difference approach and the FDMA technique used by GLONASS. Residual clock and line biases have to be estimated with a filter and contribute to the increase in the noise in the SD measurements. Other limits such as temperature effects may also be contributing to the error budget [Walsh & Daly, 1997]. This could also be the reason for a lack of accuracy improvement.

To quantify the results from the heading and pitch results as a function of inter-antenna distance, Table 6.4 lists the results of heading and pitch determination using GPS and GLONASS measurements.

**Table 6.4: Accuracy of Heading and Pitch with Different Inter-antenna Distances**

	GPS-only DD					GPS/GLONASS SD			
Inter-antenna Distances (m)	0.15	0.31	0.45	0.75	0.9	0.9	1.1	3.0	12.0
Heading (deg)	1.67	0.70	0.46	0.40	0.27	0.23	0.29	0.11	0.01
Pitch (deg)	3.27	1.66	1.07	0.89	0.43	0.93	0.78	0.14	0.03

The results listed in the first five columns are those from the previous campaign with measurements from GPS using a DD approach ([Lachapelle et al., 1996] and [Szarmes et al., 1997]). The results from the next four columns are from the results reported in this study using GPS/GLONASS SD approach. The last two columns are results obtained in static mode whereas the rest are all in kinematic mode.

Comparing the results in Table 6.4, it can be found that the accuracy of the attitude parameters is inversely proportional to the distance between the two antennas in the attitude system. This can be shown in Figure 6.18. The attitude accuracy increases with inter-antenna distance due to the decreasing effect of carrier phase noise and multipath on angular accuracy. This verifies that the statement on baseline impact on attitude accuracy made in Chapter Four is indeed true.

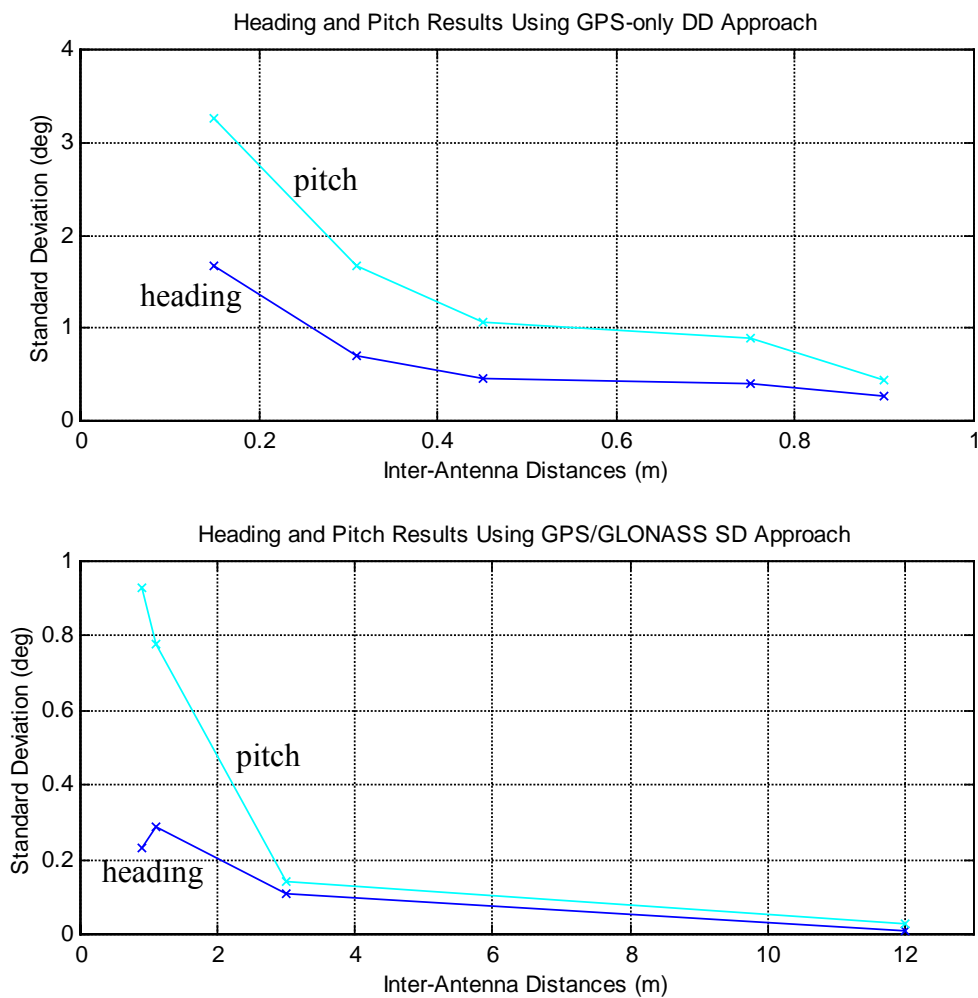


**Figure 6.18: Attitude Accuracy as a Function of Inter-Antenna Distance**

To translate the above angular accuracy into baseline positional accuracy, one may obtain a combined effect of carrier phase noise and multipath errors in the order of five-millimetre level (with an average ADOP of one and PDOP of two to three). Again, this level of errors is quite typical for an attitude system.

## CHAPTER SEVEN

### CONCLUSIONS AND RECOMMENDATIONS

An approach to combine GPS and GLONASS measurements, using a single differencing technique with a common FTS, to determine the heading and pitch parameters using a pair of non-dedicated GPS/GLONASS receivers has been presented in this thesis. The approach has been successfully applied to a two-dimensional attitude system.

#### 7.1 Conclusions

The receiver measurement noise of the GLONASS L1 C/A code is found twice as noisy as that of GPS. For the Ashtech GG24<sup>TM</sup> GPS/GLONASS receivers used in this research, the magnitudes of the code noise are 1.1 m and 2.4 m for GPS and GLONASS respectively. This is in accordance to the fact that the wavelength of GLONASS code is double the length of that of GPS. The carrier phase noise was found to be 1.1 mm for both GPS and GLONASS measurement on the Ashtech GG24<sup>TM</sup>. Therefore, it can be concluded that accuracy of L1 carrier phase, the main observable used for attitude determination, of GLONASS is compatible to that of GPS.

Besides the receiver measurement noise, multipath is a much more dominant error source in an attitude system. The effect of GPS/GLONASS carrier phase multipath on static-platform attitude estimation is investigated using a Day 1 – Day 9 repeatability test. The effect of multipath is found to be  $0.01^\circ$  for heading and  $0.03^\circ$  for pitch (about 2 mm and 6

mm, respectively, in position accuracy). This level of accuracy is similar to that of GPS-only measurements and is within the expected accuracy range of carrier phase noise with the presence of moderate multipath. In order to achieve the highest possible accuracy in attitude determination, multipath should be reduced, if not avoided, as much as possible.

Each GLONASS satellite transmitting signal with its own slightly different frequency makes the double differencing of carrier phase observables no longer possible without modification. To get around this problem, the use of the between-receiver single differencing of the carrier phase observables is found to be a feasible alternative. Using the between-receiver single differencing technique, there is a remaining error caused mainly by the clock offset and line bias. This remaining error shows up as a random bias in the residuals. The multiples of the L1 wavelength part of the error are absorbed in integer ambiguities. Therefore, only the remaining fractional part of the error, with theoretical maximum of half a wavelength, shows up as a constant bias in the single difference residual. This residual bias is shown to be common and identical in all satellites.

Given the fact that the bias in the residuals is of random bias nature, a low-pass averaging filter is used to estimate the magnitude of this residual bias. Once the biases are estimated and fed back to the carrier phase observations, zero-mean residuals can be obtained. During the convergence phase of the filter, the estimated attitude parameter accuracy will be lower than once the filter has converged. Errors in estimation, due to mainly multipath and the receiver measurement noise, will increase the single difference carrier phase observable noise and will further degrade estimated attitude parameter accuracy. The single difference accuracy of GPS/GLONASS derived attitude parameters is therefore expected to be somewhat lower than the corresponding accuracy derived using a conventional double difference approach in the case of GPS.

A static “shadow test” conducted to verify if the residuals are indeed constant over time even when no satellites are tracked concluded that the effects of clock offset and line bias

are indeed constant after the shadow period. Another static “clock test” confirmed that the quality of the FTS selected has no significant impact on the accuracy of the estimates of attitude parameters.

The results and analysis described in Chapter Six showed that, even with a current (1997 to present) GLONASS constellation of only 10 to 16 satellites, GLONASS augmentation improves the availability of attitude determination system. This is especially true under signal masking conditions. The ADOP and EDOP of the combined GPS/GLONASS solutions are always better than those of the GPS-only solutions.

With the addition of GLONASS satellites, the system is able to prevent the selection of wrong sets of ambiguities. This shows that the used of more satellites is advantageous for speed and reliability in ambiguity fixing. Also, in cases where gaps exist due to ambiguity fixing failure, GLONASS augmentation resulted in faster recovery than GPS alone.

The improvement in availability, however, comes at a cost of a slightly lower heading and pitch accuracy. This is due to the limits of the single difference approach and the FDMA technique used by GLONASS. Residual clock and line biases have to be estimated with a filter and contribute to the increase of the noise in the single difference measurements. Other limits such as temperature effects may also be contributing to the error budget. This could also be the reason for a lack of accuracy improvement.

## **7.2 Recommendations**

Based on the findings of this research, the following recommendations for future work to improve the performance of the system are suggested:

Firstly, the filter used to estimate the bias in residuals caused by the clock offset and line bias could be improved. An adaptive filter could be developed to replace the low-pass averaging filter, which is one of the causes for accuracy degradation.

Secondly, the effect of GLONASS inter-channel biases and temperature variations, due again to its FDMA characteristics, could be further investigated. With the effect investigated and calibrated, this could potentially improve the performance of the system.

Thirdly, the system performance could be tested under other different kinematic environments, such as urban downtown canyons, and for different inter-antenna distances.

Fourthly, in addition to the off-the-shelf Ashtech GG24<sup>TM</sup> GPS/GLONASS receivers used and tested in this research, implementing other brand GPS receivers in the attitude system would be desirable. Testing with the NovAtel, Javad, or some other brand GPS/GLONASS receivers, would be beneficial.

Fifthly, a GPS/GLONASS multi-antenna three-dimensional attitude system could be developed for heading, pitch, and roll determination. A full attitude system, as demonstrated in [Lu, 1995], would be highly desirable for many sea-borne and air-borne applications.

Sixthly, further augmentations of a GPS/GLONASS attitude system with other low cost sensors, such as gyro, compass, accelerometer, tiltmeter, are recommended. This types of integrated system, as shown in [Harvey, 1998], would significantly increase the reliability and speed of the carrier phase ambiguity resolution, enhance the quality assurance of the attitude results, bridge outages of satellite signals, and reduce blunders in the current system.

Lastly, a double differencing approach could be tested and implemented to be used in a system for GPS/GLONASS attitude determination. The four modified double difference techniques described in Chapter Three, particularly the ones proposed by Landau & Vollath [1996] and Rossbach & Hein [1996], worth further investigation.

## LIST OF REFERENCES

1. Axelrad, P., C.J. Comp, P.F. MacDoran [1994]. "Use of SNR for multipath error correction in GPS differential phase measurements: methodology and experimental results". *Proceedings of ION-GPS 94*, Salt Lake City, Utah, U.S.A. September 20-23, the Institute of Navigation.
2. Ball, Corp. [1993]. Precision Time & Frequency Handbook, Efratom Time and Frequency Products. Ball Corporation. Irvine, California, U.S.A.
3. Braasch, M.S. [1996]. "Multipath effects". Chapter 14 in *Global Positioning System: Theory and Application* (The Blue Book). Edited by Parkinson, B., J. Spilker, P. Axelrad, and P. Enge. American Institute of Aeronautics and Astronautics, Inc., Washington D.C., U.S.A.
4. Brown, R. [1992]. "Instantaneous GPS attitude determination". *Proceedings of IEEE PLANS*, Monterey, California, U.S.A., March, 1992.
5. Bykhanov, E. [1999]. "Timing and Positioning with GLONASS and GPS". *GPS Solution*, Vol. 3, No.1, pp. 26-31.
6. Cannon, M.E., and G. Lachapelle [1992]. "Analysis of a high-performance C/A-Code GPS receiver in kinematic mode." *Navigation*, the Institute of Navigation, Vol. 3, pp. 285 - 300.
7. Cannon M.E., E. Berry, and N. King [1993]. "Testing a lightweight GPS/GIS terminal for sub-meter DGPS positioning." *Proceedings of ION-GPS 93*, Salt Lake

- City, Utah, U.S.A. September 21-24, the Institute of Navigation. Part II, pp. 1011-1020.
8. Chen, D. [1994]. *Development of a Fast Ambiguity Search Filtering (FASF) Method for GPS Carrier Phase Ambiguity Resolution*. Master Thesis, Department of Geomatics Engineering, the University of Calgary, Calgary, Alberta.
  9. Cohen, C.E. [1992]. *Attitude Determination Using GPS*. Ph.D. Dissertation, Department of Aeronautics and Astronautics, Stanford University, California, U.S.A., 184 p.
  10. Cohen, C.E. [1995]. "Attitude determination." Chapter 11 in *Global Positioning System: Theory and Application* (The Blue Book). Edited by Parkinson, B., J. Spilker, P. Axelrad, and P. Enge. American Institute of Aeronautics and Astronautics, Inc., Washington D.C.
  11. Coordinational Scientific Information Centre [1998], *GLONASS Interface Control Document*, Coordinational Scientific Information Centre, 1998.
  12. Coordinational Scientific Information Centre [1995], *GLONASS Interface Control Document*, International Civil Aviation Organization, GNSSP/2-WP/66, Montreal, Quebec. November 14, 1995.
  13. Counselman, C.C., and S.A. Gouervitch [1981]. "Miniature interferometer terminals for earth surveying: ambiguity and multipath with Global Positioning System". *IEEE Transaction on Geoscience and Remote Sensing*, Vol. GE-19, No. 4, pp. 244-252.
  14. Daly, P. and P. Misra [1996]. "GPS and Global Navigation Satellite System (GLONASS)". Chapter 9 in *Global Positioning System: Theory and Application*

- (The Blue Book). Edited by Parkinson, B., J. Spilker, P. Axelrad, and P. Enge. American Institute of Aeronautics and Astronautics, Inc., Washington D.C.
15. Defense Mapping Agency [1987]. *Supplement to Department of Defense World Geodetic System 1984 Technical Report*, DMA Technical Report 8350.2-B, December 1, 1987.
  16. Dodson, A.H., T. Moore, D.F., Baker, J.W. Swann [1998]. "Hybrid GPS + GLONASS". Technical paper of the Institute of Engineering Surveying and Space Geodesy, University of Nottingham, England, U.K.
  17. Ford, T. and Neumann [1994]. "NovAtel's RT20- a real time floating ambiguity positioning system". *Proceedings of ION-GPS 94*, Salt Lake City, Utah, U.S.A. September 20-23, the Institute of Navigation.
  18. Georgiadou, Y and A. Kleusberg [1988]. "On carrier signal multipath effects in relative GPS positioning". *Manuscripta Geodetica*, Springer-Verlag, Vol. 13, No. 3, pp. 172-179.
  19. Goad, C.C. and L. Goodman [1974]. "A modified Hopfield tropospheric refraction correction model." Presented at the Fall Annual Meeting of the American Geophysical Union, San Francisco, California, U.S.A. December 1974.
  20. Gouzhva, G., A. Guevorkyan, A. Bassevich, and P. Bogdanov [1992]. "High-precision time and frequency dissemination with GLONASS". *GPS World*, Vol. 3, No. 4, pp. 40-49.
  21. van Grass and M. Braasch [1991]. "GPS interferometric attitude and heading determination: initial flight test results" *Navigation*, the Institute of Navigation, Vol. 38, No. 4.

22. Hall, T., B. Burke, M. Pratt, and P. Misra [1997]. "Comparison of GPS and GPS+GLONASS positioning performance." *Proceedings of ION-GPS 97*, Kansas City, Missouri. September 17-20, the Institute of Navigation, Part I, pp. 917-923.
23. Harvey, R.S. [1998]. *Development of a Precision Pointing System using an Integrated Multi-Sensor Approach*. Master Thesis, Department of Geomatics Engineering, the University of Calgary, Calgary, Alberta, 140 p.
24. Hatch R. [1990]. "Instantaneous ambiguity resolution." *Proceedings of the Kinematic Systems in Geodesy, Surveying and Remote Sensing, International Association of Geodesy Symposia 107*, Springer Verlag, New York, pp. 299-308.
25. Holmes, D. A. Last, and S. Basker [1998]. "GLONASS system performance." *Proceedings of ION-GPS 98*, Nashville, Tennessee, U.S.A. September 15-18, the Institute of Navigation, Part II, pp. 1599-1603.
26. Hopfield, H.S. [1969]. "Two-quadratic tropospheric refractivity profile for correcting satellite data." *Journal of Geophysical Research*, Vol. 74, pp. 4487-4499.
27. International Earth Rotation Services [1996]. *Annual Report 1995*. Central Bureau of International Earth Rotation Services. Paris, France.
28. Jacobson, L. [1999]. *The Business of GPS*. Course 230 of Navtech's ION-GPS99 Tutorial Series. Navtech Seminars and GPS Supply, Alexandria, Virginia, U.S.A.
29. Keong, J.H. [1999]. "GPS/GLONASS attitude determination with a common clock using a single difference approach". *Proceedings of ION-GPS 99*, Nashville, Tennessee, U.S.A. September 14-17, the Institute of Navigation.

30. Keong, J.H. and G. Lachapelle [1998]. "Heading and pitch determination using GPS/GLONASS with a common clock". *Proceedings of ION-GPS 98*, Nashville, Tennessee, U.S.A. September 15-18, the Institute of Navigation, Part II, pp. 2053-2061.
31. Kleusberg, A. [1990]. "Comparing GPS and GLONASS". *GPS World*, Vol. 1, No. 5.
32. Lachapelle, G. [1997]. *Hydrography*. UCGE Lecture Notes 10016. Department of Geomatics Engineering, the University of Calgary, Calgary, Alberta.
33. Lachapelle, G., M.E. Cannon, and R. Harvey [1996]. *Development of a Low Cost GPS Attitude Determination System*. Technical report prepared for Defense Research Establishment Ottawa, Department of Geomatics Engineering, University of Calgary, Calgary, Alberta.
34. Lachapelle, G., M.E. Cannon, and G. Lu [1992]. "High precision GPS navigation with emphasis on carrier-phase ambiguity resolution." *Marine Geodesy*, Vol. 15, pp. 253-269.
35. Landau, H., and H.J. Euler [1992]. "On-the-fly ambiguity resolution for precise differential positioning." *Proceedings of ION-GPS 92*, Nashville, Tennessee, U.S.A. September 14-17, the Institute of Navigation.
36. Landau, H., and U. Vollath [1996]. "Carrier phase ambiguity resolution using GPS and GLONASS signals." *Proceedings of ION-GPS 96*, Kansas City, Mi. September 17-20, the Institute of Navigation, Part I, pp. 917-923.
37. Langley, R.B. [1996]. "Propagation of the GPS signals." Chapter 3 and "GPS receivers and the observable." Chapter 4 in *GPS for Geodesy*, edited by Kleusberg, A., and P. Teunissen. Springer-Verlag, Berlin, Germany.

38. Langley, R.B. [1997]. "GLONASS: Review and Update". *GPS World*, Vol. 8, No. 7, pp. 46-51.
39. Lathi, B.P., [1992]. *Linear Systems and Signals*. Berkley-Cambridge, Carmichael, California, U.S.A.
40. Leick, A. [1998]. "GLONASS satellite surveying." *Journal of Surveying Engineering*, American Society of Civil Engineering, Geomatics Division, New York. Vol. 124, No. 2.
41. Leick, A. [1995]. *GPS Satellite Surveying*, 2nd ed., John Wiley & Sons, New York, U.S.A
42. Leick, A., J. Li, J. Beser, and G. Mader [1995]. "Processing GLONASS carrier phase observations: Theory and first experience." *Proceeding of ION-GPS 95*, Kansas City, Missouri, U.S.A. September 19-22, the Institute of Navigation, Part I, pp. 1041-1047.
43. Lu, Gang [1995]. *Development of a GPS Multi-Antenna System for Attitude Determination*. Ph.D. Dissertation, Department of Geomatics Engineering, the University of Calgary, Calgary, Alberta, 185 p.
44. Lu, G., M.E. Cannon, G. Lachapelle, and P. Kielland [1993]. "Attitude determination in a survey launch using multi-antenna GPS technologies". *Proceedings of ION-NTM 93*, the Institute of Navigation, pp. 251-260.
45. Magellan Corporation [1998]. *Ashtech GG24 OEM Board & Sensor GPS+GLONASS Reference Manual*. Magellan, Sunnyvale, California, U.S.A.

46. Maybeck, P.S. [1994]. *Stochastic Models, Estimation, and Control – Volume I*. Vol 141-1 in Mathematics in Science and Engineering. A series of monographs and textbooks edited by Richard Bellman, University of Southern California, U.S.A. Republished 1994 by Navtech Book & Software Store, Alexandria, Virginia, U.S.A.
47. Misra, P.N., R.I. Abbot, and E.M. Gaposchkin (1996). “Integrated use of GPS and GLONASS: Transformation between WGS 84 and PZ-90”. *Proceedings of ION-GPS 96*, Kansas City, Missouri, U.S.A. September 17-20, the Institute of Navigation, Part I, pp. 307-314.
48. Mitrikas, V. V., S.G. Revnivykh, and E.V. Bykhanov [1998]. “WGS84/PZ90 transformation parameters determination based on laser and ephemeris long-term GLONASS orbital data processing”. *Proceedings of ION-GPS 98*, the Institute of Navigation, Part II, pp. 1625-1635.
49. Neumann J.B., A. Manz, T.J. Ford, and O. Mulyk [1996]. “Test results from a new 2 cm real time kinematic GPS positioning system.” *Proceedings of ION-GPS 96*, Kansas City, Missouri, U.S.A. September 17-20, the Institute of Navigation, Part I, pp. 873-882.
50. van Nee, R.J [1994]. “The multipath estimating delay lock loop: approaching theoretical accuracy limits.” *Proceedings of IEEE PLANS*, Las Vegas, April 11-15, pp. 246-251.
51. Raquet, J.F. [1998]. *Development of a Method for Kinematic GPS Carrier-Phase Ambiguity Resolution using Multiple Reference Receivers*. Ph.D. Dissertation, Department of Geomatics Engineering, the University of Calgary, Calgary, Alberta, 259 p.

52. Ray, J.K., M.E. Cannon, and P. Fenton [1998]. "Mitigation of static carrier phase multipath effects using multiple closely-spaced antennas". *Proceedings of ION-GPS 98*, the Institute of Navigation, Part II, pp. 1025-1634.
53. Rossbach, U., H. Habrich, and N. Zarraoa (1996). "Transformation parameters between PZ-90 and WGS 84". *Proceedings of ION-GPS 96*, Kansas City, Missouri. September 17-20, the Institute of Navigation, Part I, pp. 307-314.
54. Rossbach, U. and G.W. Hein (1996). "Treatment of integer ambiguities in DGPS/DGLONASS double difference carrier phase solutions". *Proceedings of ION-GPS 96*, Kansas City, Missouri. September 17-20, the Institute of Navigation, Part I, pp. 307-314.
55. Saastamoinen, J. [1973]. "Contribution to the theory of atmospheric refraction." *Bulletin Géodésique*, Vol. 107, No. 1, pp. 13-14.
56. Schleppe J.B. [1996]. *A Real-Time Attitude System*. Master Thesis, Department of Geomatics Engineering, the University of Calgary, Calgary, Alberta, 142 p.
57. Schwarz, K.P. and J. Krynski [1992]. *Fundamentals of Geodesy*. UCGE Lecture Notes 10014. Department of Geomatics Engineering, the University of Calgary, Calgary, Alberta.
58. Skone, S. [1998]. *Wide Area Ionosphere Grid Modelling in the Auroral Region*. Ph.D. Dissertation, Department of Geomatics Engineering, the University of Calgary, Calgary, Alberta, 198 p.
59. Spilker Jr., J. J. [1996]. "GPS signal structure and theoretical performance". Chapter 3 in *Global Positioning System: Theory and Application* (The Blue Book). Edited by

- Parkinson, B., J. Spilker, P. Axelrad, and P. Enge. American Institute of Aeronautics and Astronautics, Inc., Washington D.C., U.S.A.
60. Sun, H. [1994]. *GPS/INS Integration for Airborne Applications*. Master Thesis, Department of Geomatics Engineering, the University of Calgary, Calgary, Alberta, 103 p.
61. Sun, H., M.E. Cannon, and G. Lachapelle [1997]. *HEADRTTM Operator's Manual (For G12 and GG24)*. Department of Geomatics Engineering, the University of Calgary, Calgary, Alberta.
62. Szarmes, M.C., G. Lachapelle, and M.E. Cannon [1997]. *Development of a Low Cost Real Time Twin-Antenna GPS Heading System*. Technical report prepared for Defense Research Establishment Ottawa, Department of Geomatics Engineering, University of Calgary, Calgary, Alberta.
63. Tiemeyer, B., M.E. Cannon, G. Lachapelle, and G. Schanzer [1994]. "Satellite navigation for high precision aircraft navigation with emphasis on atmospheric effects." *Proceedings of IEEE PLANS*, Las Vegas, April 11-15, pp. 394-401.
64. Torge, W. [1980]. *Geodesy*. Walter de Gruyter, New York, U.S.A.
65. Tranquilla, J.M. (1986). "Multipath and imaging problems in GPS receiver antennas." Presented at Symposium on Antenna Technology and Applied Electromagnetic, Winnipeg, Manitoba.
66. Vaníček, P., and E.J. Krakiwsky [1986]. *Geodesy: The Concepts*. 2nd rev. ed., North-Holland, Amsterdam.

67. Walsh, D., V. Ashkenazi, G. Foulkes-Jones [1995]. "Performance of OTF ambiguity resolution search algorithms for real time positioning under varying conditions." *Proceedings of ION-NTM 95*, Anaheim, California, January 18-20, 1995.
68. Walsh, D. and P. Daly [1996]. "GPS and GLONASS carrier phase ambiguity resolution." *Proceedings of ION-GPS 96*, Kansas City, Missouri, U.S.A. September 17-20, the Institute of Navigation, Part I, pp. 899-907.
69. Walsh, D. and P. Daly [1997]. "Combined GPS and GLONASS carrier phase positioning." *Proceedings of the International Symposium on Kinematic systems in Geodesy, Geomatics and Navigation (KIS-97)*, Banff, Canada. June 3-6, the Department of Geomatics engineering, the University of Calgary, pp. 205-212.
70. Weisenburger, S. D. [1997]. *Effect of constraints and multiple receivers for On-The-Fly ambiguity resolution*. Master Thesis, Department of Geomatics Engineering, the University of Calgary, Calgary, Alberta, 125 p.
71. Wells, D., N. Beck, D. Delikaroglou, A. Kleusberg, E. Krakiwsky, G. Lachapelle, R. Langley, M. Nakiboglu, J. Schwarz, J. Tranquilla, and P. Vaníček, [1986]. *Guide To GPS Positioning*. The Canadian GPS Associates, Fredericton, Canada.
72. Werts, J.R. [1978]. *Spacecraft Attitude Determination and Control*. Kluwer Academic Publishers, the Netherlands.
73. Wong R.V.C [1988]. *Development of a RLG Strapdown Inertial Survey System*. Master Thesis, Department of Geomatics Engineering, the University of Calgary, Calgary, Alberta, 73 p.

74. Zhang, J.H. [1999]. *Investigation into the Estimation of Residual Tropospheric Delay in a GPS Network*. Master Thesis, Department of Geomatics Engineering, the University of Calgary, Calgary, Alberta.
  
75. Zhang, Z. [1997]. *Impact of a Rubidium Clock Aiding on GPS Augmented Vehicular Navigation*. Master Thesis, Department of Geomatics Engineering, the University of Calgary, Calgary, Alberta, 135 p.